DEVELOPMENT OF WELDING TECHNIQUES AND FILLER METALS FOR HIGH STRENGTH ALUMINUM ALLOYS

Annual Summary Report

Project No. 07-1063

Reporting Period

27 June 1964 to 27 June 1965

to

National Aeronautics and Space Administration

George C. Marshall Space Flight Center

Purchasing Office

Huntsville, Alabama

Attn: PR-EC

Contract No. NAS8-1529

Control No. TP2-85364

October 11, 1965

SOUTHWEST RESEARCH INSTITUTE

SAN ANTONIO HOUSTON

SOUTHWEST RESEARCH INSTITUTE
8500 Culebra Road, San Antonio, Texas 78206

DEVELOPMENT OF WELDING TECHNIQUES AND FILLER METALS FOR HIGH STRENGTH ALUMINUM ALLOYS

Annual Summary Report
Project No. 07-1063

Reporting Period
27 June 1964 to 27 June 1965

for

National Aeronautics and Space Administration
George C. Marshall Space Flight Center
Purchasing Office
Huntsville, Alabama
Attn: PR-EC

Contract No. NAS8-1529
Control No. TP2-85364

October 11, 1965

Investigators:

H. C. Burghard, Jr.
N. G. Lenamond
A. L. Lowenberg
J. McDonald, Jr.
E. B. Norris
K. K. Speirs

APPROVED:

Robert D. Wylie

Robert D. Wylie, Director
Department of Materials Engineering

FOREWORD

This report entitled, "Development of Welding Techniques and Filler Metals for High Strength Aluminum Alloys", was prepared by the Southwest Research Institute under Contract No. NAS 8-1529 for the George C. Marshall Space Flight Center of the National Aeronautics and Space Administration.

The work was administered under the direction of the Propulsion and Vehicle Engineering Division, Engineering Materials Branch of the George C. Marshall Space Flight Center with Mr. Richard A. Davis acting as Project Manager.

ABSTRACT

26230

The properties of MIG and TIG weldments of 2014-T6 and 2219-T87 aluminum alloys under biaxial and uniaxial loading conditions were measured and compared. The results of this study indicate that the TIG process is superior to the MIG process for the fabrication of 2014-T6. In the case of 2219-T87, no significant differences were noted in the average properties of TIG and MIG weldments in either the biaxial or uniaxial tests.

In the course of the program, a number of observations were made which indicate that the membrane stress formula, derived for a spherical shell, is not adequate for the determination of the absolute value of biaxial ultimate strength from hydraulic bulge test data. It was concluded, however, that the bulge test does provide a satisfactory means for the comparison of weldments with similar properties.

A study of the natural aging characteristics of 0.187-inch thick MIG and TIG X7106 weldments, made with X5180, 5356 and 5556 filler metal alloys, was also carried out. A marked increase in the hardness and strength of the weld deposit and adjacent heat-affected zone on natural aging for periods in excess of eight weeks was noted for all types of X7106 weldments studied. It was observed that, in uniaxial tensile tests of such weldments, the failures occurred predominantly in the heat-affected base metal rather than in the weld deposit. This observation indicates that the increase in strength of the weld deposits, resulting from aging at room temperature, is such that the strength of the weld deposit is not the controlling factor in the strength of the X7106-T63 weldments included in this study.

The hot cracking characteristics of X7106-T63 weldments relative to those of 2219-T87 were also investigated. The Houldcroft crack susceptibility test was employed for this purpose. In these tests, the TIG process, with X5180, 5356 and 5556 filler wire, was used to make the required welds. The results of these tests indicate that X7106-T63 is more susceptible to hot cracking during welding than 2219-T87. No significant difference in the crack susceptibility of the X7106 weldments made with the three filler metals (X5180, 5356 and 5556) was noted.

Of the six combinations of welding process and filler metal included in the study of X7106 weldments, the TIG weldments, as a group, exhibited higher uniaxial tensile properties than those of the MIG weldments. Only slight differences in mechanical properties among the weldments made with the three different filler alloys by one process were noted.

TABLE OF CONTENTS

TABLE OF CONTENTS (continued)

LIST OF TABLES

LIST OF TABLES (continued)

LIST OF ILLUSTRATIONS

LIST OF ILLUSTRATIONS (continued)

LIST OF ILLUSTRATIONS (continued)

LIST OF ILLUSTRATIONS (continued)

DISTRIBUTION LIST

Name	Number of Copies
Mr. James W. Fletcher National Aeronautics & Space Administration George C. Marshall Space Flight Center Purchasing Office Huntsville, Alabama 35812 Attn: PR-EC	14
Mr. Richard A. Davis R-P&VE-MMJ-64-86 NASA George C. Marshall Space Flight Center Huntsville, Alabama 35812	1
General Dynamics/Convair P.O. Box 1128 San Diego, California 92112	1
Scientific & Technical Information Facility Attn: NASA Representative (SQT-28730) 4833 Ribgy Avenue Bethesda, Maryland 20014	2
Southwest Research Institute 8500 Culebra Road San Antonio, Texas	12

I. INTRODUCTION

In the design and construction of large aerospace vehicles, such as the Saturn V booster, extensive use is made of high-strength aluminum alloys. Alloy 2014-T6, because of its high strength to weight ratio, has been the principal material employed in the SII and SIVB upper stages of the Saturn IV vehicle. This alloy, however, has a tendency toward hot cracking during welding, particularly when the Metal Inert Gas process is employed. As a result, difficulties have been encountered in the fabrication of structural components from this alloy.

A newer high-strength aluminum alloy, designated as 2219, has been recently developed. The strength of this alloy is somewhat lower than that attainable in 2014, but 2219 exhibits a much lower susceptibility to hot cracking. Because of this latter feature, considerable interest has developed in the possible application of 2219 for welded structural components. This particular alloy was selected as the primary structural material for the tankage and certain accessory components of the S-IC booster stage of the Saturn V vehicle.

A program for the investigation of various aspects of welding 2219 and 2014 aluminum alloy has been in progress at Southwest Research Institute since 1961 (Contract NAS8-1529). During the early part of this program, the welding characteristics of relatively thick 2219-T87 plate and the mechanical properties of such weldments were established. Observations made in the program led to the question of whether or not 2219 weldments exhibited fracture characteristics under biaxial loading conditions similar to those observed in uniaxial tests. A further investigation of the properties of 3/4-inch thick 2219 weldments, employing hydraulic bulge tests, was then initiated. The bulge test was employed as a screening test to establish the location and extent of fracture with respect to the weld crown and investigate the influence of stress concentration and microstructural characteristics at the weld crown on the fracture of 2219 weldments. In addition, the test was employed for the comparison of the fracture characteristics of 2219 weldments fabricated with various welding procedures.

In the previous work, the material thicknesses were such that the bulge test produced significant bending stresses superimposed on the membrane stresses. Under these conditions, it is difficult to determine absolute values of biaxial strength. The current program was initiated to establish the biaxial properties of 2219-T87 and 2014-T6 weldments utilizing the hydraulic bulge test. This investigation was based on the use of 0.125-inch sheet material so that, in the bulge test, the bending stresses would be small relative to the membrane stresses. The program was organized to utilize both uniaxial tensile tests and bulge tests to compare the mechanical properties of Metal Inert Gas (MIG) and Tungsten Inert Gas (TIG) weldments of these alloys. Attention was also directed toward the investigation of the biaxial to uniaxial strength ratio of such weldments.

In addition to the recent alloy developments in the 2000 series aluminum alloys (resulting in alloy 2219) considerable attention has been given to the development of weldable aluminum alloys which age harden at room temperature. These materials constitute a group of Al-Mg-Zn alloys (7000 series). In general, this series of aluminum alloys exhibit poor weldability and their use has been limited to applications which do not require welding. A new, weldable Al-Mg-Zn alloy, X7106, has recently been introduced, and it has been reported that this alloy combines high-strength (attainable by natural aging) with good weldability[5]. An obvious potential application of this alloy is in the fabrication of large aerospace vehicles where post-weld heat treatment is impractical.

In view of the potential application of X7106 aluminum alloy, a study of the mechanical properties and weldability of this alloy was initiated as a separate phase of the current project. This phase of the program was organized to establish the natural aging characteristics of MIG and TIG X7106 weldments made with three potentially applicable filler alloys. In addition, the program included a study of the susceptibility of this alloy to hot cracking during welding relative to that of alloy 2219.

II. EXPERIMENTAL PROCEDURE

A. Welding Process Evaluation

The evaluation of the TIG and MIG welding processes was carried out on the basis of the mechanical properties of weldments tested under both biaxial and uniaxial loading conditions. The various combinations of material, filler metal and welding process evaluated are as follows.*

Process	Alloy	Filler Metal
TIG	2014-T6	2319
TIG	2014-T6	4043
MIG	2014-T6	4043
TIG	2219-T87	2319
MIG	2219-T87	2319

Each of these above categories included single welds, tee welds and cross welds to simulate conditions encountered in production. Tests were also conducted on parent metal specimens to provide a basis of comparison. All materials employed in this part of the program were 0.125-inch sheet stock.

The hydraulic bulge test was employed as a means for biaxial loading. In this test, a 30-inch x 30-inch panel is clamped between a lower flat die and an upper die containing a circular opening 18-inches in diameter. The lower die is equipped with an inlet for hydraulic fluid and fittings to allow for relief valve and pressure transducer connections. The lower edge of the circular opening in the upper die is machined to a radius of three-inches to eliminate any effects arising from a sharp edge. An O-ring groove is machined in the lower die to provide for a seal. The arrangement of the test panel and the bulge die is illustrated in Figure 1.

In the test, hydraulic pressure is applied to the lower side of the test panel so that the panel is bulged into the circular opening of the upper die, and the pressure is increased steadily to the point of failure of the test panel. A calibrated, strain-gage deflectometer was installed to provide a means of measuring the bulge height and a pressure transducer was employed for pressure measurement. During the course of each test the bulge height and pressure were simultaneously recorded on either a Mosely X-Y Recorder or

* MIG 2014-T6 weldments, made with 2319 filler wire were originally included in the program. This combination of filler metal and base metal, however, proved to be extremely crack sensitive, and efforts to produce sound welds with welding procedures comparable to those used for the other combinations were unsuccessful.

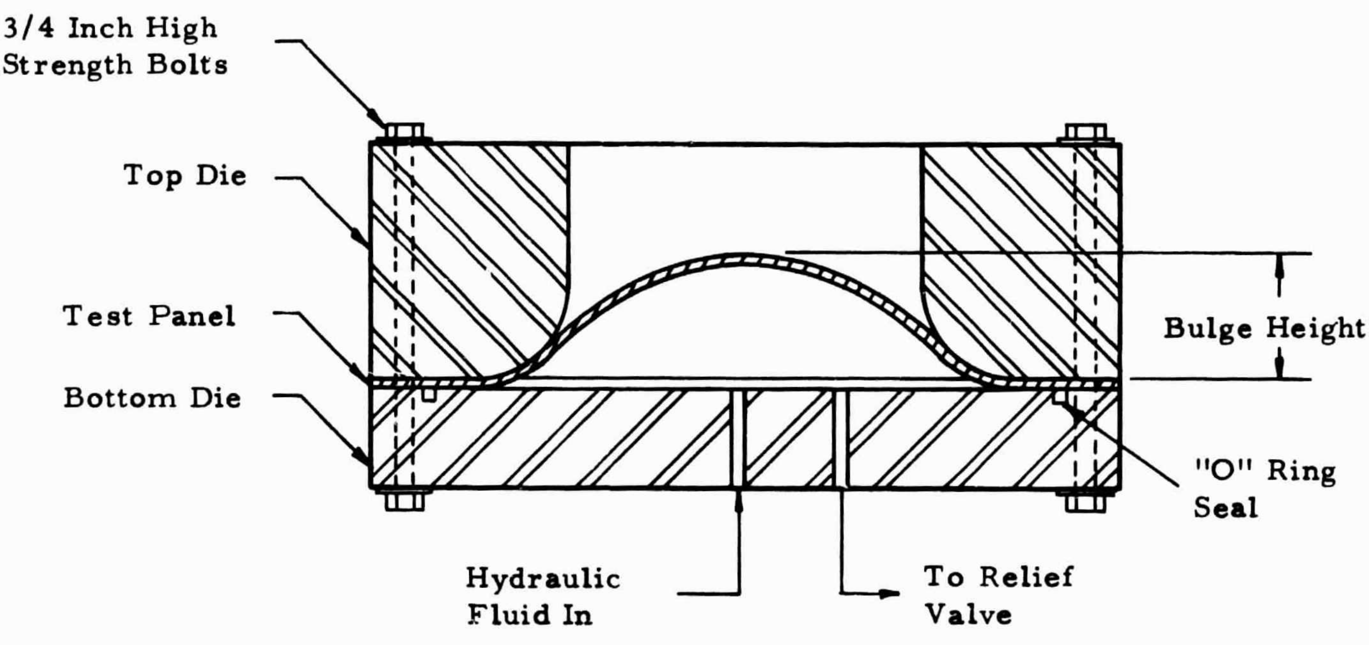

FIGURE 1. SCHEMATIC DIAGRAM OF HYDRAULIC BULGE TEST FIXTURE

a Sanborn Model 320 dual channel recorder. The test apparatus, as described above, was installed in an isolated test cell and operation and recordering were accomplished from outside the cell. The general arrangement of the test apparatus inside the cell and the recording instruments and pump outside the cell are shown in Figures 2 and 3.

The welded panels containing single welds and cross welds were prepared from two 15-inch x 36-inch blanks, cut so that the rolling direction is perpendicular to the long axis. The blanks were welded along the 36-inch dimension to form the single-weld panel. In the case of the cross welds, a single-weld panel was prepared and then sheared in half perpendicular to the single-weld. The sheared edges were then machined and the panel was completed by welding the newly formed joint.

The panels containing tee welds were prepared by first welding two 15-inch x 18-inch blanks along the 15-inch dimension. The resulting 15-inch x 36-inch weldment was then welded to a 15-inch x 36-inch blank to form a 30-inch x 36-inch weldment. The blanks for these panels were cut so that the rolling direction was perpendicular to the short weld.

In each case, the edges of the blanks were draw filed immediately prior to welding. The panel blanks were fitted up and clamped in position by an Airline positioner. A grooved, water-cooled, copper backup bar was used in the fabrication of each panel to assure reproducibility of welding conditions. During each welding operation, helium gas was directed through the groove of the backup bar to protect the underside of the weld.

The TIG welding operations were carried out using a Miller Gold Star, 600 ampere AC-DC power supply, a Linde HWM-2 contour welding head equipped with a Linde Heliarc wire feeder and a Linde HW13 TIG torch. A Linde SVI-500 constant potential power supply was used for the MIG welding operations, along with a Linde HW13 MIG torch. In both cases the welding heads and associated accessories were mounted on a Linde OM-48 side beam carriage. The carriage and wire feed motors were controlled by Linde electronic governors. During each welding operation, the voltage and current were recorded by means of Leeds and Northrup, Speedomax H, strip chart recorders.

The welding procedures employed in the fabrication of each test panel are listed in Table I.

After welding, each panel was radiographed in accordance with the procedures listed in Table II. The radiographs were graded in accordance with ASME Code porosity charts for 1/8-inch thick material. Weldments containing excessive porosity, connected pores, cracks or lack of penetration were

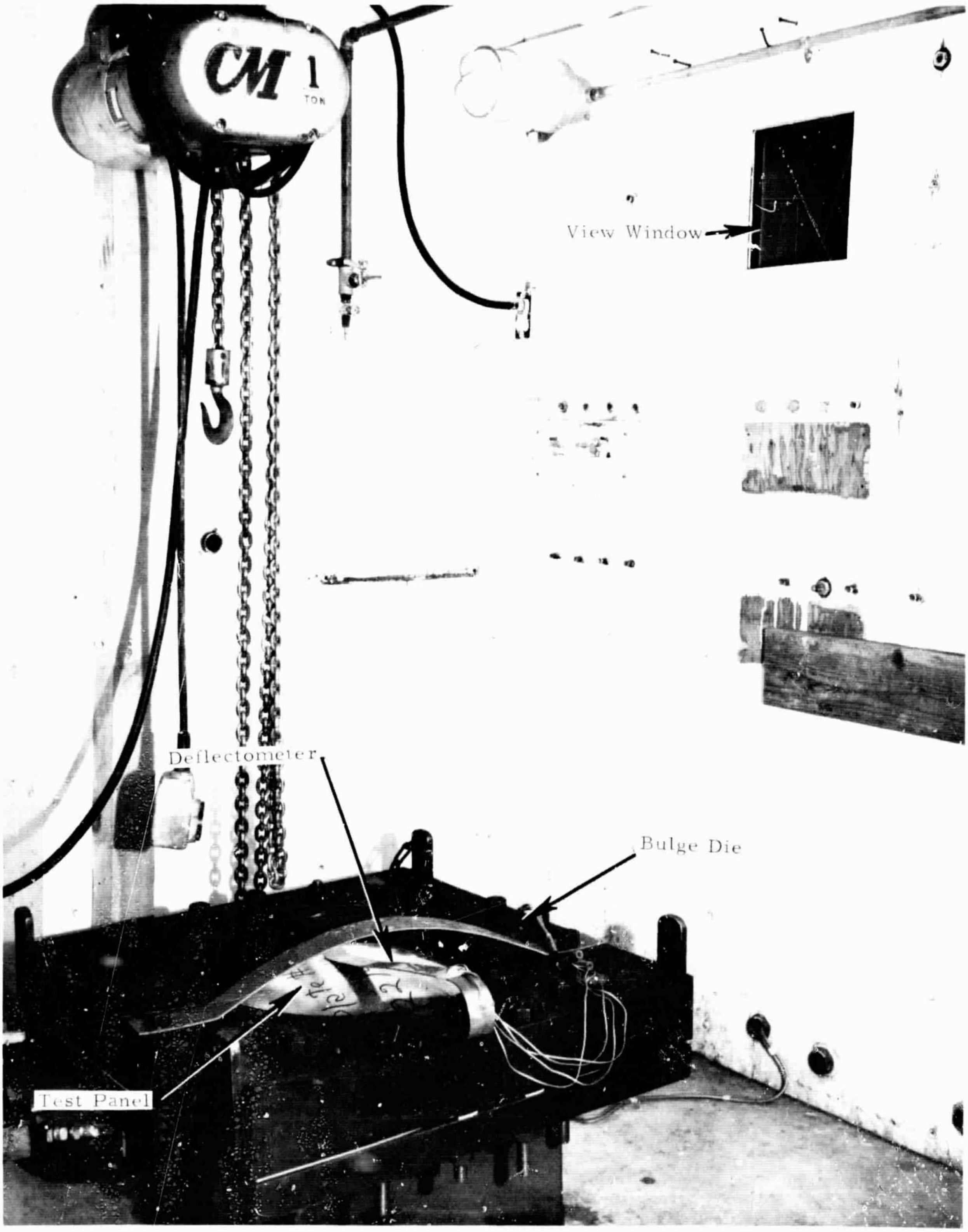

FIGURE 2. BULGE DIE AND TEST PANEL ASSEMBLY IN TEST CELL

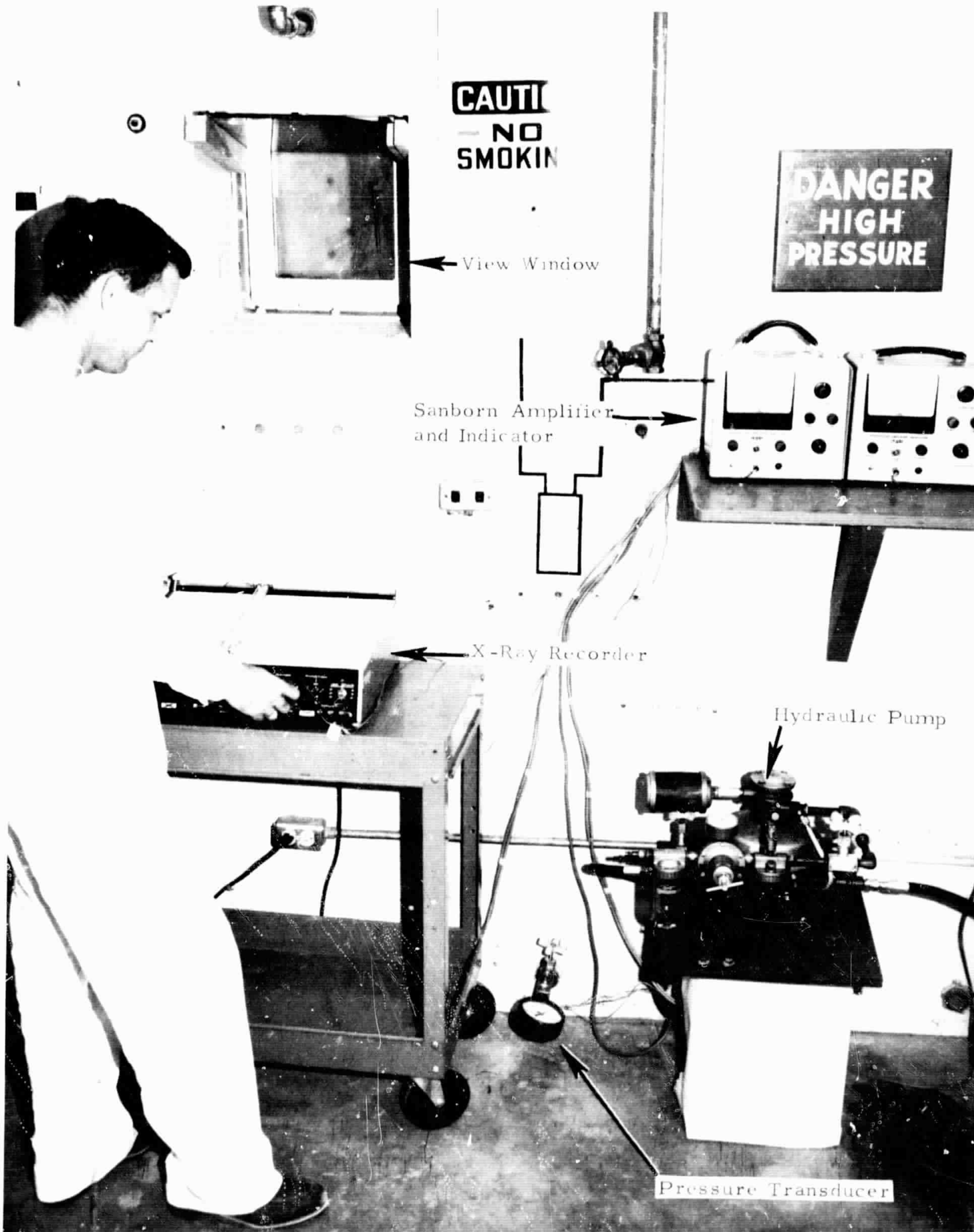

FIGURE 3. INSTRUMENTATION FOR HYDRAULIC BULGE TEST

TABLE I

WELDING PROCEDURES

Welding Procedure	Alloy/Joint Design	Material Thickness (Inches)	Welding Process	Filler Metal/ Size (Inches)	No. of Passes	Electrode Composition/Size (Inches)	Current (Amps)	Voltage (Volts)	Inert Gas/ Flow (cfh)	Travel Speed (ipm)	Filler Metal Feed (ipm)
64A-1	2014-T6/ Sq. Butt	1/8	TIG	2319/ 3/64	1	Tungsten 2% Thoria/ 1/8	180 DCSP	10.5	He/35	15	35
64A-2	2219-T87/ Sq. Butt	1/8	TIG	2319/ 3/64	1	Tungsten 2% Thoria/ 1/8	180 DCSP	10.5	He/35	15	37
64A-3	2014-T6/ Sq. Butt	1/8	MIG	4043/ 3/64	1	---	200 DCRP	33.5	A/20 He/40	50	--
64A-4	2219-T87/ Sq. Butt	1/8	MIG	2319/ 3/64	1	---	200 DCRP	33.5	A/20 He/40	50	--
64A-5	2219-T87/ Single "V" 90° Included Angle with 1/32-Inch Land	1/8	TIG	2319/ 3/64	5	Tungsten 2% Thoria/ 1/8	180 DCSP	11	He/35	17.5-40	45-68
				Individual Passes							
					1	"	"	"	"	17.5	68
					2	"	"	"	"	40	45
					3	"	"	"	"	40	45
					4	"	"	"	"	40	45
					5	"	"	"	"	40	45
64A-6	X7106-T63/ Sq. Butt	.090	TIG	X5180/ 3/64	1	Tungsten 2% Thoria 3/32	175 DCSP	11	He/35	22	64
64A-7	X7106-T63/ Sq. Butt	.090	TIG	5356/ 3/64	1	Tungsten 2% Thoria 3/32	175 DCSP	11	He/35	22	64

TABLE I (continued)

WELDING PROCEDURES

Welding Procedure	Alloy/Joint Design	Material Thickness (Inches)	Welding Process	Filler Metal/Size (Inches)	No. Passes	Electrode Composition/Size (Inches)	Current (Amps)	Voltage (Volts)	Inert Gas/Flow (cfh)	Travel Speed (ipm)	Filler Metal Speed (ipm)
64A-8	X7106-T63/ Sq. Butt	.090	TIG	5556/ 3/64	1	Tungsten 2% Thoria 3/32	175 DCSP	11	He/35	22	142
64A-9	X7106-T63/ Sq. Butt	.090	MIG	X5180/ 3/64	1	---	200 DCRP	22	A/50	58	---
64A-10	X7106-T63/ Sq. Butt	.090	MIG	5356/ 3/64	1	---	200 DCRP	22	A/50	58	---
64A-11	X7106-T63/ Sq. Butt	.090	MIG	5556/ 3/64	1	---	200 DCRP	22	A/50	58	---
64A-12	X7106-T63/ Bead-on-plate	.090	TIG	X5180/ 3/64	1	Tungsten 2% Thoria 3/32	80 DCSP	11	He/50	11	24
64A-13	X7106-T63/ Bead-on-plate	.090	TIG	5356/ 3/64	1	Tungsten 2% Thoria 3/32	80 DCSP	11	He/50	11	24
64A-14	X7106-T63 Bead-on-plate	.090	TIG	5556/ 3/64	1	Tungsten 2% Thoria 3/32	80 DCSP	11	He/50	11	24
64A-15	2219-T87 Bead-on-plate	.090	TIG	2319/ 3/64	1	Tungsten 2% Thoria 3/32	80 DCSP	11	He/50	11	24
64A-16	2014-T6/ Sq. Butt	1/8	TIG	4043/ 3/64	1	Tungsten 2% Thoria/ 1/8	200 DCSP	11	He/35	15	64

TABLE II

X-RAY PROCEDURE FOR 1/8 INCH ALUMINUM PLATES

Source - Baltospot 150

Strength - 105 KV, 3 ma

Source to Film Distance - 75 Inches

Penetrameter - .25 inch ASME, 1/8 inch shim stock

Film - Kodak Type M (90 mm strip pack)

Exposure Time - 13 minutes

Density - 2

Developing solution - Kodak X-ray developer and replenisher

Developing Time - 5 minutes at 68°F

Fixing Solution - Kodak X-ray fixer

Fixing Time - 10 minutes at 68°F

rejected. The results of the radiographic inspection of each weldment used in the program are listed in Table III.

Following radiographic inspection and acceptance, the test panels were trimmed to 30-inches x 30-inches. The drop off material from this operation was used for uniaxial tensile specimens. These specimens were cut to provide a 1/2-inch wide test section with a 2-inch gage length symmetrical about the weld. Parent metal uniaxial tensile specimens, oriented parallel to the rolling direction, were also prepared to the same dimensions. These specimens were tested in an Instron Model TTC universal testing machine in accordance with the requirement of ASTM Specification E8-57T. All welded specimens were tested with the weld crowns intact.

B. Investigation of Biaxial to Uniaxial Strength Ratio

A special series of bulge tests was conducted to determine the influence of residual stresses, welding procedure, and stress concentration at the weld crown on the biaxial to uniaxial strength ratio. This series included tests on annealed parent metal panels and weldments, multi-pass weldments and weldments with the weld crowns removed.

The influence of residual stresses was investigated by tests on the annealed panels and the multi-pass weldments. The specimens for this series of tests included three TIG 2219-T87/2319 single-weld panels (BP-40, BP-41 and BP-42) and three 2219-T87 parent metal panels (BMA1, BMA2 and BMA3), each 1/8-inch x 30-inches x 36-inches. The welded panels were fabricated by welding procedure 64A-2 (Table I). Each of the six panels was heated to 850°F ±25°F for 1-1/2 hours, furnace cooled to 200°F at a maximum rate of 50°F per hour, then air cooled. During the annealing treatment, the panels were clamped between 1/4-inch steel plates to minimize warping. The multi-pass panels (BP-47, BP-48 and BP-50) were fabricated with a single, V-groove, five-pass joint utilizing welding procedure 64A-5 (Table I).

Three single-weld panels (BP-44, BP-45 and BP-46) were fabricated with welding procedure 64A-2 (Table I) and the weld crowns were ground flush with the panel surface. These panels were tested to determine the influence of stress concentration at the weld crown.

Uniaxial tensile test specimens were cut from each of the annealed panels and special-purpose panels and tested as previously described. The results of the bulge tests and uniaxial tests on this group of panels were compared with those of the tests on as-fabricated panels performed in the MIG and TIG evaluation series.

In addition to the tests described above, direct measurements of the residual stresses in several weldments were made. For this purpose,

TABLE III

RADIOGRAPHIC RESULTS OF WELDED PANELS FOR THE WELDING PROCESS EVALUATION

Panel No.	Porosity	Lack of Penetration Length (In.)	Cracking Length (In.)	Misc.	Accepted/ Rejected
1					Accepted
2					Accepted
3					Accepted
4	Slight				Accepted
5	Slight	1/2 inch at start			Accepted
6					Accepted
7					Accepted
8					Accepted
9					Accepted
10					Accepted
12					Accepted
14	Slight				Accepted
15					Accepted
16	Gross				Rejected
17	Slight				Accepted
18					Accepted
19	Slight				Accepted
23	Slight	1/32 inch at start			Accepted
24	1 Spot			Hole	Rejected
25	Slight			Hole	Rejected
26					Accepted
27					Accepted
28	Slight				Accepted
29	Slight				Accepted
30	Slight				Accepted
31	Slight				Accepted
33	Slight				Accepted
35	Slight				Accepted
36	Slight				Accepted
37	Slight		1/4 inch in crater		Accepted
40					Accepted
41	Slight				Accepted
42					Accepted
43			1/2 inch		Rejected
44					Accepted
45					Accepted

TABLE III (continued)

RADIOGRAPHIC RESULTS OF WELDED PANELS FOR THE WELDING PROCESS EVALUATION

Panel No.	Porosity	Lack of Penetration Length (In.)	Cracking Length (In.)	Misc.	Accepted/ Rejected
46		1 inch at start			Accepted
47		1/2 inch at start			Accepted
48		1/2 inch at finish	1/2 inch at start		Accepted
49			1/2 inch		Rejected
50			1 inch at finish		Accepted
51					Accepted
52					Accepted
53					Accepted
54					Accepted
55					Accepted
56					Accepted
57				Tungsten	Accepted
58					Accepted
59				Tungsten	Accepted
60					Accepted
63					Accepted
64					Accepted
65					Accepted
68				Tungsten	Accepted
69					Accepted
70					Accepted
71				Tungsten	Accepted
72					Accepted

resistance strain gages were mounted in appropriate locations on each of the panels after fabrication. One-inch squares, containing each gage, were then cut from the panel and the relaxation strains were measured using conventional procedures and instruments. The residual stresses were calculated from these strain measurements.

The types of weldments, locations of gages and conditions of each test were as follows:

1) Panel 2-SG: TIG 2219-T87/2319 single-weld panel fabricated by procedure 64A-2. Three 120° rosettes (1/32-inch gage length) mounted on center line of the weld. Gages mounted after removal of panel from positioner. Panel replaced in positioner, clamped and strain due to clamping recorded.

2) Panels 3-SG and 5-SG: TIG 2219-T87/2319 single-weld panels fabricated by procedure 64A-2. Three 120° rosettes (1/32-inch gage length) on center line of weld and two 1/64-inch single gages mounted in heat-affected zone*, one parallel to weld center line and one perpendicular to the weld center line. Gages mounted before panel was removed from positioner. The strain arising from release of clamps was recorded.

3) Panels 6-SG and 7-SG: MIG 2219-T87/2319 single-weld panels fabricated by procedure 64A-4. Number of gages and procedure same as for Panels 3-SG and 5-SG.

4) Panels 4-SG: TIG 2219-T87/2319 single-weld panel fabricated by procedure 64A-5 (single V-groove, 5 pass). Three 120° rosettes (1/32-inch gage length) on center line of weld. Gages mounted after panel was removed from positioner. Panel replaced in positioner, clamped and strain due to clamping recorded.

C. Natural Aging Characteristics of X7106 Weldments

The study of the aging characteristics of X7106 weldments consisted of a series of uniaxial tensile tests and hardness measurements of specimens cut from 0.090-inch sheet weldments. These tests and measurements were carried out after the specimens were allowed to age at room temperature for periods of time from one day to 24 weeks. The tensile tests were performed on groups of five specimens at each aging time.

The weldments employed in this study consisted of 12-inch x 18-inch panels welded by both the TIG and MIG processes. The panels were fabricated from two 6-inch x 18-inch sheets, utilizing the welding procedures designated

---

* The term "heat-affected zone" is used in this report to describe the zone of heat-affected base metal, adjacent to the fusion line, revealed by etching.

as 64A-6 through 64A-11 in Table I. The fixtures and equipment used in the fabrication of the bulge panels, as described in Section IIA, were also employed in the fabrication of the X7106 weldments.

The tensile test specimens were cut from these panels to provide a 1/2-inch wide test section with a 2-inch gage length and were prepared so that the welded joint was located at the center of the test specimen. The specimens were tested with the weld crown intact.

The specimens used for the hardness determination consisted of coupons cut from the welded panels so as to contain a portion of the welded joint. The weld crowns were ground flush with the surface and the surface was polished and etched. With this procedure the weld metal and heat-affected base metal, as revealed by etching, may be distinguished. Rockwell hardness measurements were then made in each of the respective zones.

D. Crack Susceptibility of X7106-T63 Weldments

The study of the susceptibility of X7106-T63 alloy to cracking during welding was carried out utilizing a test as described by Houldcroft(1). This test is based on a bead-on-plate weld made on the center line of a specimen designed so as to provide a varying degree of restraint along the length of the weld. This specimen, illustrated in Figure 4, consists of a 3-inch x 1-3/4-inch coupon with slots of varying depths machined along each edge. The degree of restraint is highest near the beginning of the weld; thus, any crack produced will start at this end of the specimen and propagate in the direction of welding. The length of the crack thus formed is considered to be a measure of the susceptibility of the material to hot cracking during welding.

In this study, Houldcroft tests were performed on 0.090-inch thick specimens of X7106-T63 alloy welded with X5180, 5356 and 5556 filler metal. In addition, similar tests were carried out on specimens of 2219-T87 alloy welded with 2319 filler wire. The tests on this second alloy served as a basis of comparison for the results of this test series. Six specimens were tested for each base material/filler metal combination.

All of the welds made in this series of tests were made by the TIG process, employing the procedures designated as 65A-12 through 65A-15 in Table I. The individual parameters were selected so as to provide a full-penetration weld and to produce a weld crown of suitable width. The wire feed rate of 24 ipm was chosen as a value intermediate between the low feed rates, which were conducive to extensive cracking, and the higher rates, which prevented crack propagation beyond a few tenths of an inch. The test setup employed in this study is shown in Figure 5. During the welding operation, the specimen was clamped to a carbon block with a clamping pressure just sufficient to prevent motion during the welding operation. After welding, the length of the crack formed was measured with the aid of a fluorescent

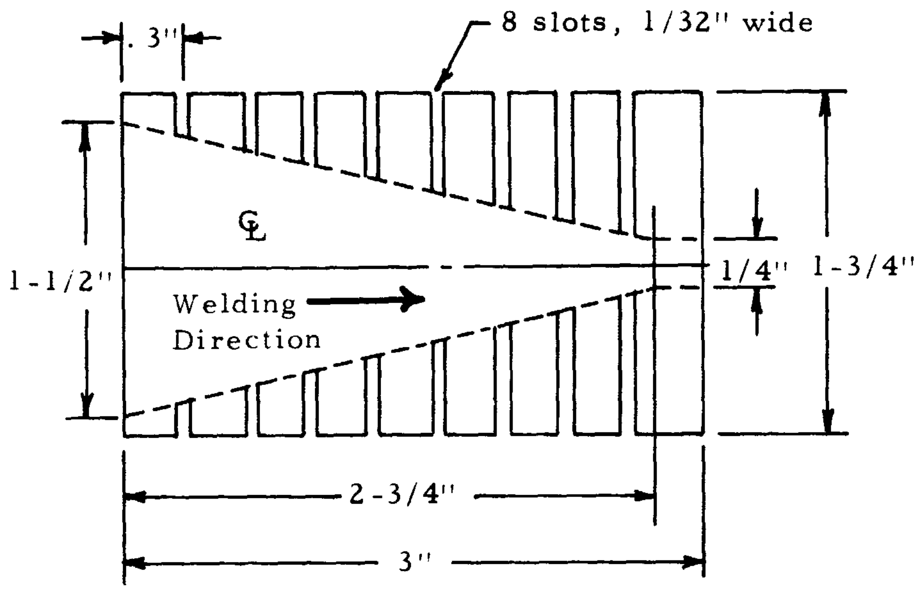

FIGURE 4. HOULDCROFT TEST SPECIMEN

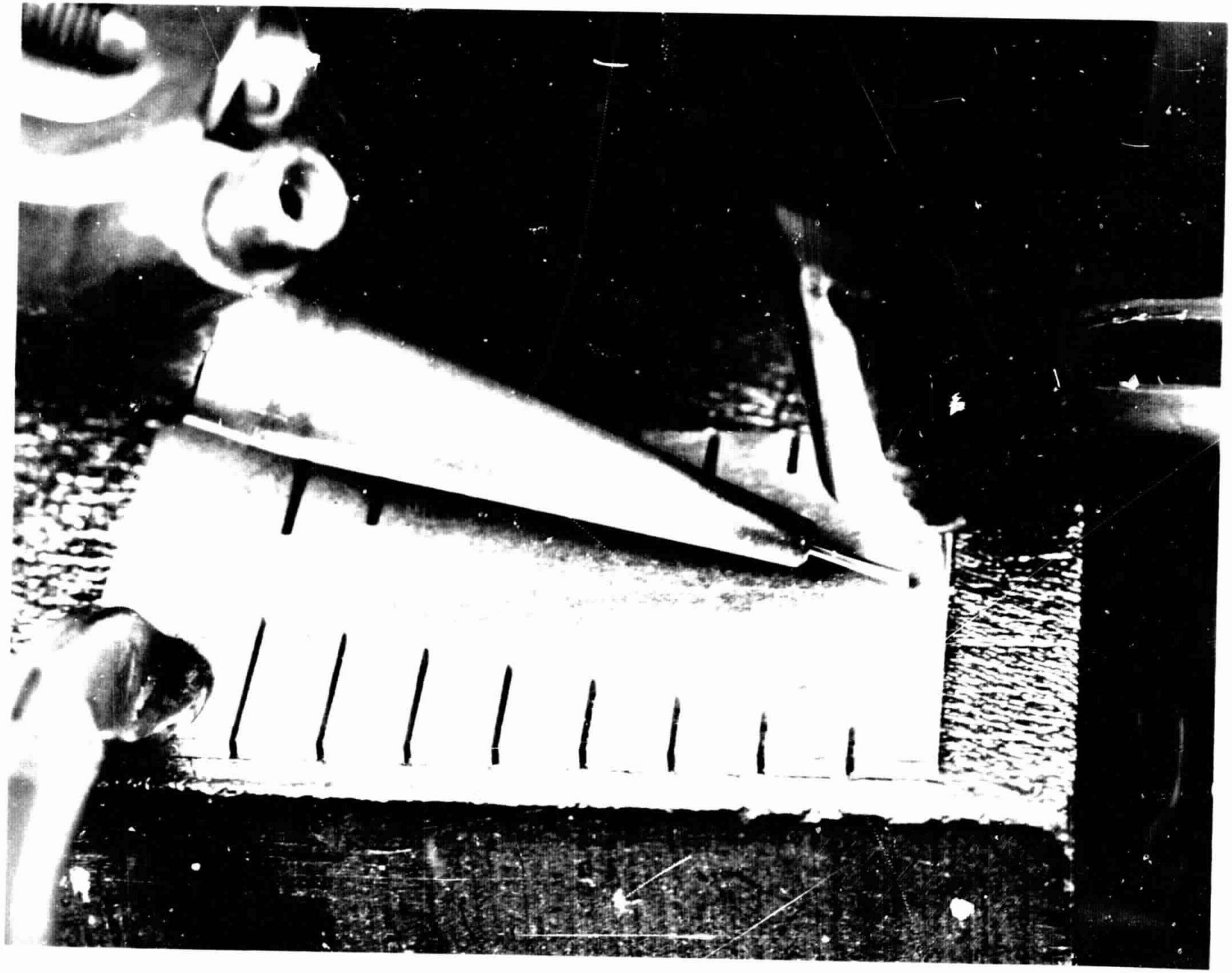

1-1/2X

FIGURE 5. SETUP FOR WELDING HOULDCROFT CRACK TEST SPECIMEN

dye penetrant. A typical welded specimen, with the crack length indicated, is shown in Figure 6.

E. Temperature Distribution Near Welded Joints

For the purpose of investigating the distribution of maximum temperatures encountered in the vicinity of welded joints, two special 0.090-inch thick welded panels were fabricated, one by the MIG process and one by the TIG process. Prior to welding, temperature indicating crayon marks were applied to the panels. The marks were oriented perpendicular to the direction of welding and extended several inches on either side of the joint. Tempilstik crayons, designated for the indication of 700, 600, 500, 400 and 300°F, were employed. The welds were then made, employing the procedures previously established for this study. After welding, the surface was cleaned and etched to reveal the fusion line. The extent to which each crayon mark had melted, relative to the fusion line of the weld, was then measured. The width of the heat-affected base metal, as revealed by etching, was also measured at the location of each respective crayon mark. The measurements made in this experiment are depicted in Figure 7.

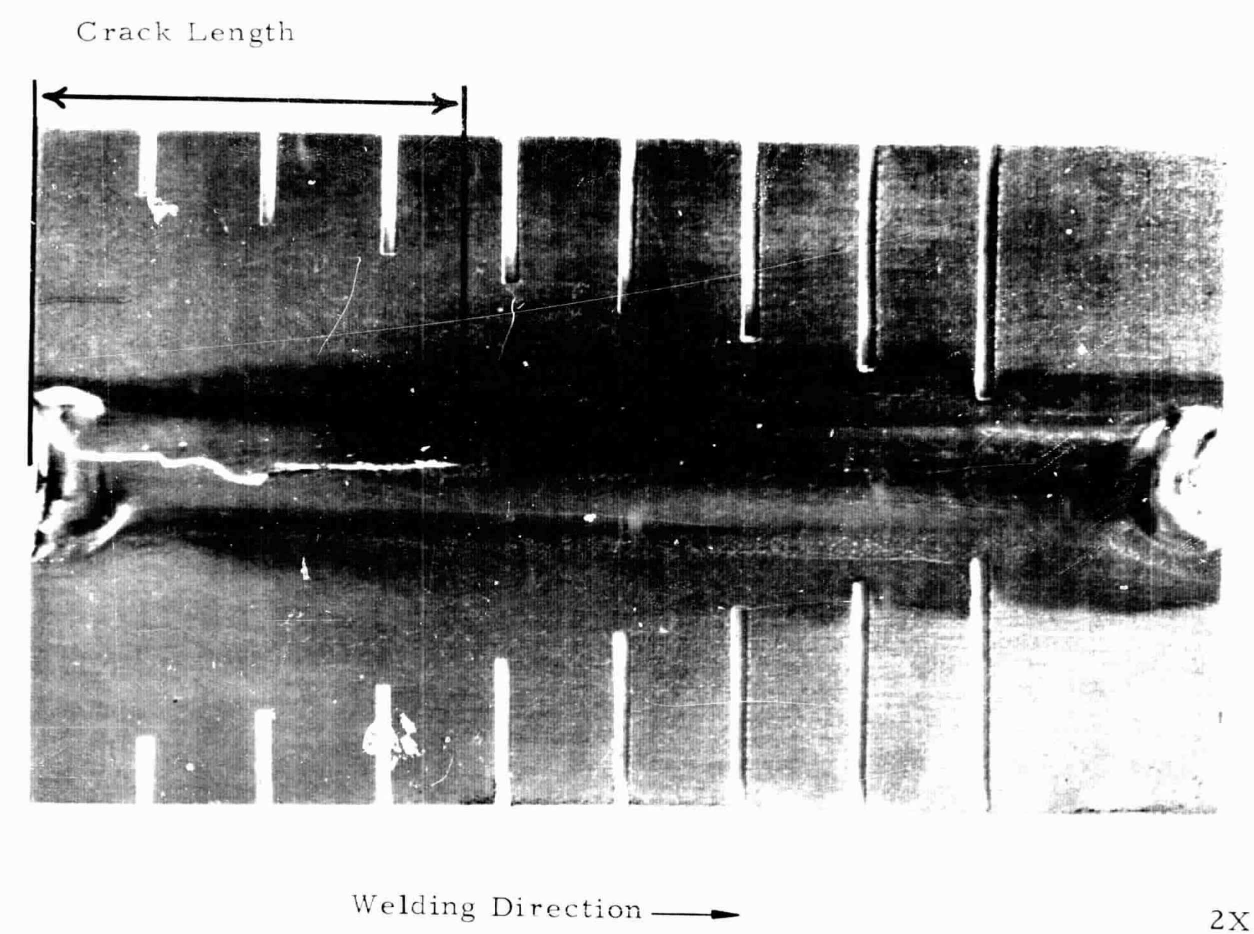

FIGURE 6. HOULDCROFT SPECIMEN AFTER COMPLETION OF TEST. Crack length indicated by fluorescent dye penetrant.

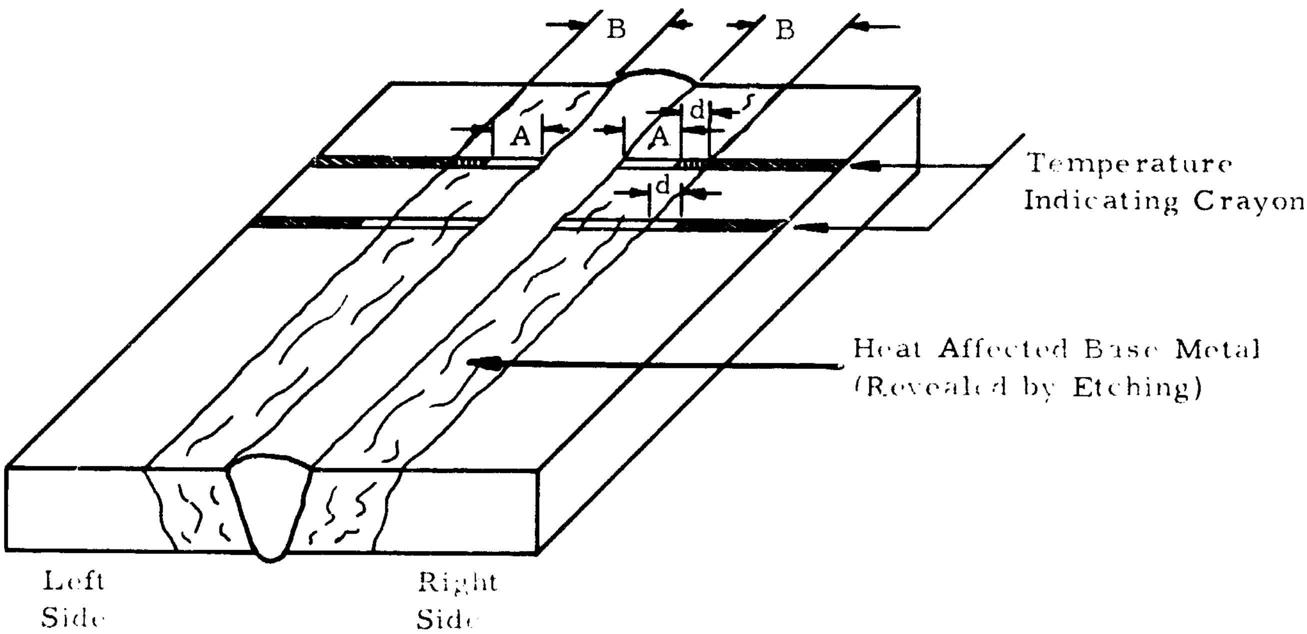

A = Extent of melted crayon
B = Extent of heat affected base metal at crayon location
d = A-B

FIGURE 7. SCHEMATIC ILLUSTRATION OF TECHNIQUE EMPLOYED FOR MEASUREMENT OF TEMPERATURE DISTRIBUTION IN VICINITY OF WELDED JOINT

III. RESULTS AND DISCUSSION

Part 1. Evaluation of Welding Processes for 2219-T87 and 2014-T6 Aluminum Alloys

A. Biaxial and Uniaxial Properties of MIG and TIG Weldments

The results of the individual bulge tests and uniaxial tensile tests conducted in the course of this program are tabulated in Appendix A (Tables A-I and A-II). The typical appearance of the various types of panels, after testing, is shown in Figures 8 through 11. In these figures, the marked difference in bulge heights between the parent metal and welded panels is evident. A summary of the average mechanical properties of the panels tested in the welding process evaluation program is given in Table IV.

In Table A-I and Table IV the biaxial ultimate strength is reported as the membrane stress at the time of failure, calculated from the equation:

$$\sigma = \frac{P \times R}{2t}$$

Where:

σ = membrane stress, psi
P = hydraulic pressure, psi
R = radius of curvature, inches
t = panel thickness, inches

In each case, the radius of curvature R was determined from the bulge height, assuming the bulged portion of the panel to be a segment of a sphere at failure. The applicability of the membrane stress formula to the determination of the biaxial ultimate strength is discussed further in Section III, Part 1-C and Appendix B.

All uniaxial tensile test specimens were cut from one end of a test panel and each specimen contained a portion of a single weld in the test section. Thus, there is no basic difference in the tensile test specimens cut from the three types of weld configuration (single, tee or cross). As a result, the mechanical properties measured in tests of all tensile specimens cut from the three weld configurations for each type of weldment were considered as a group for the purpose of computing the mean values and standard deviations listed in Table IV and V.

As may be noted in Table A-I, the values of biaxial and uniaxial ultimate strength determined from bulge tests and tensile tests exhibited considerable scatter. The degree of scatter is indicated by the standard deviations listed in Table V.

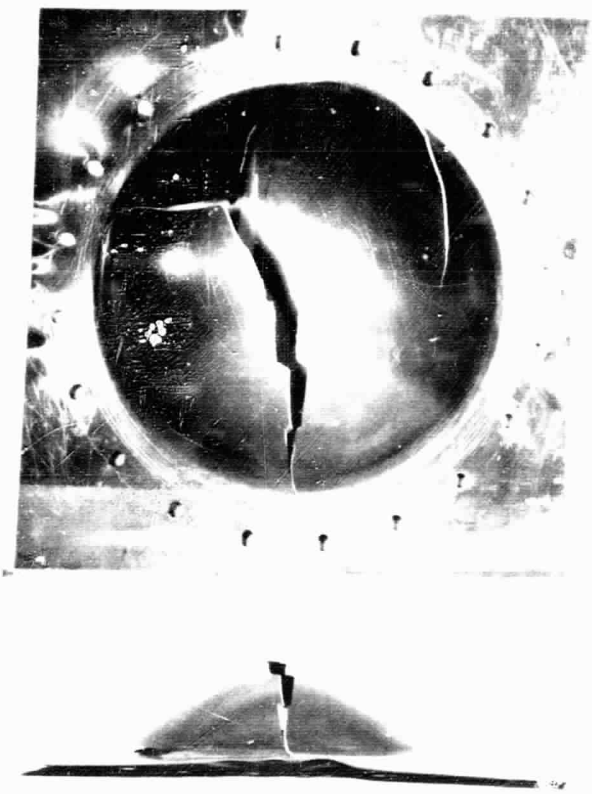

FIGURE 8. BULGE CONTOUR AND FRACTURE PATTERN OF 2014-T6 BASE METAL PANEL

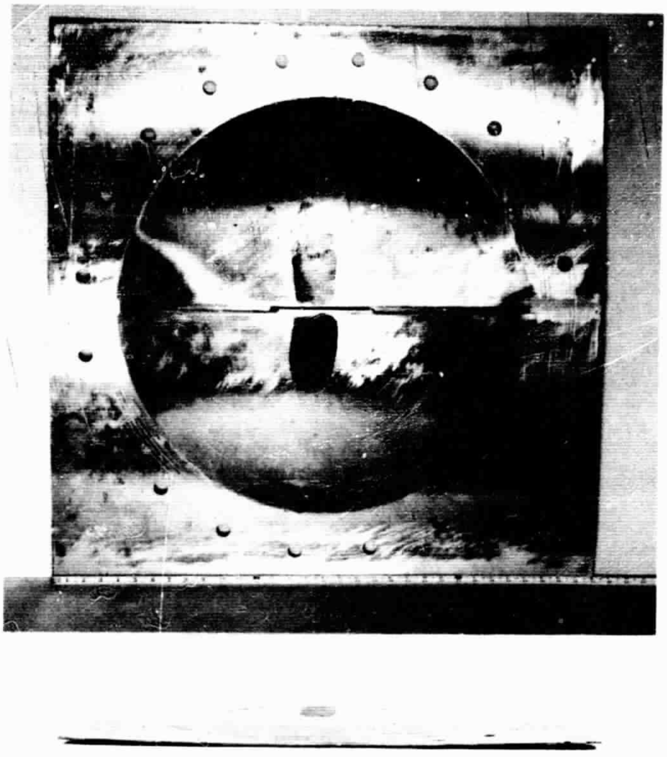

FIGURE 9. BULGE CONTOUR AND FRACTURE PATTERN OF PANEL CONTAINING SINGLE WELD

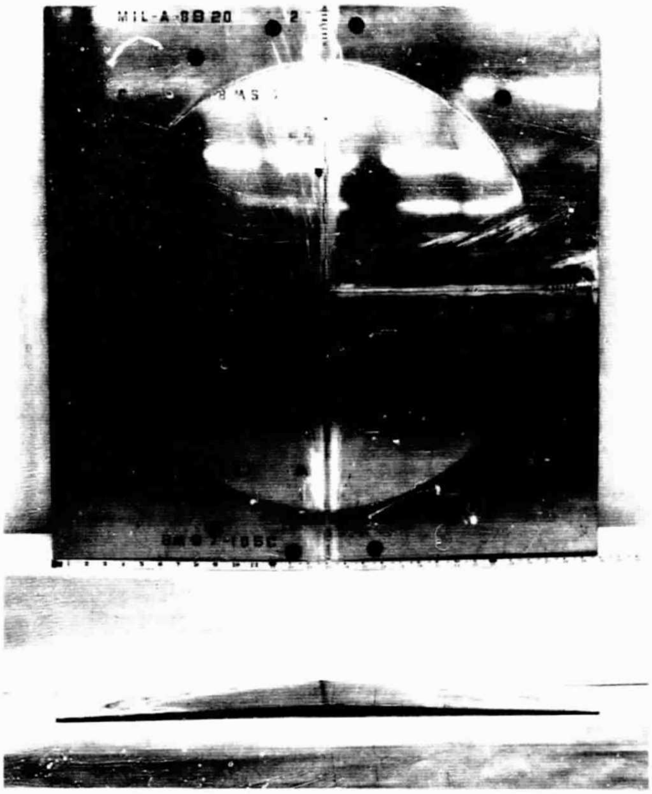

FIGURE 10. BULGE CONTOUR AND FRACTURE PATTERN OF PANEL CONTAINING TEE WELD

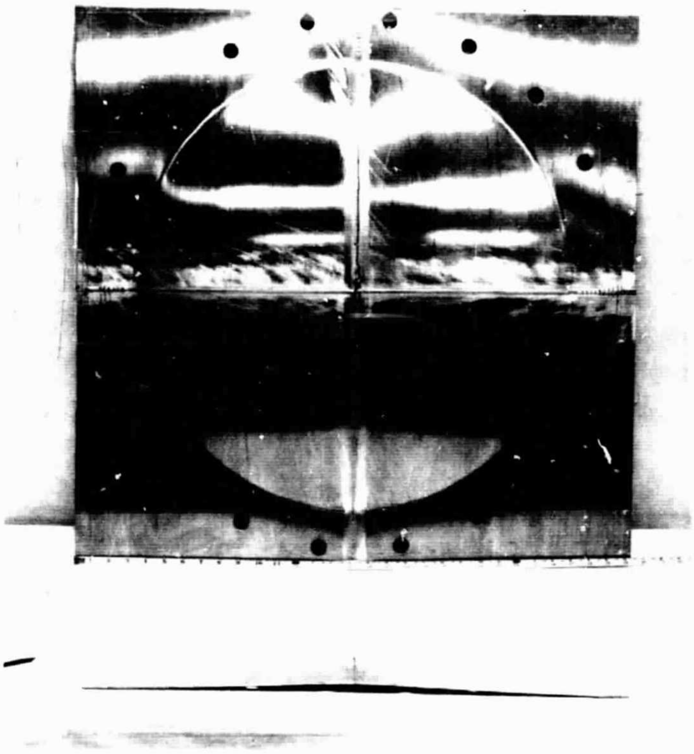

FIGURE 11. BULGE CONTOUR AND FRACTURE PATTERN OF PANEL CONTAINING CROSS WELD

TABLE IV

SUMMARY OF THE HYDRAULIC BULGE TEST AND UNIAXIAL TENSILE TEST DATA FOR VARIOUS WELD CONFIGURATIONS

Weld Configu-ration	Materials & Welding Process	Average Bulge Data				Average Uniaxial Tensile Data[1]				Biaxial / Uniaxial
		No. of Tests	Maximum Height (In.)	Maximum Pressure (psi)	Biaxial Ultimate (ksi)	No. of Tests	U. T. S. (ksi)	0.2% Y. S. (ksi)	Elongation % in 2 In.	
□	2014-T6 (Base Metal)	3	4.35	1130	77.1	10	70.8	65.0	11.2	1.09
□	2219-T87 "	3	4.20	993	70.5	10	66.8	54.9	10.9	1.06
⊟	MIG 2014-T6/4043	3	1.28	142	30.9	37	42.1	35.5	1.7	.73
⊞		3	1.36	170	35.2					.84
⊞		3	1.18	128	30.4					.72
⊟	TIG 2014-T6/4043	2	1.49	190	35.1	39	47.9	39.6	1.9	.73
⊞		3	1.45	184	34.9					.73
⊟		3	1.42	181	35.2					.74
⊟	TIG 2014-T6/2319	3	1.41	255	49.6	32	50.0	40.2	1.8	.99
⊞		3	1.29	204	44.1					.88
⊞		2	1.45	228	43.1					.86
⊟	MIG 2219-T87/2319	3	1.31	172	36.1	46	42.7	28.6	2.9	.85
⊞		3	1.43	193	37.3					.87
⊞		4	1.49	198	36.4					.85
⊞	TIG 2219-T87/2319	3	1.23	171	38.2	48	43.5	33.4	1.8	.88
⊞		3	1.49	182	33.7					.78
⊞		3	1.41	174	33.7					.78

(1) Average results from tests on specimens from all three weld configurations.

TABLE V

SUMMARY OF BIAXIAL AND UNIAXIAL ULTIMATE STRENGTHS FOR MIG AND TIG WELDMENTS

Weldment Type	Biaxial				Uniaxial				Biaxial/Uniaxial
	No. of Tests	Ultimate Strength (ksi)	Standard Deviation (ksi)	99% Lower Tolerance Limit(ksi)	No. of Tests	Ultimate Strength (ksi)	Standard Deviation (ksi)	99% Lower Tolerance Limit (ksi)	
MIG 2014-T6/4043	9	32.1	2.76	20.7	37	42.1	4.14	29.9	0.76
TIG 2014-T6/4043	8	35.0	1.86	27.0	39	47.9	4.74	33.9	0.73
TIG 2014-T6/2319	8	45.9	3.54	30.5	32	50.0	2.84	41.4	0.92
MIG 2219-T87/2319	10	36.6	2.33	27.3	46	42.7	1.91	37.2	0.86
TIG 2219-T87/2319	9	35.3	3.13	22.3	48	43.5	2.20	37.2	0.81

An examination of selected bulge panels and tensile specimens was conducted to ascertain whether or not the low values of biaxial and uniaxial ultimate strength correlated with any observable feature of particular specimens or panels. In this study, described in Appendix C, no significant variations in weld bead size or shape were noted among the three panels inspected. Certain variations in the size and shape of the weld beads in the uniaxial test specimens were noted but these variations are considered to be comparable to those which may be expected in production. Since no unusual variations in weld bead profile or other abnormal defects were noted, the observed differences in biaxial ultimate strength and uniaxial ultimate strength must be considered as inherent in the particular type of weldments tested and in the test procedures employed.

It was observed that the uniaxial mechanical properties of the 2014-T6/4043 weldments exhibited a higher degree of scatter than the other types (Table V). Such a result may be expected, since the strength of weldments made with 4043 filler wire depends upon alloying of the filler metal with the base metal and is thus subject to variation. In addition, 2014 alloy is widely recognized as exhibiting poor weldability, and the probability of low values of ultimate tensile strength for weldments of this alloy is higher than that for 2219 weldments. The results of the examination of the fractured panels and tensile specimens and the factors associated with the 2014-T6 weldments are such that discarding the results of any particular tensile test is not warranted.

The scatter in the values of biaxial ultimate strength is considered reasonable in the light of the current status of the interpretation of the bulge test data. At this state of the development, some uncertainty exists in the determination of the biaxial ultimate strength by means of the membrane stress equation (See Section III, Part 1-C and Appendix B). Thus, at the present time, the observed scatter must be considered as inherent in the bulge test.

The average biaxial ultimate strength for each weld type and configuration and the average uniaxial ultimate strength of each weldment type are plotted in Figure 12. In this figure, the standard deviations for the uniaxial tensile data and the range of results of the bulge tests are also indicated. This plot of the results illustrates that the indicated differences in biaxial ultimate strength for the different weld configurations are of the same order as the range of results for one type of configuration. Thus, these data do not show any significant difference in strength between the three weld configurations for any one type of weldment. On the basis of this observation, the results of the three types of weld configuration may be treated as a single group of data for each type of weldment.

The mean values of biaxial ultimate strength and uniaxial tensile strength for each type of weldment (computed from the results of all tests for a given process-filler metal combination) are listed in Table V and presented graphically in Figure 13. The standard deviations and lower tolerance limits are also included in Table V and Figure 13. The lower tolerance limit is computed as a 99% limit for a 95% confidence level (Appendix D).

The results of the tests on 2014-T6/4043 weldments indicate that for this material-filler metal combination the TIG process is superior to the MIG process. The TIG weldments exhibit a slightly higher mean uniaxial

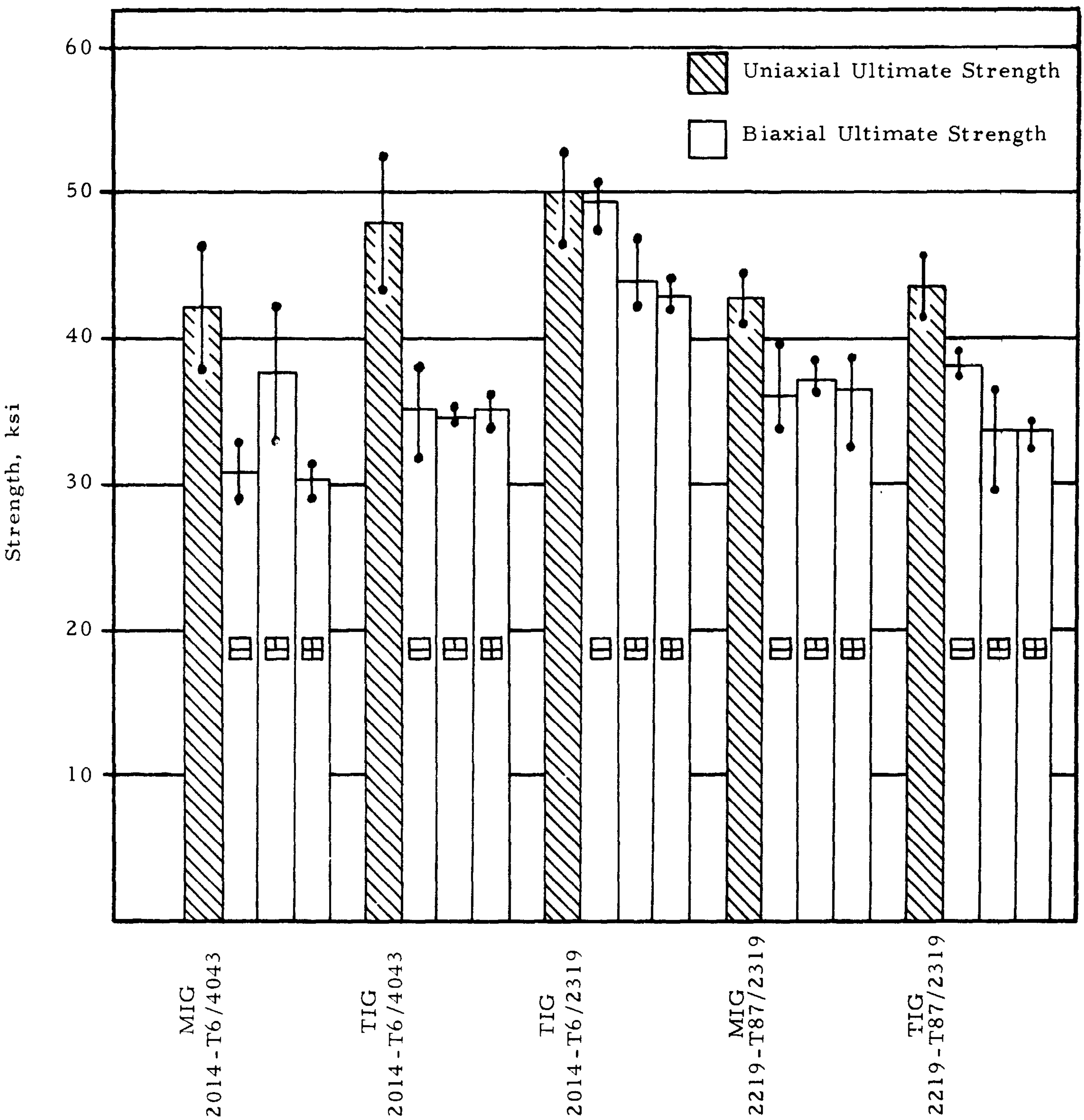

FIGURE 12. AVERAGE UNIAXIAL AND BIAXIAL ULTIMATE STRENGTHS FOR VARIOUS WELD CONFIGURATIONS

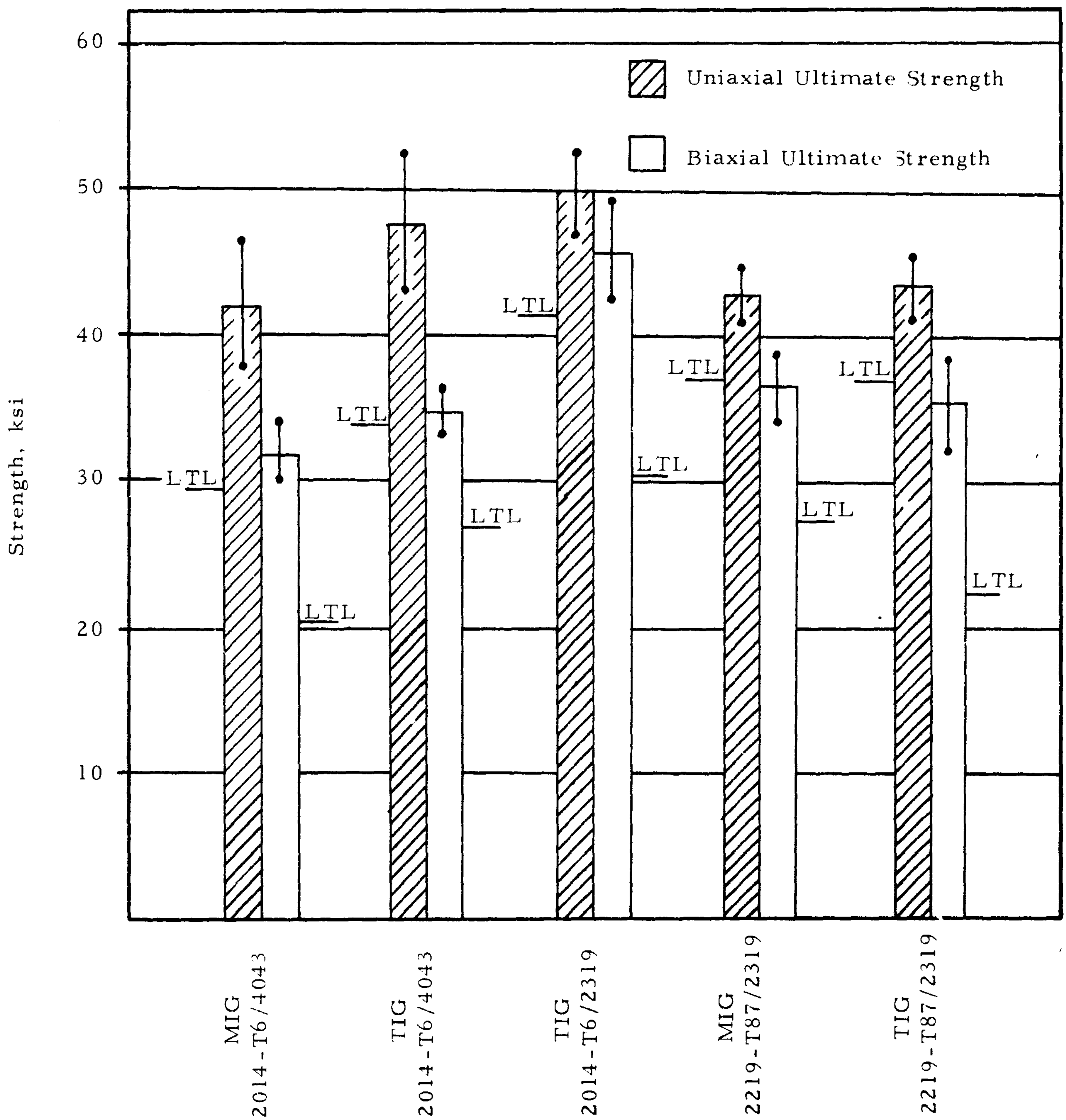

FIGURE 13. AVERAGE UNIAXIAL AND BIAXIAL ULTIMATE STRENGTHS FOR MIG AND TIG WELDMENTS

ultimate strength and a slightly higher mean biaxial ultimate strength than the MIG weldments. The biaxial and uniaxial lower tolerance limits of ultimate strength for the TIG weldments exceed those of the MIG weldments by 6.3 ksi and 2.7 ksi respectively. The TIG 2014-T6/2319 weldments exhibit a uniaxial ultimate strength comparable to that of the TIG 2014-T6/4043 weldments. The biaxial ultimate strength of the TIG 2014-T6/2319 panels is significantly higher than that of both of the MIG and TIG weldments employing 4043 filler metal. Both the biaxial and uniaxial lower tolerance limits indicate that the TIG weldments made with 2319 filler metal are superior to both TIG and MIG weldments made with 4043 filler wire. It should also be noted that the TIG 2014-T6/2319 weldments exhibit the highest biaxial to uniaxial strength ratios of all the weldments tested.

No significant differences were observed in the mean values of biaxial and uniaxial ultimate strengths for the MIG 2219-T87/2319 and TIG 2219-T87/2319 weldments. The uniaxial lower tolerance limits for these two types of weldments are also comparable. The results of the hydraulic bulge tests on the TIG 2219-T87/2319 weldments exhibited a higher degree of scatter than those for MIG 2219-T87/2319 weldments, see Table V and Figure 12. As a result, the lower tolerance limit of biaxial ultimate strength computed for the MIG 2219-T87/2319 weldments is significantly higher (5.0 ksi) than that of the TIG 2219-T87/2319 weldments.

The above comparison of the various weldments is based on the values of biaxial ultimate strength computed by means of the membrane stress formula. As a result, the conclusions drawn are subject to the limitations of the applicability of that formula (See Section III, Part 1-C and Appendix B).

B. Investigation of Biaxial to Uniaxial Strength Ratio

The results of the measurements of residual stresses in welded panels are given in Table VI. In general, the residual stresses in both TIG and MIG welds are roughly equal to the uniaxial yield stresses normally found for the weld metal, as would be expected. In most cases, the maximum principal stress was considerably larger than the minimum principal stress. In all cases, the maximum principal stresses were tensile stresses, oriented in a direction parallel to the length of the weld. Very often the minimum principal stress was observed to be compressive, probably resulting from the relatively high value of the maximum principal stress. Although the stress profile through the panel is unknown, in one case the stresses on the underside of the panel (as positioned during welding) were found to be about 4,000 psi less than those measured on the top of the panel. The residual stresses in the heat-affected base metal were, in general, roughly the same magnitude as in the weld metal and in the same direction.

Clamping stresses were observed to differ widely in value and in direction. Most of the clamping stresses measured were lower in magnitude than the residual welding stresses and in a direction perpendicular to the direction of the maximum residual welding stresses. The stresses calculated from the strain arising from reclamping the panels in the welding positioner

TABLE VI

RESULTS OF RESIDUAL STRESS MEASUREMENTS IN 1/8 INCH THICK, TIG AND MIG, 2219-T87/2319 WELDED PANELS

Panel No.	Location of Gages	Clamping Stress Maximum/Minimum/Direction(1) (ksi/ksi/Degrees) Strain Gage No.			Residual Stress Maximum/Minimum/Direction(1) (ksi/ksi/Degrees) Strain Gage No.		
		No. 1	No. 2	No. 3	No. 1	No. 2	No. 3
2-SG	Weld	14.3/4.9/82°	15.9/7.8/90°	14.8/11.5/75°	- - - - -	14.6/-8.0/01°	3.5/-8.6/07°
3-SG	Weld	2.6/1.8/-65°	-0.3/0.1/-64°	- - - - -	18.1/0.6/02°	19.8/-1.2/02°	- - - - -
	Heat Affected						
	Base Metal	- - - - -	1.6/0.8/90°	- - - - -	- - - - -	16.9/-0.6/00°	- - - - -
4-SG	Weld	18.3/14.5/77°	22.2/7.1/-85°	4.8/2.8/-86°	13.0/2.9/00°	12.5/2.8/06°	20.1/5.1/02°
5-SG	Weld	-1.2/0.3/33°	1.9/1.6/61°	-1.2/0.6/29°	15.5/5.5/03°	16.6/7.1/08°	21.2/4.7/07°
	Heat Affected						
	Base Metal	- - - - -	0.5/0.5/0°	- - - - -	- - - - -	-19.5/8.2/90°	- - - - -
6-SG	Weld	-1.4/-0.1/-14°	1.6/0/17°	-2.8/0.4/-26°	18.9/-17.4/14°	18.2/-2.2/05°	22.3/0.3/01°
7-SG	Weld	2.9/-1.2/90°	3.8/-1.2/-75°	2.9/-2.7/-86°	15.2/-4.8/0°	12.5/-2.7/05°	18.3/2.5/08°
	Heat Affected						
	Base Metal	- - - - -	7.3/2.3/90°	- - - - -	- - - - -	14.5/-10.6/0°	- - - - -

(1) Maximum refers to maximum principal stress.
Minimum refers to minimum principal stress.
Direction refers to direction of the maximum principal stress in relation to the center-line of the weld. Center-line of the weld is zero.

Note: Minus sign "-" refers to compressive stress. No sign means tensile stress.

(Panels 2 S.G. and 4 S.G.) were considerably higher than the stresses determined from the strain occurring on release of the positioner clamps (Panels 3 S.G., 5 S.G., 6 S.G. and 7 S.G.).

One additional set of measurements was made to determine the magnitude of the residual stresses in base metal plates prior to welding. These measurements were made on a 1/8-inch x 16-inch x 16-inch panel employing a three-gage rosette mounted at the center of the panel. The residual stresses in the panel were found to be less than 2.0 ksi. Stresses of this magnitude are not considered to be significant relative to the residual stresses measured for welded panels.

The measurements of residual stresses and the significance of such measurements are discussed further in Appendix E.

The results of the individual bulge tests and uniaxial tensile tests conducted to investigate the factors influencing the biaxial to uniaxial strength ratio are tabulated in Appendix A (Tables A-III and A-IV) and a summary of the average mechanical properties determined in these tests is given in Table VII. The average results of tests on the TIG-2219-T87/2319 weldments (bulge test panels BP7, BP8 and BP9) from the welding process evaluation program are included in Table VII to serve as a basis of comparison.

It may be noted in Table VII that the biaxial to uniaxial strength ratios for all the welded panels (annealed, multipass and crowns removed) were less than one (0.84 to 0.88) and comparable in magnitude to that of the as-welded panels. These results indicate that neither the residual stresses arising from the welding operation nor the stress concentration associated with the weld crowns influences the biaxial to uniaxial strength ratio. The tests on the annealed 2219 base metal panels resulted in a biaxial to uniaxial strength ratio of 0.89 in contrast to a value of 1.06 measured for 2219-T87 panels (See Table IV).

It should also be noted that the mechanical properties of the annealed weldment and annealed base metal panel are comparable, and are significantly lower than those of the as-welded panels. The biaxial and uniaxial strengths measured for the multipass weldments are comparable to those of the panels welded with a single pass. The panels tested with weld crown removed exhibited a lower strength (both uniaxial and biaxial) than the as-welded panel but were significantly stronger than either of the annealed panels.

As in the case of the welding process evaluation, the above conclusions are subject to the limitations inherent in the application of the membrane stress formula to the determination of the biaxial ultimate strength from bulge test results (See Section III, Part 1-C and Appendix B).

TABLE VII

RESULTS OF HYDRAULIC BULGE TESTS AND UNIAXIAL TENSILE TESTS RUN TO STUDY BIAXIAL/UNIAXIAL STRENGTH RATIO

Panel Description	Average Bulge Test Data				Average Uniaxial Tensile Data				
	No. of Tests	Bulge Height (Inches)	Max. Press. (psi)	Biaxial U.S. (ksi)	No. of Tests	U.S. (ksi)	Y.S. 0.2% Offset (ksi)	Elong.% in 2 Inches	Biaxial Ult. / Uniaxial Ult.
TIG 2219-T87/ 2319 Single weld As-welded	3	1.23	171	38.5	18	43.7	35.1	1.8	.88
2219-T87 Base Metal Annealed	3	7.53	481	24.3	5	27.2	13.6	22.3	.89
TIG 2219-T87/ 2319 Single weld Annealed	3	5.62	449	23.3	15	27.6	13.2	19.3	.84
TIG 2219-T87/ 2319 Single weld Weld Crowns Removed	3	1.31	165	34.9	15	39.8	26.8	3.2	.88
TIG 2219-T87/ 2319 Single weld Multipass	3	1.57	217	37.8	14	45.2	28.0	3.2	.84

C. Interpretation of Bulge Test Results

The membrane stress formula, as given in Section III, Part 1-A, is derived for a thin sheet formed into a spherical section by hydrostatic pressure. Thus this formula is strictly applicable to the bulge test only in those cases which result in a spherical bulge. In the course of the bulge test program, it was observed that all of the welded panels failed at very low bulge heights, giving rise to doubt as to whether or not such bulged sections were near spherical. In order to check this point, measurements of the shape of the bulge section were made on one annealed base metal panel and one as-welded 2219-T87 panel. In addition, the strain in the base metal of a welded panel was measured as a function of bulge pressure.

This study, described in detail in Appendix B, revealed that the bulged section of both panels deviated from a true spherical section. This deviation was more pronounced in the welded panel (at a low bulge height) than in the case of the base metal panel.

The stresses in the welded panel as determined from the strain measurements, the membrane formula and the formula given by Timoshenko [2] for a uniformly loaded, circular, flat plate (See Appendix B) were compared. This comparison indicated that, in this case, the flat plate formula gives a better estimate of the stress than does the membrane formula. The observation of this limited study points out that further investigation is necessary for the proper interpretation of bulge test data. Such an investigation will require instrumented bulge tests to provide the information necessary to establish the relationship between biaxial ultimate strength and the parameters involved in the bulge test.

At the present stage of development some uncertainty exists as to the applicability of the membrane stress formula to the hydraulic bulge test. However, only very limited data exists as to the suitability of any other formula for this application. It is felt that the use of any of the available formulae is satisfactory for comparative purposes, even though these formulae may not give the correct absolute value of biaxial strength. As a result, the data from the current bulge test series have been analyzed on the basis of the membrane stress formula. It must be emphasized that the conclusions drawn from the analysis are subject to the applicability of the membrane formula. In the event that further investigation provides a stress formula more suitable to the bulge test, the data from this program should be re-evaluated.

III. RESULTS AND DISCUSSION

Part 2. Weldability of X7106-T63 Aluminum Alloy

A. Literature Survey and Plant Visits

A survey of the literature pertaining to the 7000-series aluminum alloys was conducted and visits were made to several industrial plants and laboratories with experience in the manufacture and fabrication of X7106 and similar alloys. These surveys were made to consolidate all available information related to the weldability of X7106 prior to the initiation of a detailed laboratory investigation. The results of the literature survey and the plant visits are summarized in Appendix F.

B. Mechanical Properties and Microstructure of X7106-T63 Parent Metal

The results of the individual uniaxial tensile tests conducted to establish the mechanical properties of X7106-T63 base material are tabulated in Appendix A, Table A-V. The average properties for each of the thicknesses tested are summarized in Table VIII and plotted in Figure 14. As may be noted in Table VIII and Figure 14, the 0.187-inch material exhibited the highest strength (longitudinal and transverse) of the four thicknesses, while the lowest values of ultimate strength were recorded for the 0.090-inch material. Three thicknesses (0.187 inch, 0.500 inch and 1.00 inch) exhibited higher properties in the longitudinal direction than in the transverse direction. In the case of the 0.090-inch material, however, the yield strength and ultimate strength in the transverse direction exceeded those in the longitudinal direction. The range of differences between the longitudinal and transverse ultimate strengths for specific thicknesses was from 0.6 to 2.6 ksi. A general increase in elongation at fracture with increasing thickness was observed. The average value of elongation noted ranged from 11.5 percent for the 0.090-inch material to 14.4 percent for the 1.00-inch material.

The microstructure of specimens of each of the four thicknesses was examined. The typical structures observed in longitudinal sections of the 0.090-inch material and the 1.00-inch material are shown in Figures 15 and 16. The 0.090-inch and 0.187-inch material exhibited similar structures, and the structures of the 0.500-inch and the 1.00-inch material were comparable. Pronounced elongation of the grains in the rolling direction was evident in all four thicknesses of material. The grain boundaries of the thicker plates, however, were not as clearly defined as those of the thinner plates. In the 0.090-inch and the 0.187-inch material the appearance of the grain boundaries at high magnification suggests that the grains are outlined by an intermetallic precipitate. Figure 15. No similar indications were noted in the structure of the thicker materials. Large, dark-etching constituents were present throughout the structure of all specimens examined.

TABLE VIII

SUMMARY OF MECHANICAL PROPERTIES OF
X7106-T63 PARENT METAL

Thickness (Inch)	Grain Direction	Yield Strength, ksi (0.2% Offset)	Ultimate Strength, ksi	Elongation % (2 Inches)	Hardness Rb
.090	Long.	54.0	59.9	11.5	79.5
	Trans.	55.7	62.5	10.5	
.187	Long	61.0	68.0	10.9	80.0
	Trans.	58.8	65.9	12.3	
.500	Long.	59.1	64.9	17.7	76.5
	Trans.	58.8	64.3	16.0	
1.00	Long.	58.3	64.4	20.7	74.5
	Trans.	56.1	62.0	19.4	

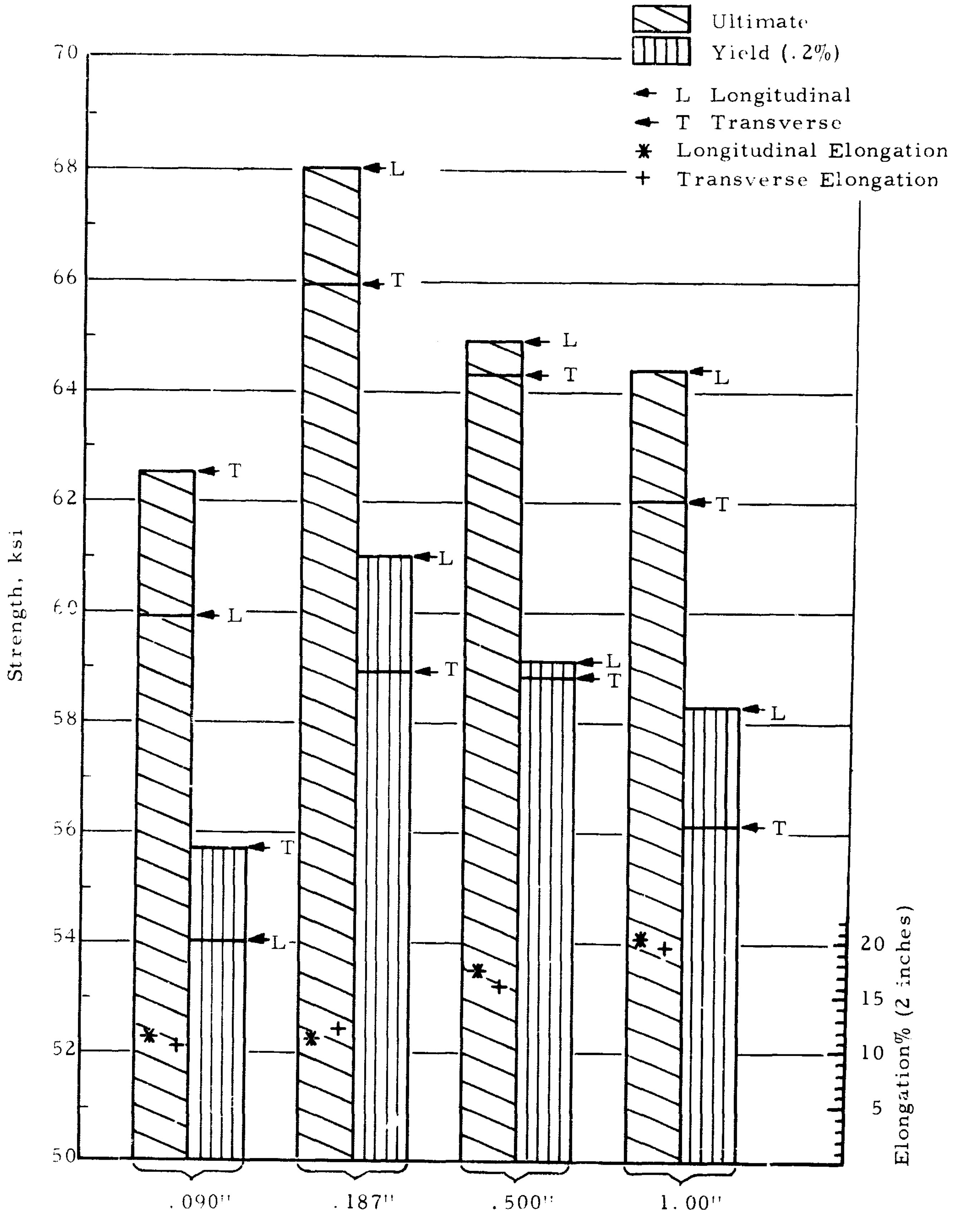

FIGURE 14. BAR GRAPH OF MECHANICAL PROPERTIES OF VARIOUS THICKNESSES OF X7106-T63

100X

Etchant-Keller's 1500X

FIGURE 15. MICROSTRUCTURE OF X7106-T63 .090 INCH SHEET

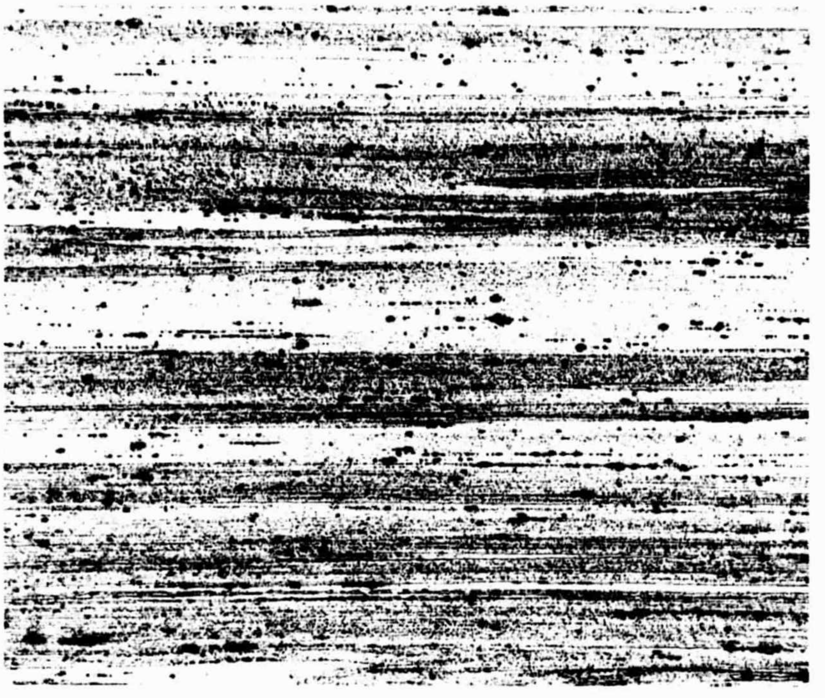

100X

Etchant-Keller's 1500X

FIGURE 16. MICROSTRUCTURE OF X7106-T63 1.00 INCH PLATE

C. Natural Aging Characteristics of X7106-T63 Weldments

The results of the individual tensile tests conducted to establish the natural aging characteristics of X7106-T63 aluminum alloy weldments are listed in Appendix A (Table A-VI). The average mechanical properties for both MIG and TIG weldments made with the three types of filler wire (X5180, 5356 and 5556) are summarized in Tables IX and X. These average properties of the weldments are plotted as a function of aging time in Figures 17 through 20. It may be noted in these figures that each type of weldment exhibits little or no increase in ultimate strength or yield strength beyond an aging time of twelve weeks. Thus a reliable comparison of the properties of these weldments may be made after an aging time of twelve weeks or longer.

The mechanical properties after an aging period of 24 weeks of all types of X7106 weldments included in this program are presented in Table XI. In this table, the standard deviation and the 99 percent lower tolerance limits (95 percent confidence) for the ultimate strengths and yield strengths are also listed. (See Appendix D for sample calculations.) These results are presented graphically in Figure 21.

This comparison of results shows that, as a group, the TIG weldments exhibited higher ultimate strengths than the MIG weldments (53.8 to 55.0 ksi as compared to 52.3 to 52.6 ksi). In addition to the higher average ultimate strength, the degree of scatter in the data was less for the TIG weldments than for the MIG weldments. As a result, the lower tolerance limits of ultimate strength for the TIG weldments are significantly higher than that of the MIG weldments.

The TIG/X5180 and TIG/5356 weldments exhibited slightly higher average yield strengths than the three MIG weldments, although the difference is not as significant as that noted in the ultimate strength. The average yield strength measured for the TIG/5556 weldments is comparable to those of the MIG weldments. The elongation at fracture of the TIG weldments was also noted to be slightly higher than that of the MIG weldments.

Within the group of three types of TIG weldments, those made with the 5556 filler wire exhibited a significantly lower ultimate strength than the other two types tested (3.8 ksi difference in LTL). No significant differences in ultimate strength were noted between the TIG/X5180 and TIG/5356 weldments. The average yield strength for the three types are comparable; however, the higher degree of scatter exhibited by the 5356 weldments resulted in a lower tolerance limit of yield strength significantly lower than those of the other two types of weldments. No significant differences in either yield strength, ultimate strength or elongation were noted between the three types of MIG weldments tested.

TABLE IX

SUMMARY OF AVERAGE MECHANICAL PROPERTIES OF 0.090 INCH TIG-X7106-T63 WELDMENTS

Filler Metal	Aging Time	No. of Tests	Yield Strength (0.2% Offset) ksi	Ultimate Strength ksi	Elong. in 2 in. %	% Failures in HAZ
X5180 (Panel A&B)	1 day	10	30.8	46.1	4.6	20
	1 week	10	36.0	50.6	4.2	60
	2 weeks	10	37.4	52.2	4.4	90
	4 weeks	10	38.2	52.9	4.8	90
	8 weeks	10	39.6	52.4	4.3	90
	12 weeks	5	40.9	54.7	4.7	80
	19 weeks	5	41.6	55.8	4.5	100
	24 weeks	10	41.1	54.9	5.0	90
5356 (Panel C)	1 day	5	29.2	44.6	4.7	20
	1 week	5	35.0	51.0	4.6	60
	2 weeks	5	36.3	51.5	4.5	60
	4 weeks	5	38.0	52.3	3.7	40
	8 weeks	5	38.7	52.7	4.4	60
	12 weeks	5	39.5	53.2	4.5	80
	24 weeks	5	40.6	55.0	5.9	80
5556 (Panel D)	1 day	5	33.2	45.4	4.1	100
	1 week	5	37.4	50.5	4.4	100
	2 weeks	5	37.8	52.0	4.0	60
	4 weeks	5	38.8	52.2	4.2	60
	8 weeks	5	38.7	52.0	4.4	60
	12 weeks	5	39.8	54.0	5.2	80
	24 weeks	5	39.1	53.8	4.8	80

TABLE X

SUMMARY OF AVERAGE MECHANICAL PROPERTIES
OF 0.090 INCH MIG-X7106-T63 WELDMENTS

Filler Metal	Aging Time	No. of Tests	Yield Strength (0.2% Offset) ksi	Ultimate Strength ksi	Elong. in 2 in. %	% Failures in HAZ
X5180 (Panel E)	1 day	5	31.9	46.5	4.7	100
	1 week	5	35.6	50.1	5.3	100
	2 weeks	5	37.0	50.5	4.5	60
	4 weeks	5	36.7	50.8	4.8	80
	8 weeks	5	38.0	52.1	4.9	100
	24 weeks	2	39.5	52.4	4.0	100
5356 (Panel F)	4 weeks	5	36.1	50.2	4.5	80
	24 weeks	5	38.7	52.6	4.1	60
5556 (Panel G)	4 weeks	5	36.3	49.5	4.5	80
	24 weeks	5	39.9	52.3	4.2	100

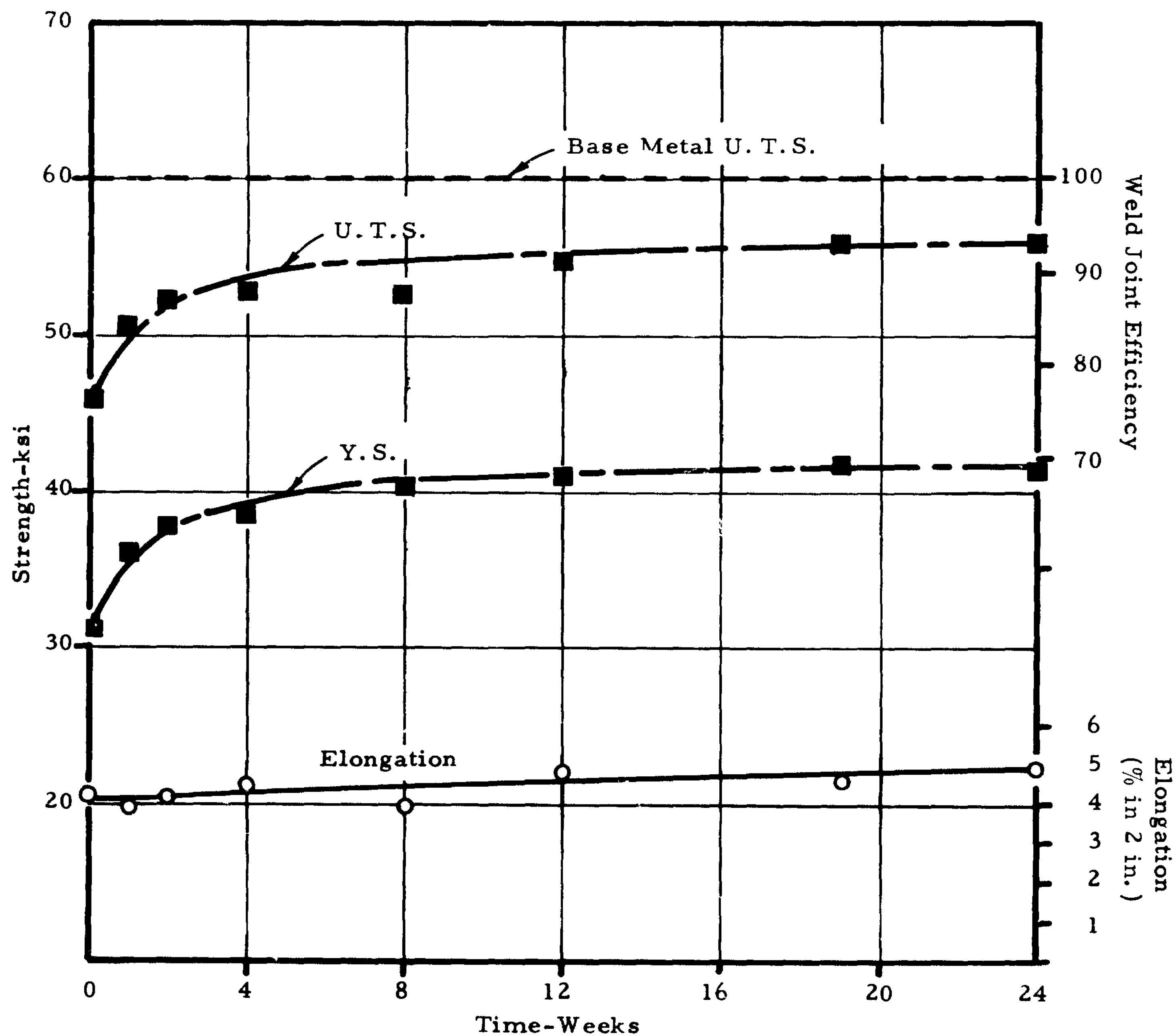

FIGURE 17. MECHANICAL PROPERTIES OF TIG-X7106/X5180 WELDMENTS

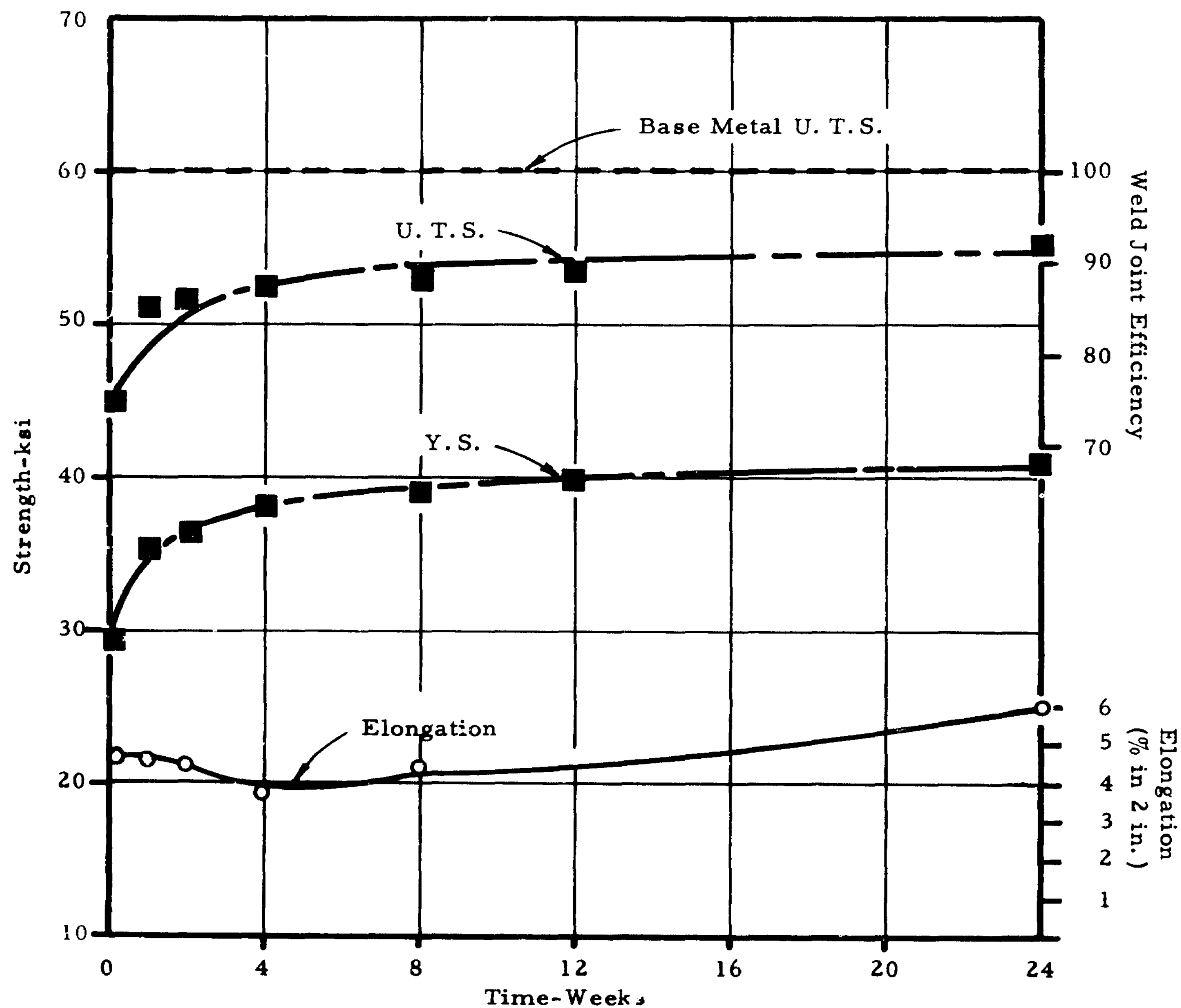

FIGURE 18. MECHANICAL PROPERTIES OF TIG-X7106/5356 WELDMENTS

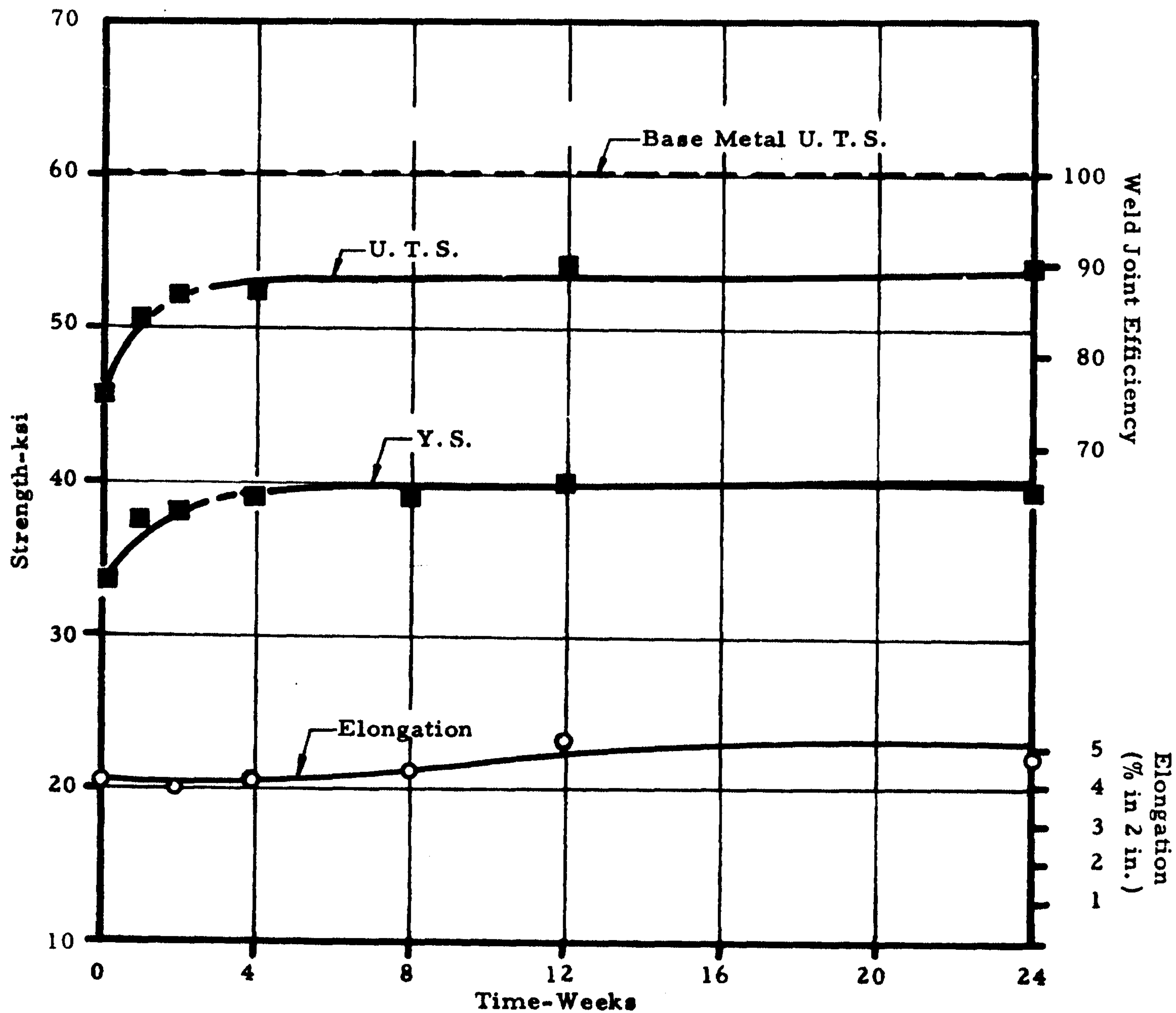

FIGURE 19. MECHANICAL PROPERTIES OF TIG-X7106/5556 WELDMENTS

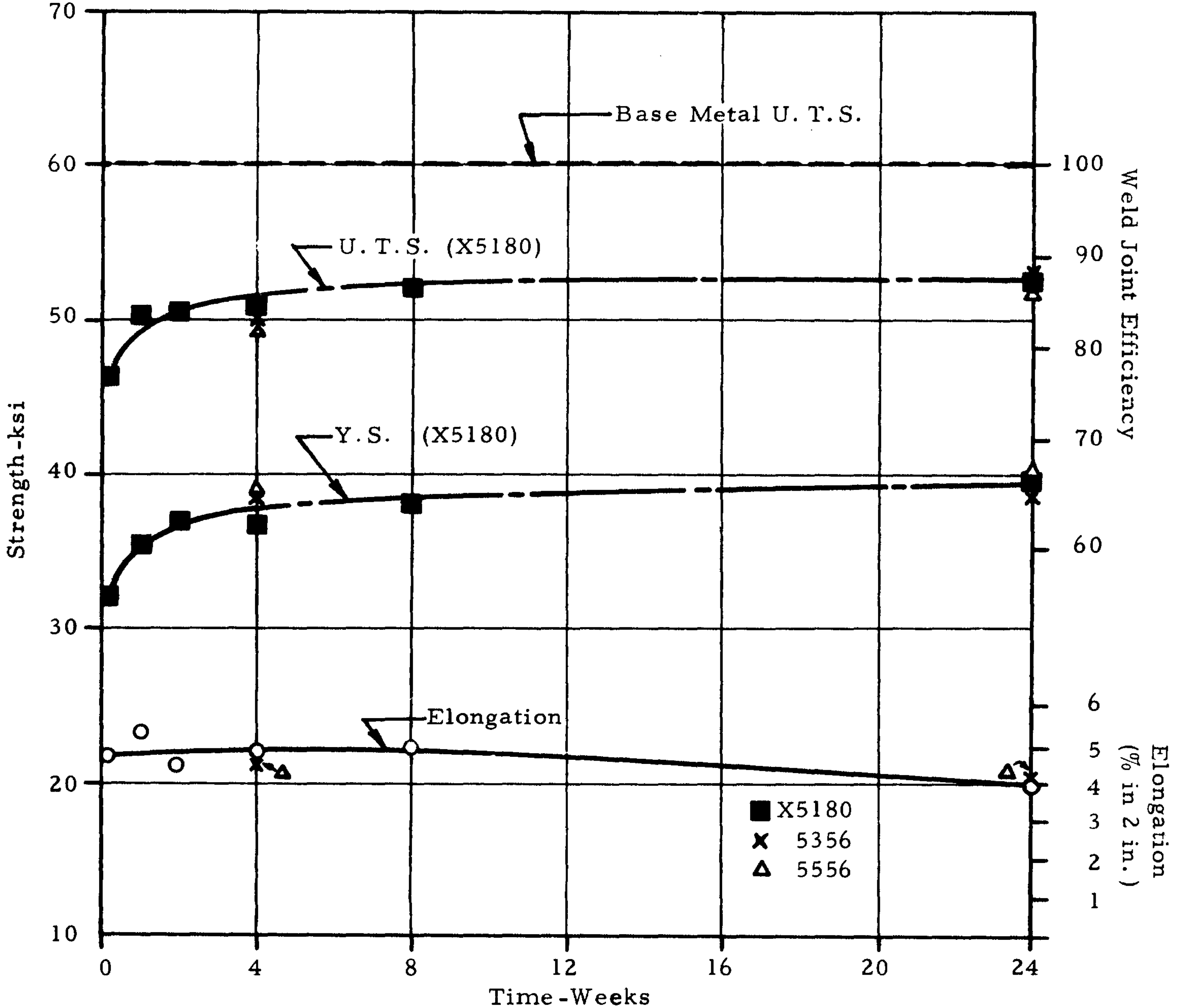

FIGURE 20. MECHANICAL PROPERTIES OF MIG X7106-T63 WELDMENTS

TABLE XI

SUMMARY OF MECHANICAL PROPERTIES OF X7106-T63 WELDMENTS AFTER 24 WEEKS NATURAL AGING

Process and Filler Metal	Yield Strength				Ultimate Strength				Elongation in 2 inches %
	No. of Tests	Avg. ksi	S_y (1) ksi	LTL ksi	No. of Tests	Avg. ksi	S_x (1) ksi	LTL ksi	
TIG/X5180	10	41.1	0.64	38.5	10	54.8	1.51	48.8	5.0
TIG/5356	5	40.6	0.96	35.1	5	55.0	0.37	52.9	5.9
TIG/5556	5	39.1	0.18	38.1	5	53.8	0.82	49.1	4.8
MIG/X5180	2	39.5	1 3 (2)	----	2	52.4	0.15 (2)	----	4.0
MIG/5356	5	38.7	1.26	31.5	5	52.6	0.96	47.1	4.1
MIG/5556	4	39.9	0.24 (2)	----	5	52.3	0.86	47.4	4.2

(1) S_x = Standard deviation, Ultimate Strength.

S_y = Standard deviation, Yield Strength.

(2) Insufficient number of test for determination of standard deviation. S_x and S_y reported as range of data above and below mean value.

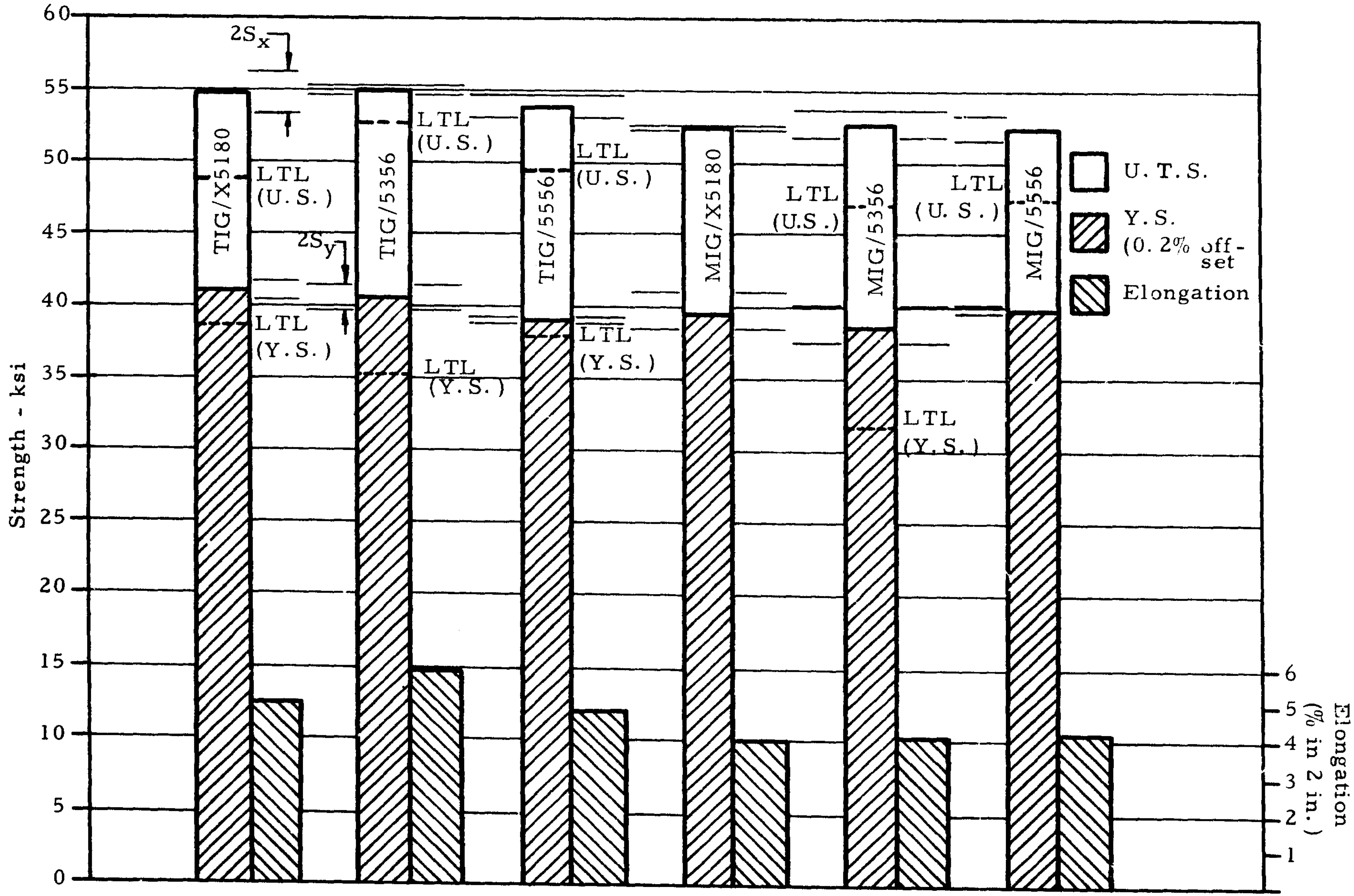

FIGURE 21. AVERAGE MECHANICAL PROPERTIES OF X7106-T63 WELDMENTS AGED 24 WEEKS

Of the six types of weldments included in the program, the TIG/X5180 weldments exhibited both the highest ultimate strength and the highest yield strength after 24 weeks aging. In addition, the average elongation recorded for this process-filler combination was either higher than, or comparable to, that of all other types.

For comparison purposes, the average tensile properties of the six types of X7106 weldments after four weeks aging are presented in Figure 22. It may be noted that, at this shorter aging time, the strength of the six weldment types exhibit the same general relationship as was noted for an aging time of 24 weeks.

In the course of the tensile tests conducted on the X7106 weldments, it was observed that all of the failures occurred at one of two locations; within the heat-affected zone or at the fusion line. Examples of failures at these two locations are shown in Figures 23 and 24. The location of the fracture in each individual tensile specimen is listed in Appendix A (Table A-IV) and the percentage of failures occurring in the heat-affected zone is indicated in Tables IX and X. It may be noted in Tables IX and X that in a large majority of the tests the failures occurred within the heat-affected zone. Only three sets of tests exhibited a predominance of fusion line failures; TIG/X5180 and TIG/5356 weldments aged one day and TIG/5356 weldments aged four weeks. It should be pointed out that X7106 is the only alloy tested in this program for which the strength of the weld deposit was not the limiting factor. Apparently, in this alloy, age hardening of the weld deposit brings about an increase in strength of the weld deposit which, combined with the reinforcement provided the weld crown, is sufficient to shift the fracture to the heat-affected base metal.

In the specimens which failed in the heat-affected zone, failures were located in a region between 0.08-inch and 0.32-inch from the fusion line. Cracks were frequently observed at the toes of the welds in these specimens. These cracks were found to extend along the fusion line.

The fractured edge of a heat-affected base metal failure is shown in Figure 25. The elongated grains are deformed near the fracture surface. At the higher magnification (500X, Figure 25b), the failure appears to be a mixture of transgranular and intergranular fracture.

The toes of the weld crown of one tensile specimen are shown in Figure 26 and are arbitrarily designated "A" and "B". The cast structure of the weld deposit and elongated grains of the heat-affected base metal are clearly distinguished. The arrow points to the toe region of the weld crown where a crack has occurredduring tensile testing. This crack is located along the line where the toe of the weld crown overlaps the heat-affected base metal. The crack at Toe "B" is smaller than that at Toe "A"

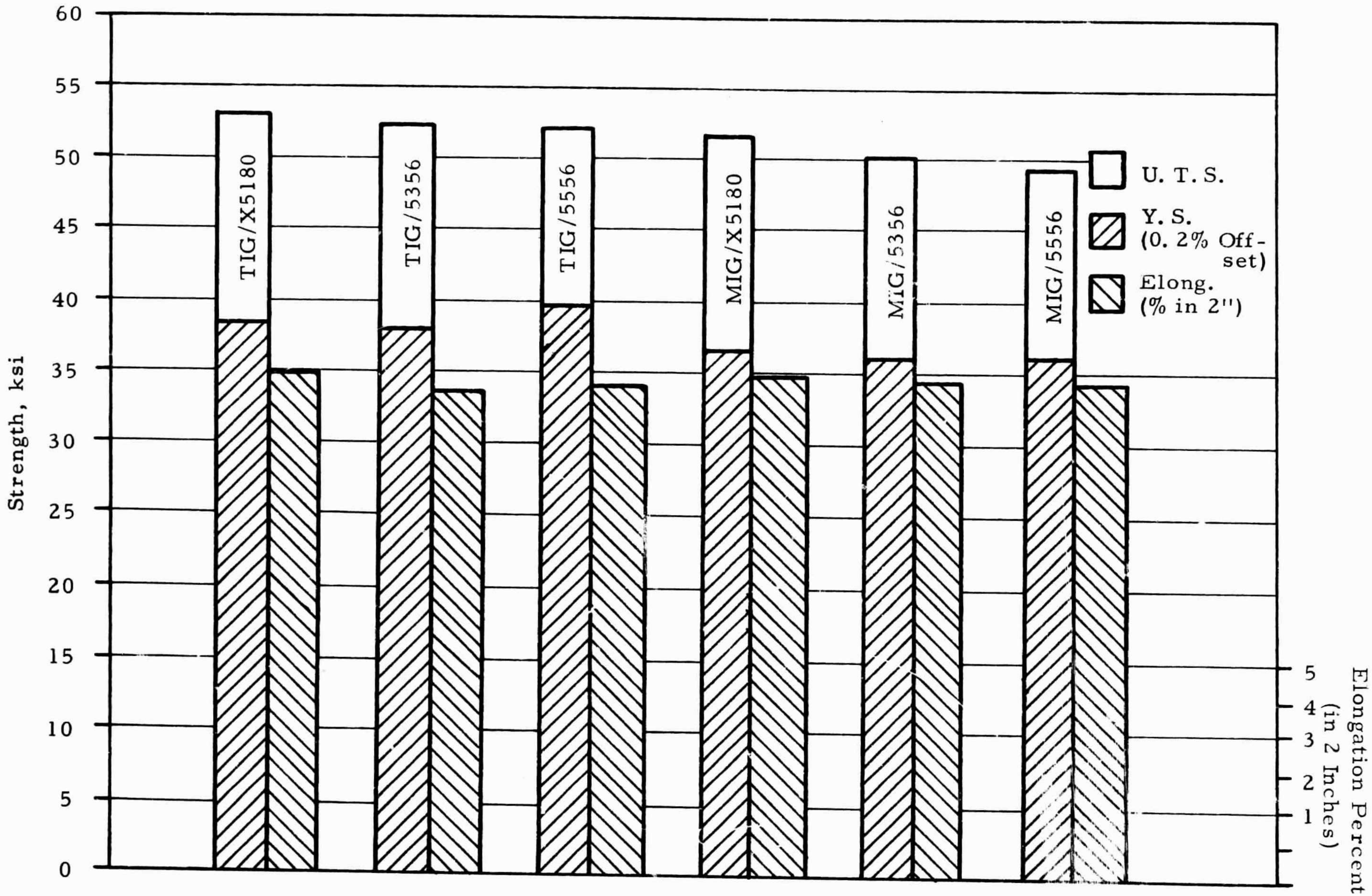

FIGURE 22. AVERAGE MECHANICAL PROPERTIES OF X7106-T63 WELDMENTS AGED 4 WEEKS

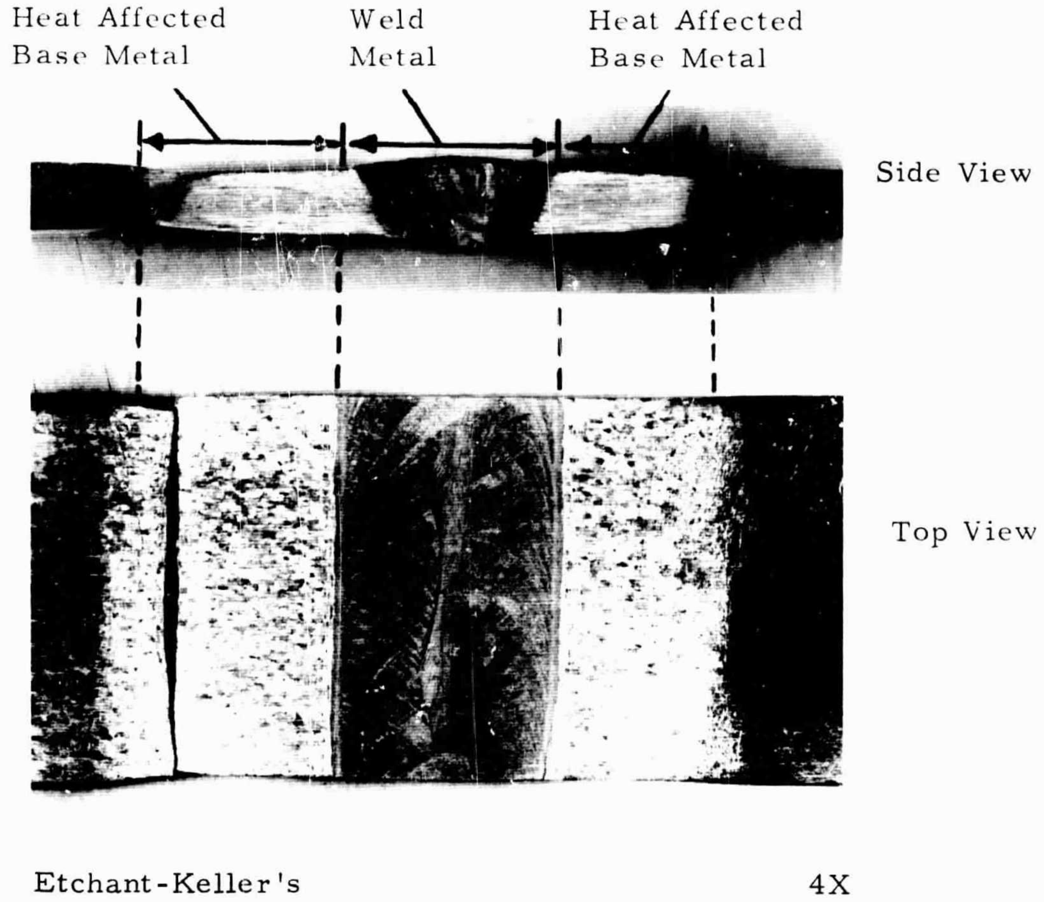

FIGURE 23. MIG X7106 TENSILE SPECIMEN. FAILURE LOCATED IN HEAT AFFECTED BASE METAL.

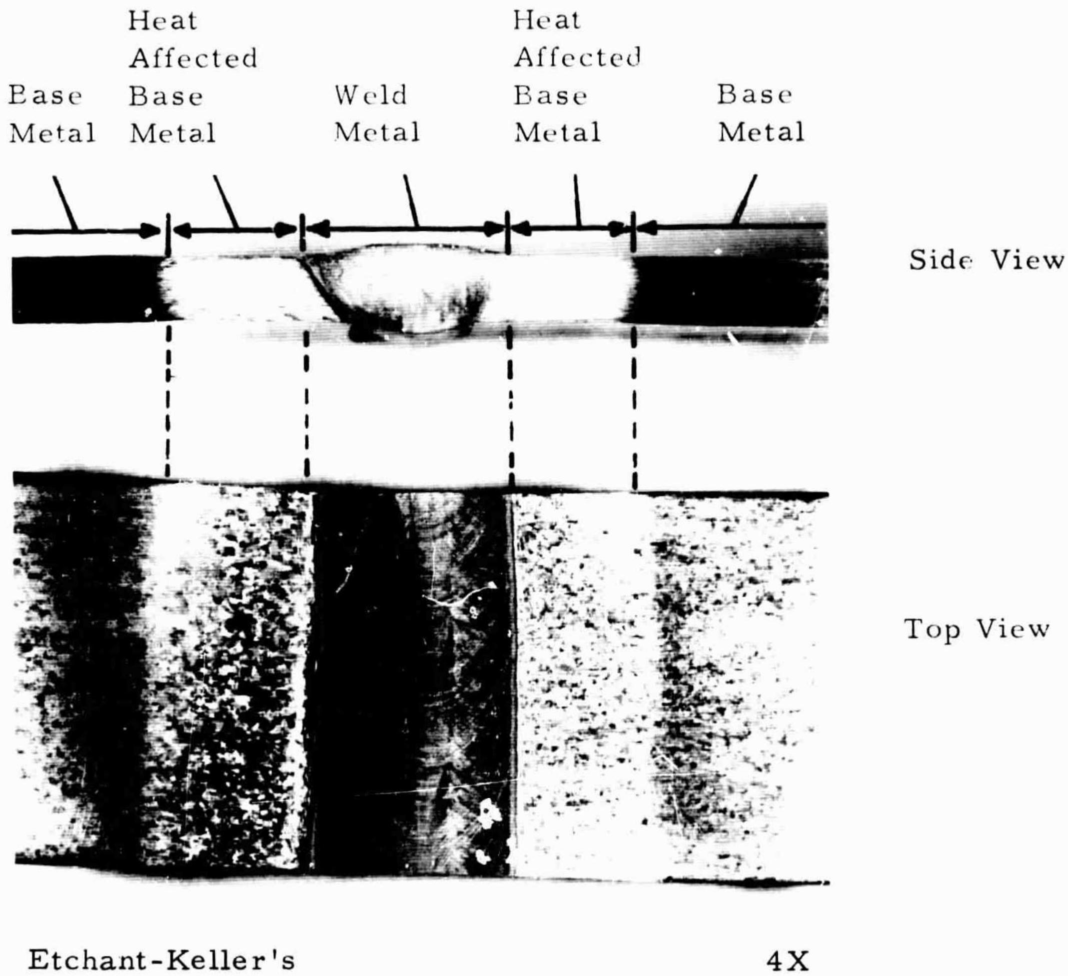

FIGURE 24. MIG X7106 TENSILE SPECIMEN. FAILURE LOCATED AT FUSION LINE.

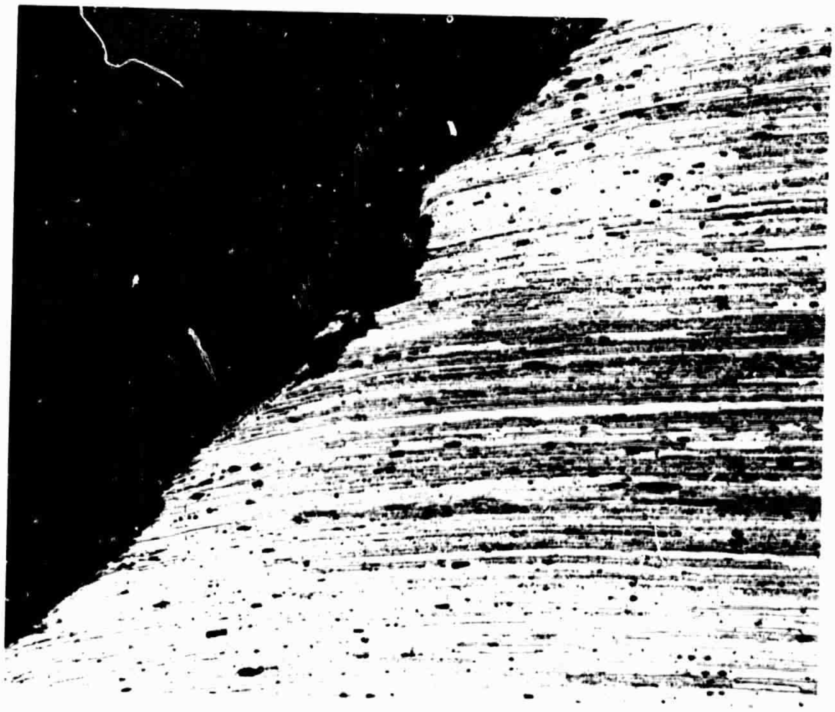

(a)

100X

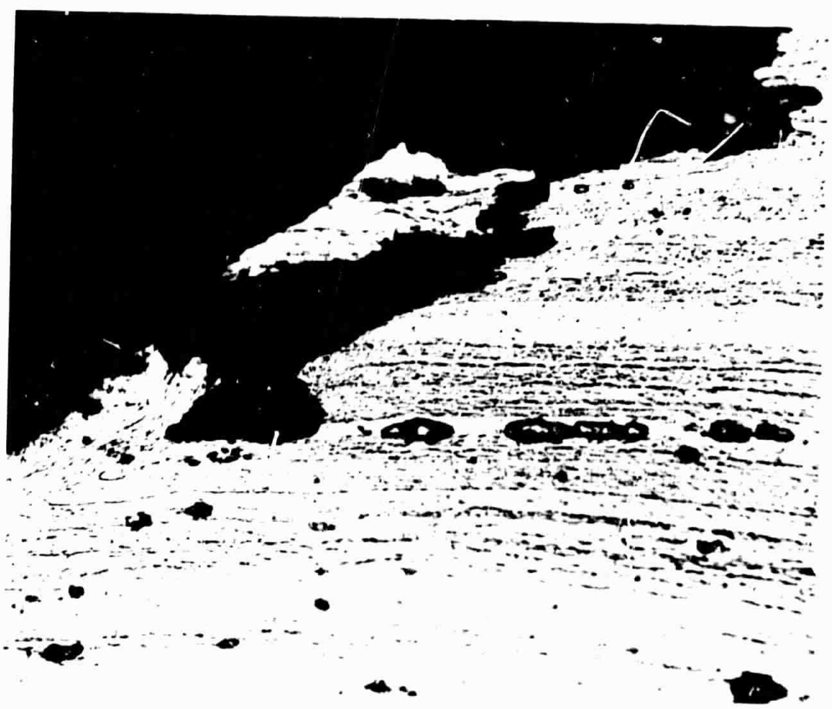

(b)

Etchant-Keller's

500X

FIGURE 25. FRACTURED EDGE IN HEAT AFFECTED BASE METAL X7106 WELDMENT

Toe "A"

100X

Toe "B"

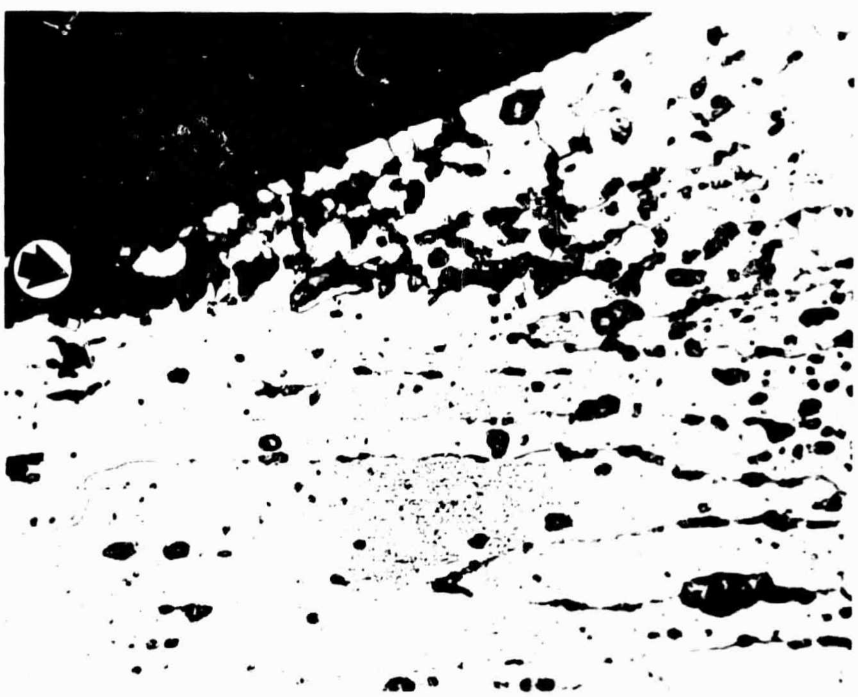

Etchant-Keller's

500X

FIGURE 26. TOES OF WELD CROWN OF A MIG X7106 TENSILE SPECIMEN THAT FAILED IN THE HEAT AFFECTED BASE METAL

The intermetallic constituents in Toe "B" are clearly resolved at 500X. The concentration of these constituents in the vicinity of the boundry between the toe and the heat-affected zone is markedly higher than at other locations within the weld metal. This region of high concentration of intermetallic particles is the location where cracks are consistently initiated in tensile test specimens.

Microhardness surveys were conducted on three specimens to establish the variation in hardness across the heat-affected zone. The specimens used for these surveys were as follows:

1) TIG X7106/X5180 (Panel B) aged 2 weeks
2) TIG X7106/5356 (Panel C) aged 4 weeks
3) TIG X7106/X5180 (Panel B) aged 8 weeks

The results of these surveys are presented in Figure 27. Each of the three specimens exhibited a soft region near the outer edge of the heat-affected zone (identified by "S" in Figure 27).

The points of low hardness were all located from 0.105-inch to 0.135-inch from the fusion line. Such a region is within the range of the locations of fracture determined for specimens which failed in the heat-affected base metal. This observation suggests that the soft regions are the points of initiation of fracture when failure occurs in the heat-affected zone.

This occurrence of a soft area in the heat-affected zone may be expected on the basis of the time-temperature aging effect of the heat of welding. There is a zone at the lower temperature end of the heat-affected band which reaches a temperature (below the solution temperature) at which overaging occurs.

A limited investigation of the microstructure of the X7106/X5180 specimen (aged 2 weeks) in the vicinity of the soft region was carried out. The microhardness indentation corresponding to the low hardness point (S) and the two adjacent indentations are shown in Figure 28, together with the microstructure associated with two of the indentations. The microstructures observed (Figures 28b and c) are characteristic of heat-affected base metal in X7106 weldments. There is some indication of a larger quantity of a finely dispersed, light colored precipitate in the region of lower hardness (circles in Figures 28b and c) than in the harder region. The size of these precipitates approaches the limit of resolution of optical microscopy. Further investigation of the structure in these regions would require the utilization of electron microscopy.

The hardness of profiles for a TIG/X5180 weldment at various aging times is shown in Figure 29. The general character of the hardness profile for this weldment is typical of that observed in each type.

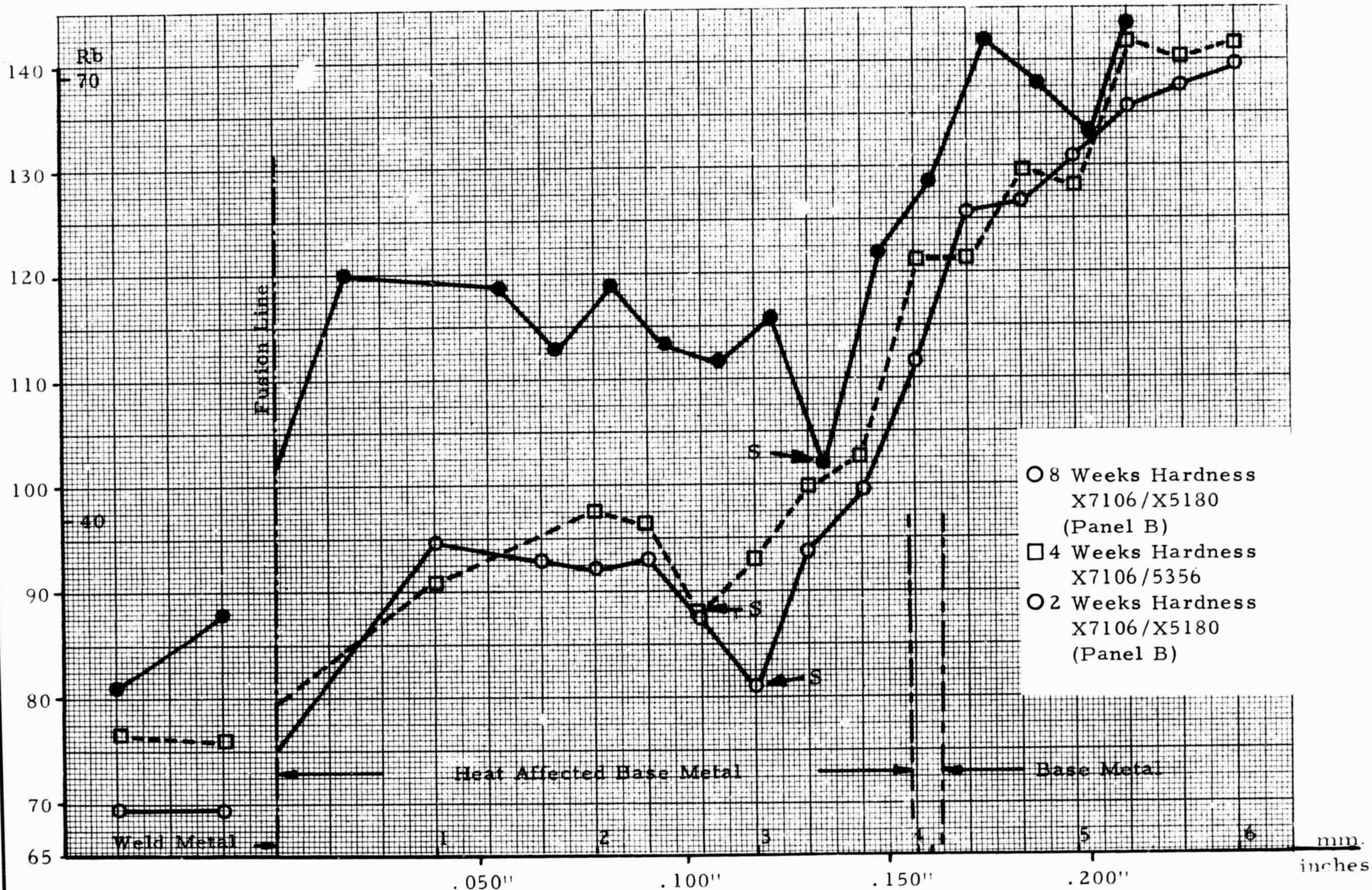

FIGURE 27. MICRO-HARDNESS SURVEY OF X7106 WELDMENTS AFTER VARIOUS NATURAL AGING TIMES

Weld Metal ←   Base Metal →

(a)

100X

(b)

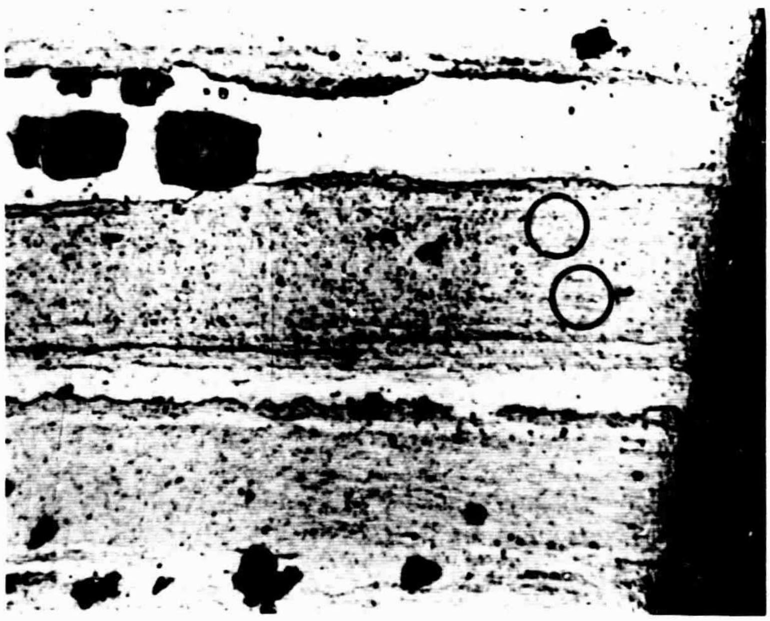

"H" Indentation

1500X

(c)

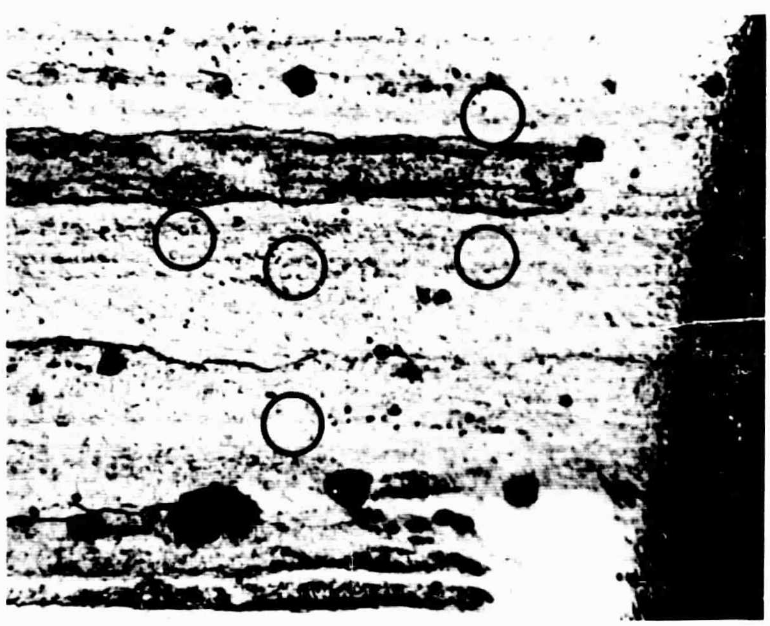

"S' Indentation

Etchant-Keller's   1500X

FIGURE 28. STRUCTURE IN HEAT AFFECTED BASE METAL

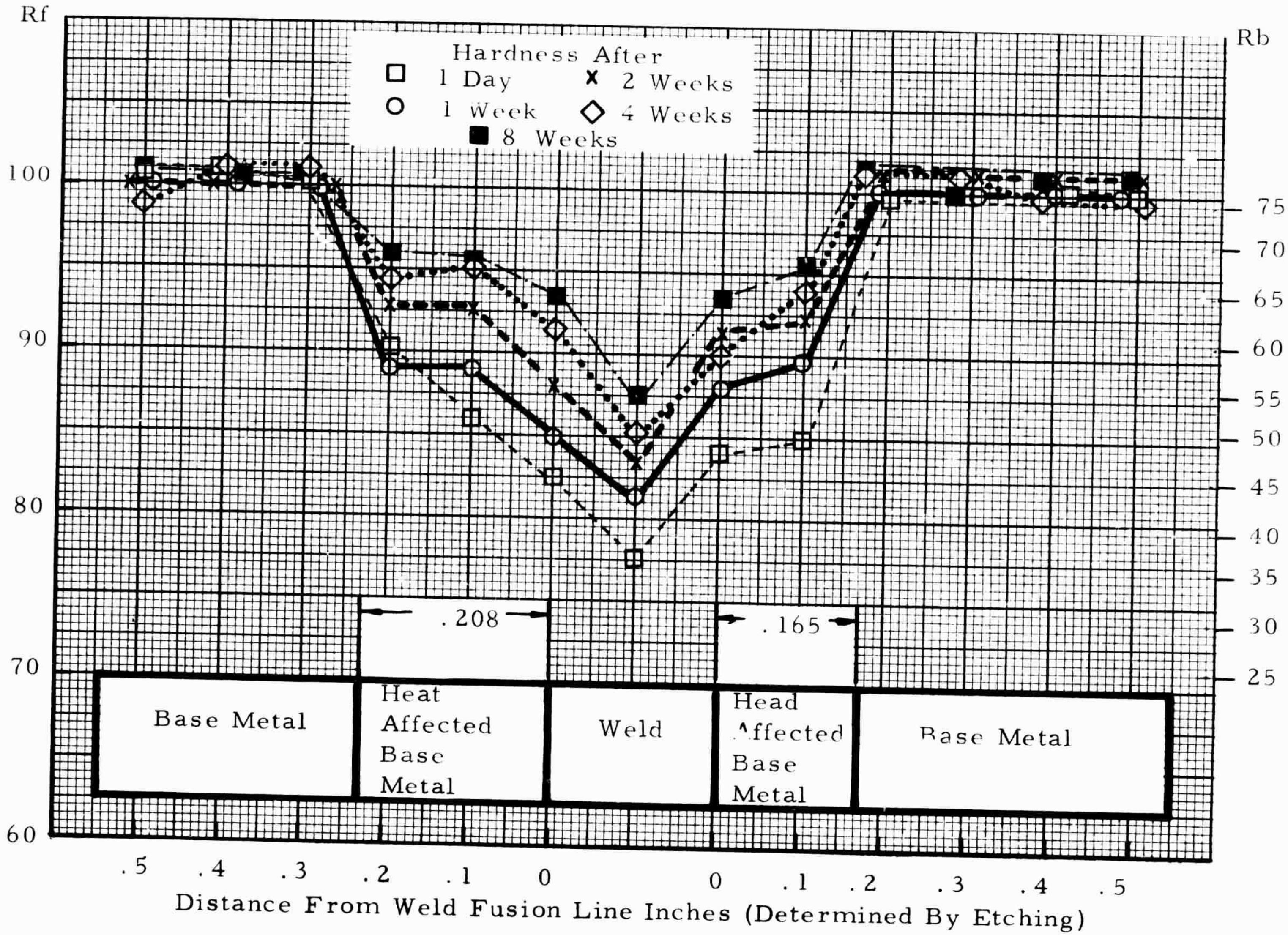

FIGURE 29. HARDNESS SURVEYS OF X7106/X5180 WELDMENT AFTER VARIOUS NATURAL AGING TIMES (PANEL B)

The results of the hardness surveys made on the TIG weldments are presented as hardness versus aging time in Figure 30. In the case of these weldments, hardness measurements were made at various aging times at the center line of the weld, at the fusion line and 0.10-inch from the fusion line in the heat-affected base metal. These measurements were made after five different aging times (1 day to 8 weeks) for the TIG/X5180 weldments and at one day and eight weeks for the TIG weldments employing 5356 and 5556 filler wire. As may be noted in Figure 30, all measurements made in the heat-affected zone for the X5180 weldment fell in a band representing the normal scatter to be expected in Rockwell hardness measurements. The hardness values at the fusion line for the 5356 and 5556 weldments, after one day, were noted to be somewhat lower than that of the X5180 weldments. After eight weeks aging, however, the hardness at both locations within the heat-affected zone was comparable for all three types of TIG weldment.

The hardness at the weld center line for the TIG/5356 and TIG 5556 weldments aged one day were both lower than that for the X5180 weldments. After eight weeks aging, the weld metal hardness valves for the X5180 and 5356 welds were comparable and somewhat higher than that of the 5556 weld metal (See Figure 30).

The results of the hardness surveys made on the MIG/X7106-T63 weldments, aged up to eight weeks, are shown in Figure 31. In this case, hardness measurements were made at the center line of the weld, 1/16-inch and 1/8-inch from the fusion line in the heat-affected zone and in the base metal.

At each aging time, the hardness measured at both points in the heat-affected zone of all three types of MIG weldments fell within a normal scatter band. Thus no significant differences in hardness at these two points are indicated. The hardness of the heat-affected base metal at these two points, as a function of time, for all three types of MIG weldments may thus be considered as a band rather than as individual curves, Figure 31.

The hardness measurements taken in the weld metal indicate some differences in the natural aging characteristics of the three types of filler metal in the case of the MIG weldments. At short aging times, the hardness values for the three types of weld metal fell within or near a normal scatter band. At longer aging times, (4 weeks and 8 weeks) differences in hardness greater than normal scatter were noted. This, coupled with the fact that at lower aging times the recorded hardness of each type of filler metal fell in the same order (5556 highest, X5180 intermediate and 5356 lowest), allows presentation of the data for the MIG weldments as three separate curves, Figure 31. It is evident from these three curves that, after an aging period of eight weeks, a higher hardness results in the fusion zone of the MIG weldments made with X5180 and 5556 filler metal than in that of the MIG/X7106-T63/5356 weldments. The X5180 weldments exhibited the highest hardness of the three MIG weldments at this aging time, but the difference in

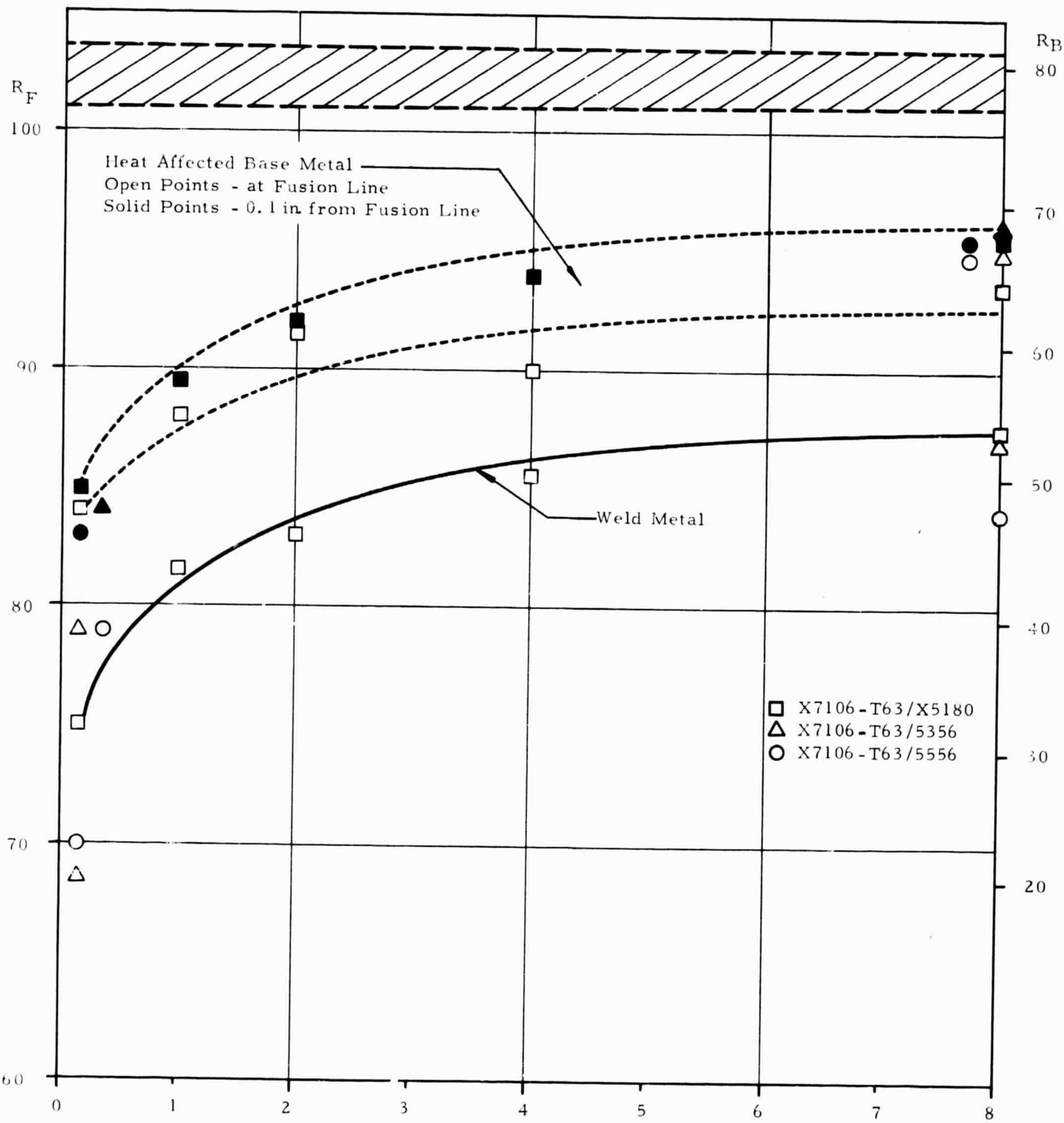

FIGURE 30. INCREASE IN HARDNESS OCCURRING IN TIG X7106-T63 WELDMENTS ON NATURAL AGING

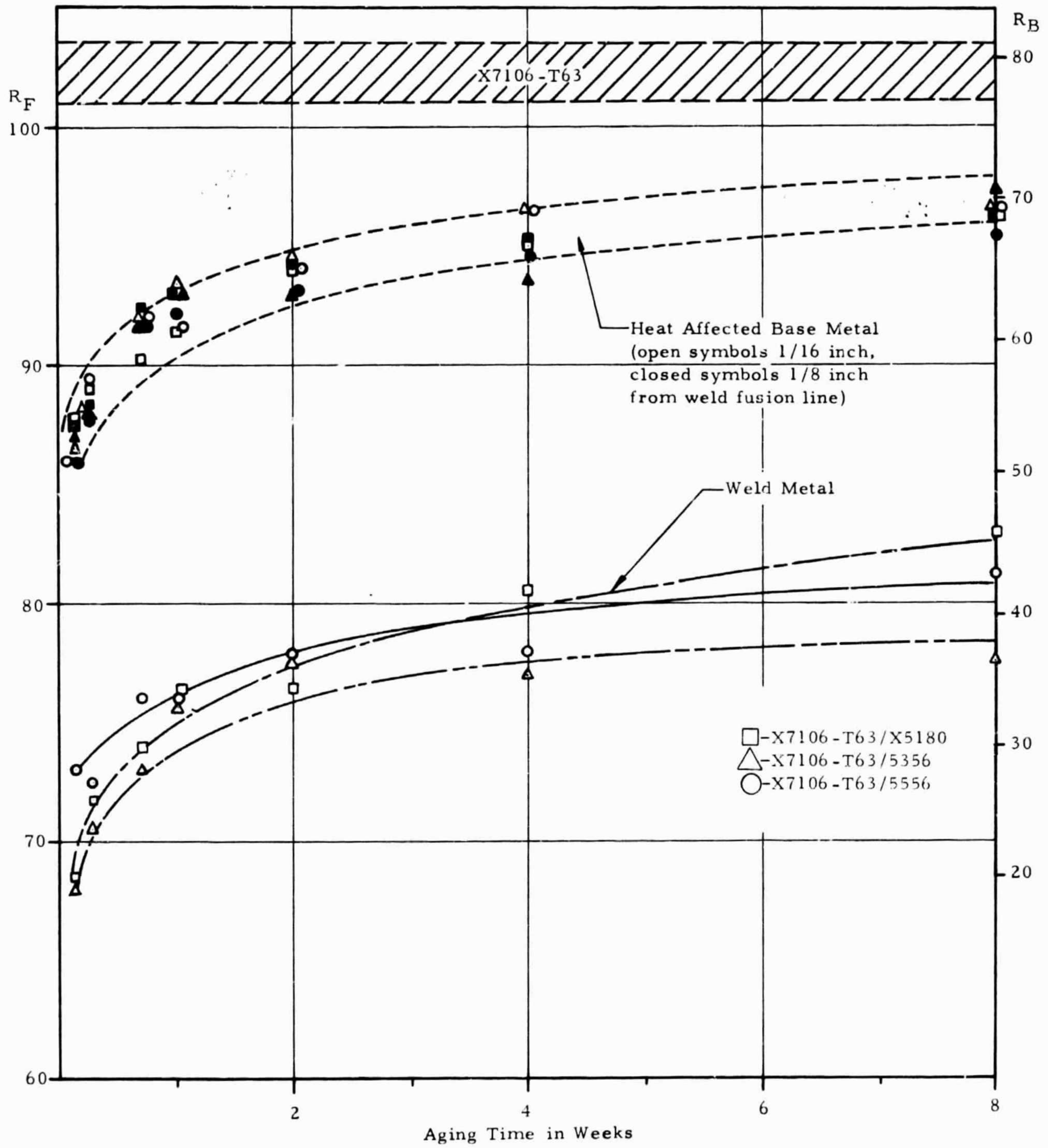

FIGURE 31. INCREASE IN HARDNESS OCCURRING IN MIG X7106-T63 WELDMENTS ON NATURAL AGING

hardness between the X5180 and 5556 weld metal is within the normal scatter to be expected in hardness measurements.

For all types of X7106-T63 weldments studied in this program, the hardness of the heat-affected base metal, in the immediate vicinity of the fusion line, increased to a value near that of the base metal after an aging period of eight weeks (R_B 70 as compared to R_B 77), as may be noted in Figures 30 and 31. On the other hand, a maximum hardness of only R_B 55 was recorded for the weld metal in any of the types of weldments. The slopes of the hardness versus time curves, for both the heat-affected base metal and the weld metal, indicate that near maximum hardness was attained after an aging time of eight weeks.

The observed natural aging characteristics of the heat-affected base metal and the weld metal are consistent with the thermal conditions that prevail during welding. At a point in the immediate vicinity of the fusion line, the base metal may be heated to a sufficiently high temperature and cooled rapidly enough, to constitute a partial solution treatment. Such a condition would allow for a considerable increase in hardness on aging, but result in a maximum hardness somewhat lower than the base metal, as was noted in this case.

The weld metal, however, has an alloy content significantly lower than the base metal, particularly in the concentration of zinc. In addition, the weld metal cools at a slower rate from the welding temperature and the cast structure permits some greater degree of segregation. Each of these factors would contribute to limiting the maximum hardness obtainable in the weld metal on aging. Since the natural aging characteristics are dependent to a great extent on the zinc content, it is reasonable that the X5180 filler metal, which contains approximately 2 percent zinc, should show the optimum aging response. Because of the influence of zinc concentration, the relative dilution of the weld deposit with the base metal becomes an important consideration. This is governed by a series of welding variables which establish weld size and shape. Consequently, it is somewhat difficult to compare the aging response of welds made with non-zinc bearing filler metals without a more statistical sampling of various heats of base metal, filler wires and variations in welding sequence. In this particular series of tests the MIG weldments made with 5556 filler wire, which has a nominally higher magnesium level, proved to have better age hardening characteristics than the MIG 5356 weldments. Such a result could be expected because of the zinc-magnesium precipitation reaction in these alloys. A final rating of these two filler metals, however, should await a much more comprehensive statistical sampling.

A comparison of the results of the tensile tests (Figures 19 and 20) and the hardness measurements (Figures 30 and 31) demonstrates that each of the types of information gives a similar description of the natural aging characteristics of X7106-T63 weldments. The comparison of the increase in ultimate strength and yield strength with the increase in hardness for TIG/X5180 weldments, shown in Figure 32, is typical of the weldment listed in this study. Each set of data exhibits approximately logarithmic dependence of strength and hardness on aging time. It may be concluded, therefore, that an adequate description of the aging characteristics may be obtained from hardness measurements alone.

D. Crack Susceptibility of X7106-T63 Weldments

The results of the series of crack susceptibility tests on Houldcroft test specimens are given in Table XII and Figure 33. The mean crack length observed for each of the three X7106-T63 weldments exceeded that of the 2219-T87/2319 specimen. These results indicate that the X7106-T63 alloy is more susceptible to hot cracking during welding than the 2219-T87 alloy. A comparison of the results, taking the calculated standard deviation into consideration, verifies that the observed difference in the two alloy types is real. By the same token, however, no difference in the crack susceptibility of the three types of X7106-T63 weldments were detected by these tests. A modified Houldcroft test specimen has been proposed by Rogerson, et al[3]. This specimen employs an integral tab to stabilize heat flow and is reported to provide a less severe but more sensitive test. Utilization of this modified test specimen could possibly differentiate between the crack susceptibility of the three types of X7106-T63 weldments.

E. Temperature Distribution Near Welded Joints

The results of the investigation of the temperature distribution in the vicinity of welded joints are given in Figures 34 and 35. In these figures the data are plotted as indicated peak temperatures versus the distance from the outer edge of the zone of heat-affected base metal as revealed by etching (Dimension d, Figure 7). This method of plotting was necessitated by the inherent irregularities in the width of the heat-affected zone. Since the Tempilstik marks were located at various points along the direction of welding, the variations in width of this zone reflect as irregularities in a plot of indicated temperature versus distance from the center line (or fusion line) of the weld. The method of presentation used in Figures 34 and 35 eliminates such irregularities and simplifies interpretation of the results.

It is recognized that the technique used in this study is somewhat limited in accuracy and some scatter in the data is evident. The degree of scatter is not serious, however, and the technique is considered to give a satisfactory indication of the distribution of peak temperatures.

As may be noted in Figures 34 and 35, the results indicate that the zone of heat-affected base metal, as revealed by etching, consists of material heated to a temperature of approximately 500°F or higher during the welding operation. The results are comparable for both the MIG and TIG processes.

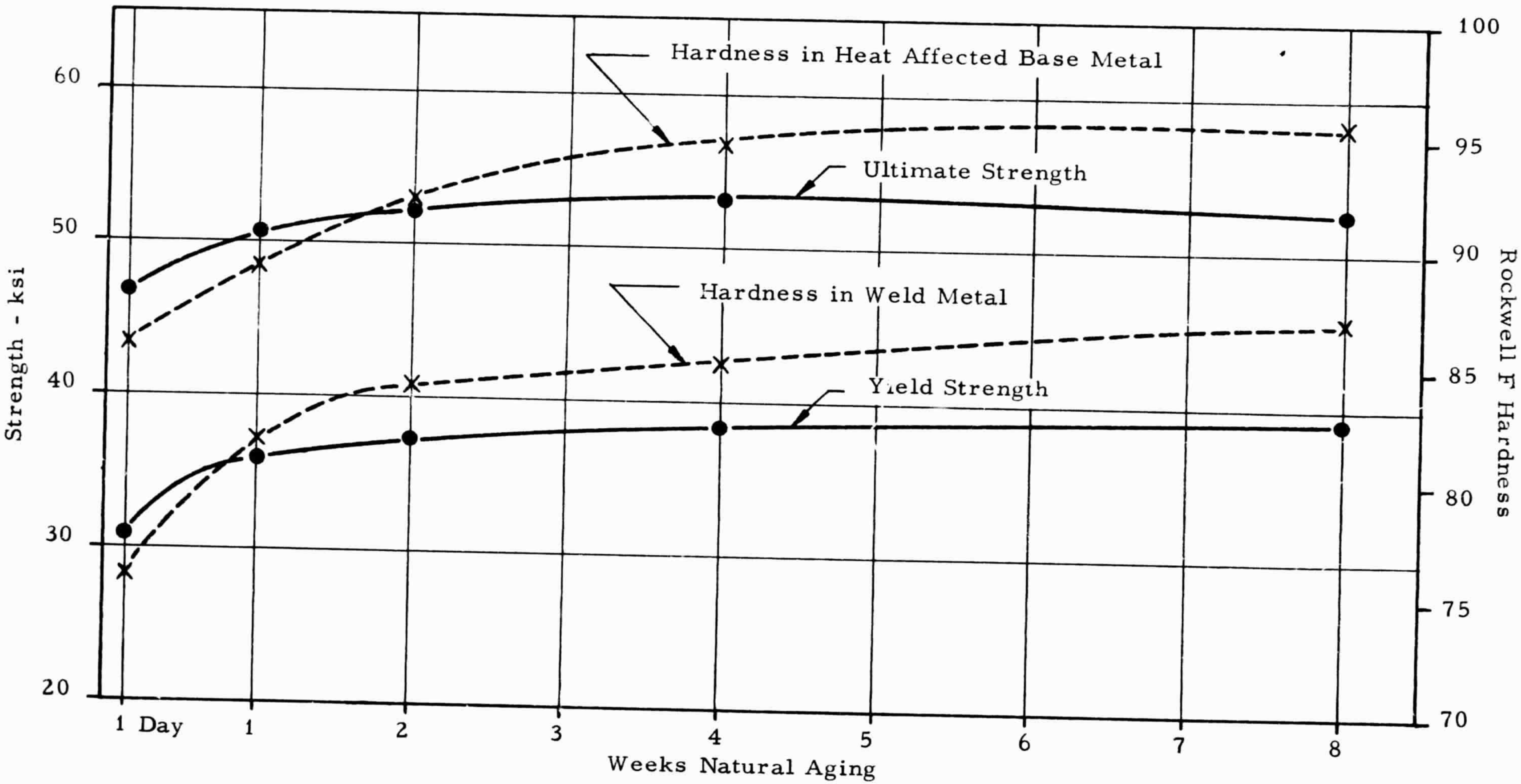

FIGURE 32. RELATIONSHIP BETWEEN HARDNESS, YIELD AND ULTIMATE STRENGTH OF A TIG X7106/X5180 WELDMENT (PANEL B)

TABLE XII

HOULDCROFT CRACK TEST RESULTS FOR
0.090 INCH X7106-T63 AND 2219-T87 WELDMENTS

Parent Metal & Filler Metal	Individual Crack Lengths* in.	Mean Crack Length in.	Standard Deviation in.
X7106-T63/X5180	1.25, 1.30, 1.15 1.31, 1.01, 0.90	1.15	0.17
X7106-T63/5356	1.30, 1.12, 1.29 1.55, 1.06, 1.26	1.26	0.18
X7106-T63/5556	0.73, 1.19, 1.38 1.31, 1.05, 0.75	1.07	0.28
2219-T87/2319	0.61, 0.15, 0.79 0.63, 0.39, 0.42	0.50	0.26

* Crack length in weld crown as determined from fluorescent dye penetrant indication.

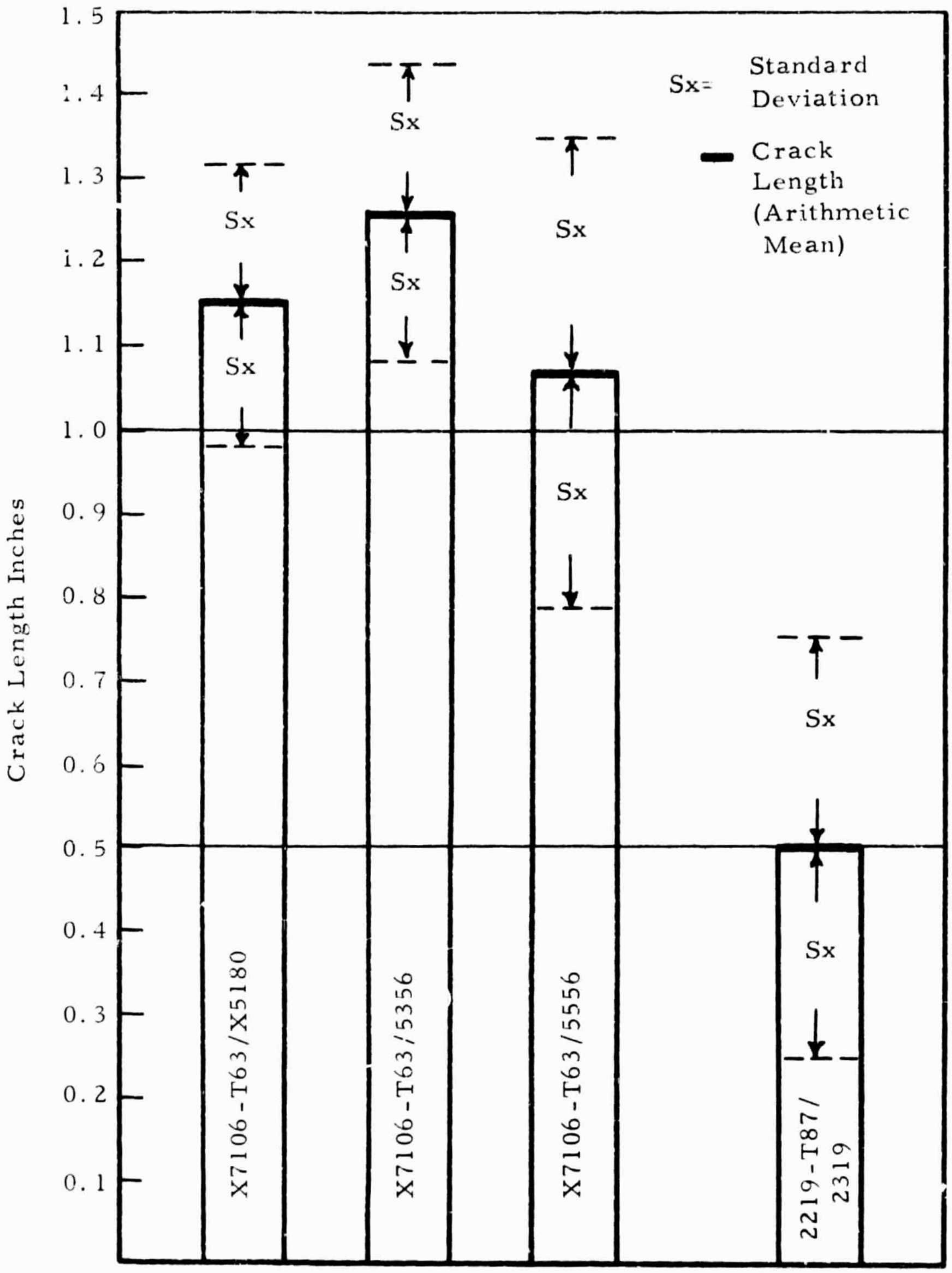

FIGURE 33. GRAPHICAL PRESENTATION OF CRACK DATA OBTAINED FROM HOULDCROFT TESTS

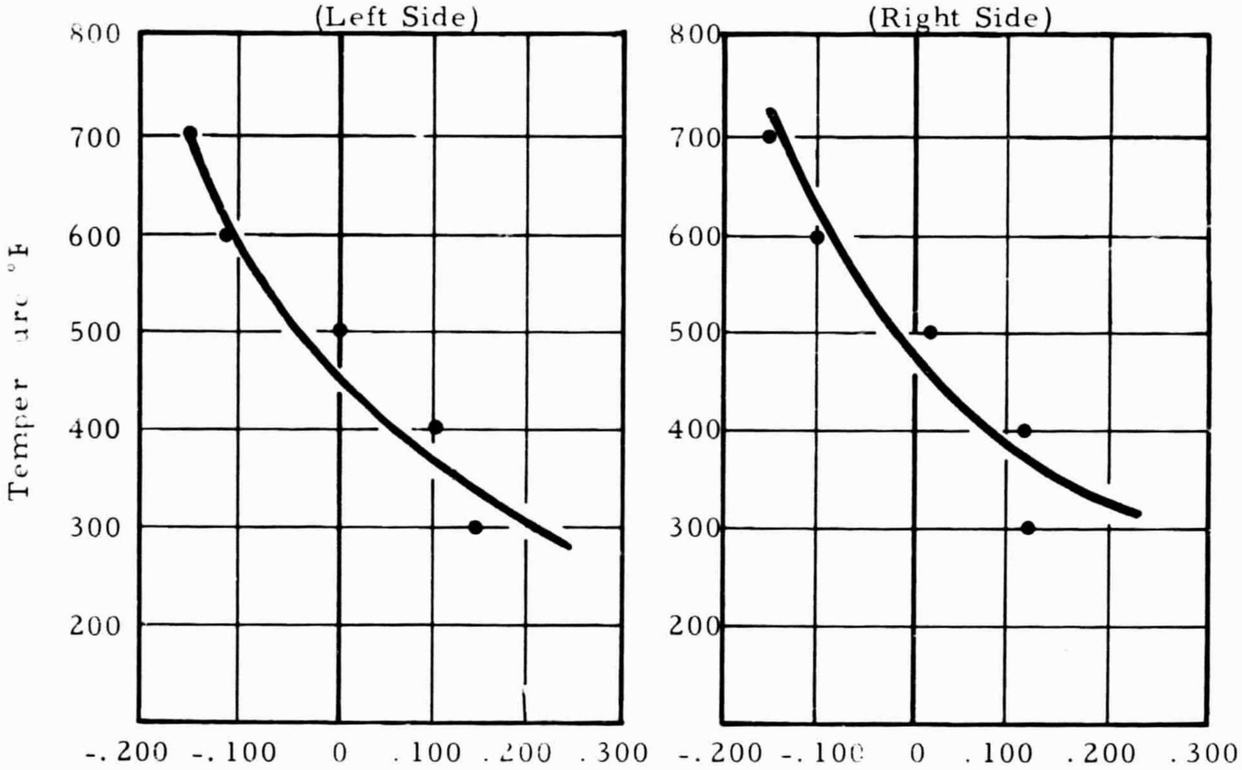

Distance from outer edge of HAZ* (inches)

Distance from outer edge of HAZ* (inches)

*HAZ: Zone of heat affected base metal revealed by etching.

FIGURE 34. TEMPERATURE DISTRIBUTION IN THE VICINITY OF JOINT IN A TIG WELDED X7106-T63/X5180 PANEL AS REVEALED BY TEMPERATURE SENSITIVE CRAYONS

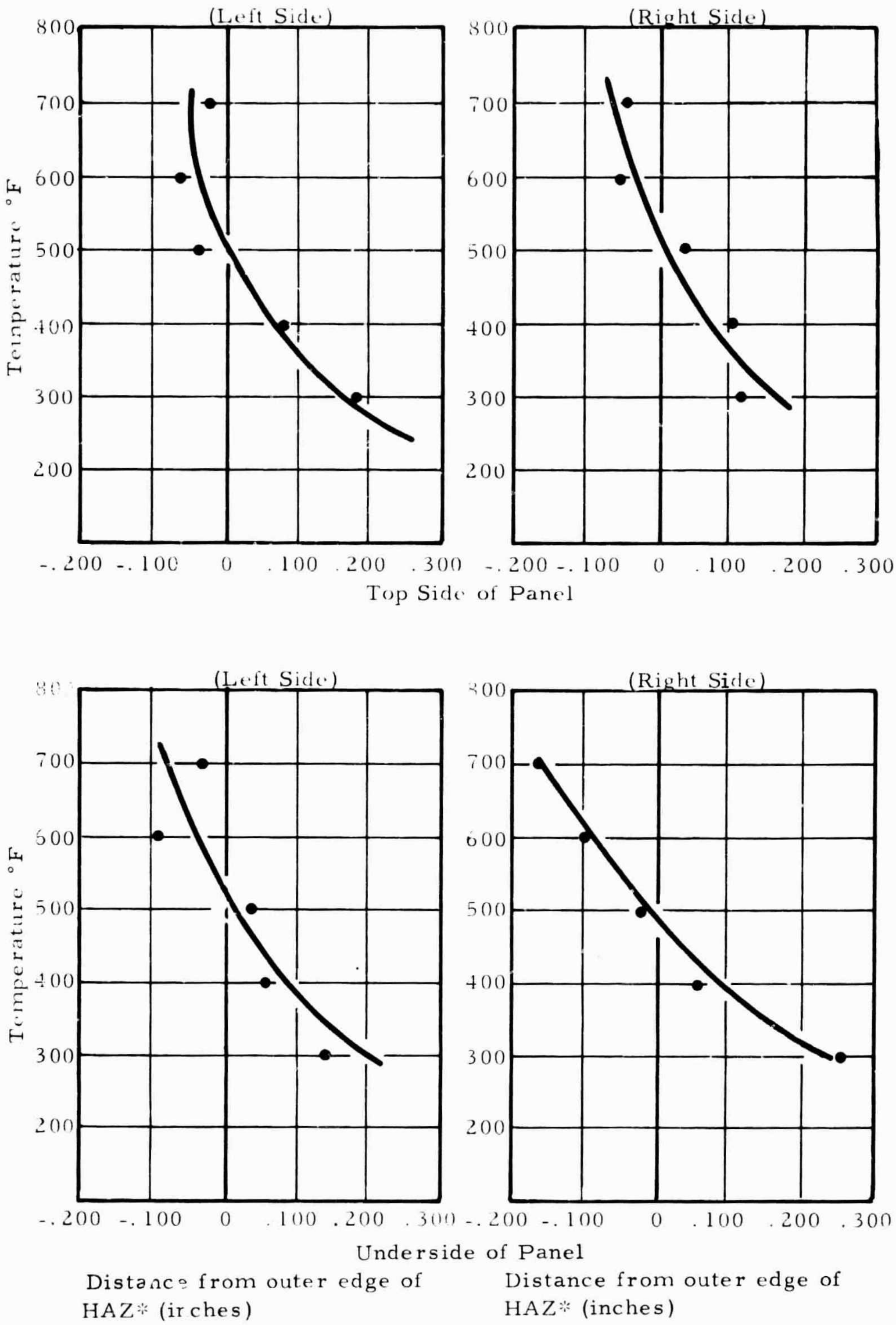

*HAZ: Zone of heat affected base metal revealed by etching.

FIGURE 35. TEMPERATURE DISTRIBUTION IN THE VICINITY OF JOINT IN A MIG WELDED X7106-T63/X5180 PANEL AS REVEALED BY TEMPERATURE SENSITIVE CRAYONS

In the course of the mechanical testing carried out in the aging study, it was observed that a large majority of the tensile test fractures were located within the heat-affected zone. This observation, coupled with the temperature distribution study, indicates that the point of minimum strength in both TIG and MIG weldments (as long as the weld metal is reinforced by the weld crown) is associated with base metal which has been heated to a temperature of 500°F or higher. These results are consistent with the observed reduced hardness in the heat-affected zone relative to that of the base metal (Figures 30 and 31).

Similar results have also been obtained in other studies of Al-Mg-Zn alloys. Rogerson[4] found the weakest point in a weldment of such an alloy to occur in a zone corresponding to peak temperatures of 392-482°F. In addition, information published by Alcoa[5] indicates that X7106 alloy may be heated to temperatures up to 350°F for periods of ten minutes without degrading the mechanical properties by more than 5 percent. In the same publication, however, it is suggested that exposure to temperatures higher than 400°F will result in significant deterioration of the mechanical properties.

It is apparent then, from the results of this study and other investigations, that the location of failures in X7106-T63 weldments may be associated with a region of base metal which has experienced a time-temperature cycle sufficient to bring about some degree of overaging of the previously age-hardened material.

BIBLIOGRAPHY

1. Houldcroft, P. T.: "A Simple Cracking Test for Use with Argon-Arc Welding." British Welding Journal, Oct. 1955, pp. 471-475.

2. Timoshenko, S.: "Theory of Plates and Shells." McGraw-Hill, 1930, pp. 333-337.

3. Rogerson, J. H., Cotterell, B., and Borland, J. C.: "An Analysis and Evaluation of the Houldcroft Weld Cracking Test." Welding Journal, Welding Research Supplement, June, 1963, pp. 264s-268s.

4. Rogerson, J. H.: "Microstructure and Properties of Heat-Affected Zones in Medium Strength Al-Zn-Mg Alloys." British Welding Journal, Jan. 1962, pp. 12-17.

5. Nuernberger, H. H.: "Alcoa Aluminum Alloy X7106." Aluminum Company of America, Sales Development Division, New Kensington Pa., Oct. 1, 1963.

6. Young, J. G.: "New Weldable Aluminum--Zinc--Magnesium Alloys." Light Metals Industry, Nov. 1963, pp. 47-50.

7. Houldcroft, P. T.: "Investigation of Filler Materials for Welding Al-Zn-Mg Alloys." British Welding Journal, July, 1961, pp. 360-365.

8. Polmear, I. G.: "Studies on High-Strength Aluminum Alloys in Australia." Metals Progress, Jan. 1962, pp. 82-84, 124-130.

9. Dix, E. H., Jr.: "Aluminum-Zinc-Magnesium Alloys." A. S. M. Transaction, Vol. 42, 1950, pp. 1057-1127.

10. Polmear, I J.: "The Aging Characteristics of Ternary Aluminum-Zinc-Magnesium Alloys." Journal of the Institute of Metals, 1957-1958, Vol. 86, pp. 113-121.

11. Thomas, G. and Nutting, J.: "The Aging Characteristics of Aluminum Alloys." Journal of the Institute of Metals, Vol. 88, 1959-1960, pp. 81-90.

12. D'Annessa, A. T. and Friend, R. C.: "Properties of X7000-Series Aluminum Alloy Weldments." Welding Journal, August, 1964 Welding Research Supplement, pp. 337s-343s.

13. Polmear, I. J. "The Upper Temperature Limit of Stability of G. P. Zones in Ternary Aluminum-Zinc-Magnesium Alloys." Journal of the Institute of Metals, 1958-1959, Vol. 87, pp. 24-25.

14. General Dynamics/Astronautics Report No. 63-0705 (Nova Technical Memorandum 35), August, 1963.

15. D'Annessa, A. T.: "Properties of X7002, X7006 and X7039 Aluminum Alloy Weldments." Lockheed Missile and Space Company, Technical Report, Feb. 1964.

16. Anderson, W. A., Kaufman, J. G. and Kane, J. E.: "Notch Sensitivity of Aluminum-Zinc-Magnesium Alloys at Cryogenic Temperatures. Reprinted from Advances in Cryogenic Engineering, Vol. 9 Plenum Press, New York, 1964.

17. Taylor, I.: "74S and C74S." Metal Progress, Nov. 1963, pp. 74-77, Dec. 1963, pp. 96-100.

18. Correspondence with R. C. Forrest, Technical Service and Development Dow Chemical Company Metals Division, Midland, Mich., (August, 1964).

19. Dowd, J. D.: "Weld Cracking of Aluminum Alloys." Welding Journal Oct. 1952, Welding Research Supplement, pp. 448s-456s.

20. Pumphrey, W. I. and Lyons, J. V.: "Cracking During the Casting and Welding of the More Common Binary Aluminum Alloys." Journal of the Institute of Metals, Vol. 74, 1948, pp. 439-455.

21. Houldcroft, P. T.: "Dilution and Uniformity in Aluminum Alloy Weld Beads." British Welding Journal, Oct. 1954, pp. 468-471.

22. Young, J. G.: "Significance of Filler Metal Composition in Aluminum Alloy Welding." British Welding Journal, Dec. 1961, pp. 568-574.

23. Houldcroft, P. T. and Fidgeon, F.: "Aging Characteristics of 'As Deposited' Aluminum Alloy Weld Metal." British Welding Journal, 1958, pp. 319-326.

24. Conference with Messrs. G. O. Hoglund and J. H. Dudas, Aluminum Company of America, New Kensington, Pa. (August, 1964).

25. Conference with Messrs. F. R. Baysinger and F. E. Gibbs, Kaiser Aluminum and Chemical Corporation, Spokane, Washington (August, 1964).

26. Conference with R. C. Manary, General Dynamics, San Diego, Calif. (August, 1964).

27. Conference with Messrs. A. T. D'Annessa and A. A. Pfluger, Lockheed, Palo Alto, Calif. (August, 1964).

28. Conference with Mr. D. Lovell and Associates, Boeing Company, Seattle, Wash. (August, 1964).

29. Randall, M. D., Monroe, R. E., and Rieppel, P. J.: "Methods of Evaluating Welded Joints." Defense Metals Information Center (DMIC) Report 165, Dec. 1962, pp. 52-64.

30. Cranjon, H.: "Information on Cracking Test." Welding Abroad, Nov. 1963, pp. 65-77.

31. Baysinger, F. R.: "Determination of Engineering Properties of Aluminum Weldments." Interim Project Report No. MS PR 58-101, Dec. 31, 1958, Kaiser Aluminum Chemical Corporation, Spokane, Wash.

32. Levy, A. V., and Kennedy, H. E.: "Stresses in Circular-Patch Weld-Test Specimens." Welding Journal, Welding Research Supplement, Sept. 1952, pp. 402s-405s.

33. Borland, J. C., and Rogerson, B. A.: "Examination of the Patch Test for Assessing Hot Cracking Tendencies of Weld Metal." British Welding Journal, August, 1962, pp. 494-499.

34. Arnold, P. C.: "Problems Associated with the Welding of T-1 Material". Welding Journal, Welding Research Supplement, August, 1957, pp. 373s-381s.

35. Conference with Messrs. J. Stadick, D. Bertossa, and O. Seth, Chicago Bridge and Iron, Chicago, Ill. (August, 1964).

36. D'Annessa, A. T.: "Fracture Toughness of X7006-T6351 Aluminum Alloy Plate Weldments." Lockheed Missile and Space Company, Technical Report, July, 1964.

37. DeMoney, F. W.: "Performance of a New Cryogenic Aluminum Alloy, 7039." Advances in Cryogenic Engineering, Vol. 9, Plenum Press, New York, 1963, pp. 112-123.

38. Campus, F.: "Effects of Residual Stresses on the Behavior of Structures." Residual Stresses in Metals and Metal Construction, W. R. Osgood, Editor, Reinhold, 1954, p. 9.

39. Drucker, D. C.: "A Continuum Approach to the Fracture of Metals". Fracture of Solids, Drucker and Fillman, Editors, Interscience, 1962.

APPENDIX A

APPENDIX A

RESULTS OF INDIVIDUAL BULGE TESTS AND UNIAXIAL TENSILE TESTS

The results of the individual bulge tests and uniaxial tensile tests conducted in the course of the program are presented in Tables A-I through A-VI. Summaries of these results are included in the body of the report.

TABLE A-I

HYDRAULIC BULGE TEST RESULTS
2014-T6 and 2219-T87 Parent Metal and Weldments

Panel Description				Maximum Pressure psi	Bulge Height in.	Biaxial Ult. Str ksi
Material & Process	Type	Welding Procedure	No			
2014-T6	Parent Metal	----	----	1060 (980)*	4.30 (3.10)*	79.3
		----	----	1200 (1080)	4.40 (3.80)	76.4
		----	----	-- (670)	-- (2.40)	75.6
2219-T87	Parent Metal	----	----	930 (780)	3.48 (2.80)	74.1
			----	1040 (750)	4.53 (2.90)	69.8
			----	1010 (850)	4.60 (3.40)	67.6
TIG 2014-T6 2319	Single Weld	64A-1	BP1	255	1.47	47.4
			BP2	250	1.35	50.6
			BP3	260	1.40	50.7
	Tee Weld	64A-1	BP17	190	1.12	47.0
			BP18	206	1.33	42.9
			BP19	217	1.41	42.4
	Cross Weld	64A-1	BP14	218	1.44	42.0
			BP15	237	1.45	44.3
TIG 2014-T6 4043	Single Weld	64A-16	BP54	186	1.58	31.9
			BP56	195	1.40	38.4
	Tee Weld	64A-16	BP57	180	1.43	34.6
			BP58	188	1.46	35.4
			BP59	184	1.46	34.6
	Cross Weld	64A-16	BP51	180	1.41	35.1
			BP52	186	1.41	36.3
			BP53	177	1.43	34.1

* Values in parenthesis indicate pressure and bulge height corresponding to biaxial ultimate strength.

TABLE A-I (Continued)

HYDRAULIC BULGE TEST RESULTS
2014-T6 and 2219-T87 Parent Metal and Weldments

Panel Description				Maximum	Bulge	Biaxial
Material & Process	Type	Welding Procedure	No.	Pressure psi	Height in.	Ult. Str. ksi
MIG 2014-T6 4043	Single Weld	64A-3	BP29	158	1.33	33.0
			BP30	134	1.28	29.2
			BP37	134	1.23	30.4
	Tee Weld	64A-3	BP35	177	1.40	35.1
			BP36	143	1.21	33.0
			BP70	189	1.39	37.4
	Cross Weld	64A-3	BP28	127	1.13	31.4
			BP31	124	1.18	29.3
			BP33	133	1.22	30.4
TIG 2219-T87 2319	Single Weld	64A-2	BP7	178	1.25	39.2
			BP8	162	1.16	38.6
			BP9	174	1.27	37.8
	Tee Weld	64A-2	BP10	197	1.53	35.2
			BP12	172	1.30	36.5
			BP60	176	1.64	29.4
	Cross Weld	64A-2	BP4	178	1.49	32.6
			BP5	171	1.38	34.1
			BP6	173	1.37	34.3
MIG 2219-T87 2319	Single Weld	64A-4	BP26	159	1.24	34.7
			BP27	156	1.28	33.7
			BP65	201	1.41	39.8
	Tee Weld	64A-4	BP68	210	1.51	38.6
			BP69	181	1.35	37.0
			BP71	188	1.42	36.4
	Cross Weld	64A-4	BP23	175	1.48	32.5
			BP63	215	1.57	37.5
			BP64	196	1.39	38.8
			BP72	206	1.59	36.7

TABLE A-II

UNIAXIAL TENSILE TEST RESULTS
2014-T6 and 2219-T87 Parent Metal and Weldments

Material & Process	Panel No.	Specimen No.	Yield Str. 0.2% Offset ksi	Ultimate Strength ksi	Elongation in 2 in. %
2014-T6 Parent Metal	-----	1	63.0	69.6	8.0
		2	63.0	69.6	10.1
		3	62.7	69.6	10.8
		4	62.5	69.6	10.6
		5	62.5	69.6	10.2
		6	66.3	71.5	10.6
		7	65.7	71.0	11.0
		8	65.1	70.6	11.0
		9	65.1	70.6	10.7
		10	65.4	70.8	10.4
2219-T87 Parent Metal	-----	1	54.8	66.5	11.0
		2	54.9	66.8	10.3
		3	54.9	66.7	10.3
		4	54.7	66.7	10.3
		5	54.5	66.5	10.0
		6	55.4	67.0	12.1
		7	55.6	67.9	11.0
		8	55.0	67.2	11.5
		9	54.4	66.2	11.2
		10	55.0	66.7	11.3

TABLE A-II (Continued)

UNIAXIAL TENSILE TEST RESULTS
2014-T6 and 2219-T87 Parent Metal and Weldments

Material & Process	Panel No.	Specimen No.	Yield Str. 0.2% Offset ksi	Ultimate Strength ksi	Elongation in 2 in. %
TIG 2014-T6 2319	BP1	1	46.1	56.7	1.5
		2	43.6	51.1	2.2
		3	43.7	56.3	2.2
		4	41.7	54.3	2.2
		5	43.2	53.1	4.0
		6	40.9	51.6	1.7
	BP17	1	41.4	51.4	1.9
		2	38.6	48.7	1.9
		3	37.8	49.5	2.0
		4	38.1	48.6	1.6
		5	40.3	47.1	1.6
	BP18	1	38.8	48.1	1.8
		2	38.6	47.1	1.4
		3	38.4	46.4	1.7
		4	38.0	45.1	1.5
		5	40.2	45.9	1.5
	BP19	1	40.3	51.9	1.6
		2	38.1	50.3	2.0
		3	39.2	48.4	1.4
		4	40.6	50.7	1.9
		5	39.9	47.3	1.4
		6	37.8	44.7	1.2
	BP14	1	40.2	51.6	1.5
		2	40.5	51.2	1.9
		3	40.1	50.5	1.7
		4	39.6	50.1	1.6
		5	40.7	52.0	1.6
	BP15	1	41.9	50.7	1.6
		2	39.5	49.5	1.6
		3	41.1	48.7	1.6
		4	38.8	51.4	1.5
		5	40.1	50.5	1.9

TABLE A-II (Continued)

UNIAXIAL TENSILE TEST RESULTS
2014-T6 and 2219-T87 Parent Metal and Weldments

Material & Process	Panel No.	Specimen No.	Yield Str. 0.2% Offset ksi	Ultimate Strength ksi	Elongation in 2 in. %
TIG 2014-T6 4043	BP54	1	41.0	50.8	1.8
		2	39.9	54.3	1.8
		3	39.1	47.4	2.0
		4	37.5	47.2	1.6
		5	38.6	46.8	2.0
	BP56	1	42.7	51.6	2.3
		2	37.3	47.5	1.6
		3	38.1	51.9	1.6
		4	36.2	43.2	1.4
		5	38.2	45.9	1.6
	BP57	1	39.4	49.6	2.0
		2	38.4	47.8	2.3
		3	41.3	51.1	2.3
		4	39.6	53.1	2.4
		5	39.1	53.9	3.0
	BP58	1	40.4	54.0	2.5
		2	38.6	51.6	2.6
		3	37.3	53.1	2.8
		4	39.0	46.9	1.9
		5	38.1	43.3	2.2
	BP59	1	38.1	49.4	2.3
		2	41.5	57.2	2.4
		3	41.3	55.9	3.0
		4	40.1	57.4	2.1
		5	39.9	46.5	2.1
	BP51	1	39.7	47.0	1.5
		2	40.7	41.1	1.0
		3	42.9	43.6	1.5
		4	39.2	42.8	1.7
	BP52	1	41.4	47.9	1.8
		2	41.0	46.7	1.6
		3	41.5	46.5	1.4
		4	40.2	45.4	1.5
		5	39.0	43.7	1.1
	BP53	1	38.2	42.0	1.6
		2	40.9	41.1	1.5
		3	39.1	40.0	1.5
		4	39.8	42.3	1.3
		5	39.5	42.1	1.9

TABLE A-II (Continued)

UNIAXIAL TENSILE TEST RESULTS
2014-T6 and 2219-T87 Parent Metal and Weldments

Material & Process	Panel No.	Specimen No.	Yield Str. 0.2% Offset ksi	Ultimate Strength ksi	Elongation in 2 in. %
MIG 2014-T6 4043	BP29	1	34.6	48.9	2.9
		2	36.2	45.0	1.6
		3	34.7	45.5	2.0
		4	29.9	36.3	1.2
		5	32.4	38.1	1.7
	BP30	1	35.1	46.1	2.2
		2	36.1	43.4	1.2
		3	34.2	43.9	2.1
		4	30.5	36.0	1.3
		5	34.6	39.2	1.3
	BP35	1	34.8	42.4	1.3
		2	36.2	40.3	1.8
		3	31.4	31.4	1.3
		4	33.2	35.4	1.3
	BP36	1	38.0	44.1	2.1
		2	38.6	45.1	1.3
		3	35.0	43.6	1.8
		4	40.6	45.5	1.1
		5	32.6	34.9	1.3
	BP70	1	37.1	41.7	2.3
		2	36.6	44.3	2.5
		3	36.7	43.7	2.5
	BP28	1	35.5	43.5	1.9
		2	37.5	45.2	1.9
		3	36.1	45.5	1.9
		4	34.9	42.6	1.4
		5	36.1	44.9	2.3
	BP31	1	36.3	44.4	1.6
		2	35.4	40.7	1.6
		3	36.6	46.0	2.0
		4	35.8	45.1	2.0
		5	33.0	34.0	1.4
	BP33	1	36.6	40.6	1.2
		2	36.6	40.4	1.5
		3	38.6	45.0	1.8
		4	37.4	47.8	1.8
		5	38.6	38.6	1.6

TABLE A-II (Continued)

UNIAXIAL TENSILE TEST RESULTS
2014-T6 and 2219-T87 Parent Metal and Weldments

Material & Process	Panel No.	Specimen No.	Yield Str. 0.2% Offset ksi	Ultimate Strength ksi	Elongation in 2 in. %
TIG 2219-T87 2319	BP7	1	37.9	41.8	1.7
		2	34.9	41.9	1.1
		3	34.5	47.8	2.2
		4	34.4	48.0	1.5
		5	35.8	47.5	1.8
		6	34.1	41.2	1.8
	BP8	1	35.5	42.8	1.8
		2	37.5	41.3	1.8
		3	33.3	41.6	1.3
		4	36.1	42.1	1.5
		5	37.9	47.8	1.5
		6	33.8	40.9	1.9
	BP9	1	34.0	40.9	2.1
		2	35.5	42.6	2.0
		3	35.9	47.7	1.4
		4	32.1	41.3	1.9
		5	33.5	42.3	1.9
		6	35.3	46.8	1.9
	BP10	1	31.2	42.3	1.7
		2	30.4	40.4	2.1
		3	31.8	42.7	2.1
		4	31.6	42.2	2.4
		5	31.5	44.3	2.0
	BP12	1	31.7	43.7	2.0
		2	32.1	44.1	1.8
		3	31.9	41.6	1.8
		4	34.5	45.3	2.1
		5	31.4	43.2	2.5
	BP60	1	34.1	45.2	2.1
		2	30.9	42.8	1.7
		3	30.9	43.2	2.1
		4	32.4	45.5	2.1
		5	34.5	46.1	2.5
	BP4	1	34.6	44.0	1.4
		2	35.6	43.5	1.4
		3	31.4	43.6	1.4
		4	34.3	44.2	1.5
		5	32.8	43.5	2.1

TABLE A-II (Continued)

UNIAXIAL TENSILE TEST RESULTS
2014-T6 and 2219-T87 Parent Metal and Weldments

Material & Process	Panel No.	Specimen No.	Yield Str. 0.2% Offset ksi	Ultimate Strength ksi	Elongation in 2 in. %
TIG 2219-T87 2319 (Continued)	BP5	1	31.7	43.5	1.6
		2	31.7	43.9	2.1
		3	32.5	45.5	2.0
		4	33.4	46.0	2.0
		5	33.0	46.0	2.1
	BP6	1	33.0	42.4	1.7
		2	29.7	39.6	1.4
		3	34.1	41.5	1.6
		4	32.2	40.3	1.8
		5	32.4	42.5	1.8
MIG 2219-T87 2319	BP26	1	28.6	47.3	3.4
		2	27.4	43.6	3.2
		3	30.9	45.9	3.2
		4	28.4	45.0	2.4
		5	26.7	42.8	3.2
	BP27	1	27.6	41.9	2.3
		2	29.6	40.5	1.9
		3	28.9	39.9	2.7
		4	29.5	39.7	2.0
		5	27.6	39.1	2.3
	BP65	1	30.0	45.1	3.0
		2	26.8	40.5	2.0
		3	29.1	45.0	2.1
		4	28.0	45.2	3.6
		5	28.4	42.0	2.1
	BP68	1	28.6	43.7	3.2
		2	28.7	43.4	3.0
		3	28.9	41.9	3.4
		4	28.8	43.5	2.9
		5	28.2	43.7	3.1
	BP69	1	27.7	42.1	3.3
		2	29.5	43.6	3.6
		3	27.7	42.0	3.4
		4	28.8	41.6	2.2
		5	29.7	41.1	3.3

TABLE A-II (Continued)

UNIAXIAL TENSILE TEST RESULTS
2014-T6 and 2219-T87 Parent Metal and Weldments

Material & Process	Panel No.	Specimen No.	Yield Str. 0.2% Offset ksi	Ultimate Strength ksi	Elongation in 2 in. %
MIG 2219-T87 2319 (Continued)	BP71	1	26.2	41.3	3.3
		2	31.8	40.7	3.2
	BP23	1	25.5	40.6	2.9
		2	29.6	41.6	2.1
		3	32.3	45.4	2.1
		4	26.0	42.9	2.8
		5	26.7	40.6	2.9
	BP63	1	31.3	47.7	4.8
		2	28.9	44.5	4.0
		3	26.0	42.6	3.5
		4	29.2	43.4	3.2
		5	29.5	42.3	3.5
	BP64	1	29.4	43.2	2.6
		2	30.6	42.7	2.2
		3	29.5	42.3	2.2
		4	30.3	43.5	2.7
	BP72	1	28.9	40.9	2.3
		2	27.4	42.4	2.8
		3	27.4	41.5	3.2
		4	29.3	41.9	3.1
		5	28.4	41.8	2.5

TABLE A-III

HYDRAULIC BULGE TEST RESULTS

Annealed 2219-T87 Parent Metal and Weldments
and Special Purpose 2219-T87 Weldments

Panel Description				Maximum Pressure psi	Bulge Height in.	Biaxial Ult. Str. ksi
Material & Process	Type	Welding Procedure	Number			
2219-T87	Annealed Parent Metal		BMA1 BMA2 BMA3	475 482 485	7.95 7.55 7.10	23.6 24.2 25.4
TIG 2219-T87 2319	Single Weld (Annealed)	64-A2	BP40 BP41 BP42	476 440 430	6.00 5.90 4.95	23.8 21.9 24.2
TIG 2219-T87 2319	Single Weld (Crowns Removed)	64-A2	BP44 BP45 BP46	166 174 156	1.35 1.30 1.27	33.9 36.9 33.9
TIG 2219-T87 2319	Single Weld (Multipass)	64-A5	BP47 BP48 BP50	222 216 212	1.70 1.50 1.52	35.7 39.6 38.2

TABLE A-IV

UNIAXIAL TENSILE TEST RESULTS

Annealed 2219-T87 Parent Metal and Weldments
and Special Purpose 2219-T87 Weldments

Material & Process	Panel Number	Specimen Number	Yield Strength 0.2% Offset ksi	Ultimate Strength ksi	Elongation in 2 inches %
2219-T87 Parent Metal (Annealed)	BMA1	1	13.8	27.1	22.2
		2	13.7	27.3	22.2
		3	13.8	27.5	22.3
		4	13.5	27.1	22.1
		5	13.4	27.0	22.6
TIG 2219-T87 2319 (Annealed)	BP40	1	12.8	27.7	19.6
		2	13.1	27.4	18.2
		3	13.5	28.2	21.2
		4	13.6	27.8	19.2
		5	12.5	26.8	18.3
	BP41	1	13.1	27.4	19.3
		2	12.9	27.0	19.8
		3	13.4	28.0	19.2
		4	13.0	27.7	19.3
		5	13.4	28.1	20.1
	BP42	1	13.2	27.3	19.5
		2	12.9	27.4	19.8
		3	13.6	28.3	19.8
		4	13.4	27.8	17.2
		5	13.2	27.9	19.7

TABLE A-IV (continued)

UNIAXIAL TENSILE TEST RESULTS

Annealed 2219-T87 Parent Metal and Weldments
and Special Purpose 2219-T87 Weldments

Material & Process	Panel Number	Specimen Number	Yield Strength 0.2% Offset ksi	Ultimate Strength ksi	Elongation in 2 inches %
TIG 2219-T87 2319 (Crowns Removed)	BP44	1	---	37.2	3.8
		2	27.4	39.1	3.3
		3	28.0	40.4	2.6
		4	25 6	39.4	3.6
		5	25.0	38.6	3.3
	BP45	1	26.7	40.4	2.5
		2	27.2	40.3	3.0
		3	25.9	40.3	3.3
		4	26.5	40.6	3.3
		5	27.1	40.5	2.4
	BP46	1	28.0	40.2	2.9
		2	27.9	40.0	3.0
		3	26.0	40.0	3.3
		4	27.7	40.3	3.3
		5	27.0	40.3	3.3
TIG 2219-T87 2319 (Multipass)	BP47	1	25.8	43.8	2.7
		2	28.4	45.3	2.7
		3	27.2	45.0	2.9
		4	28.3	46.1	3.0
		5	29.1	44.0	2.2
	BP48	1	26.8	45.7	3.5
		2	28.5	45.2	3.5
		3	27.3	46.9	4.0
		4	28.7	46.2	4.0
		5	28.7	45.8	3.4
	BP50	1	28.3	43.6	2.5
		2	29.1	45.8	3.3
		3	27.5	45.2	3.4
		4	27.7	45.9	3.4

TABLE A-V

RESULTS OF UNIAXIAL TENSILE TESTS ON X7106-T63 PARENT METAL

Thickness in.	Grain Direction	Yield Strength (0.2% Offset) ksi	Ultimate Strength ksi	Elongation in 2 inches %
.090	Long	54.7	60.7	11.7
		53.9	60.1	11.2
		54.3	60.0	11.2
		53.7	59.4	11.8
		53.6	59.4	11.5
	Trans.	55.6	62.4	10.2
		56.0	62.8	10.7
		55.9	62.8	10.7
		55.3	62.1	10.2
		55.6	62.4	10.5
.187	Long	61.0	67.8	11.2
		61.3	68.3	10.0
		60.7	67.8	11.0
		60.9	67.8	11.2
		61.0	68.1	11.1
	Trans	59.0	66.1	11.6
		58.6	65.7	12.5
		58.8	66.2	12.5
		58.9	65.7	13.3
		58.8	65.7	12.0

TABLE A-V (continued)

RESULTS OF UNIAXIAL TENSILE TESTS ON X7106-T63 PARENT METAL

Thickness in.	Grain Direction	Yield Strength (0.2% Offset) ksi	Ultimate Strength ksi	Elongation in 2 inches %
.500	Long	59.0	64.6	17.7
		60.1	65.8	17.8
		58.5	64.4	17.8
		59.1	65.0	17.8
		58.8	64.8	17.5
	Trans.	58.5	64.2	16.6
		58.9	64.4	17.0
		58.8	64.3	15.2
		59.1	64.3	15.7
		58.7	64.2	15.7
1.00	Long.	58.1	64.1	20.7
		58.4	64.5	20.9
		57.9	64.0	20.9
		58.8	64.9	20.7
		58.4	64.3	20.5
	Trans.	56.0	61.9	19.4
		56.2	62.2	19.1
		56.1	62.1	19.4
		56.1	61.9	19.9
		56.2	62.1	19.3

TABLE A-VI

RESULTS OF UNIAXIAL TENSILE TESTS ON 0.090 INCH THICK X7106-T63 WELDMENTS

Process and Filler Metal	Panel	Aging Time	Yield Str. 0.2% Offset ksi	Ultimate Strength ksi	Elong in 2 in. %	Failure Location*
TIG X5180	A	1 day	31.3	46.0	5.3	HAZ
			30.1	46.0	5.9	HAZ
			31.1	45.6	3.0	FL
			31.3	45.2	3.3	FL
			31.2	45.7	3.3	FL
	B	1 day	30.5	46.5	5.5	FL
			31.2	46.5	4.5	FL
			30.7	46.9	5.1	FL
			30.7	46.6	4.5	FL
			30.6	46.3	5.1	FL
	A	1 wk.	34.8	49.9	3.1	HAZ
			35.8	50.9	3.7	FL
			36.8	49.9	2.7	FL
			36.5	51.1	4.9	HAZ
			35.9	51.6	4.9	HAZ
	B	1 wk.	35.2	50.9	4.7	HAZ
			35.7	50.2	3.6	FL
			36.2	50.0	3.6	FL
			37.3	51.1	4.1	HAZ
			35.0	50.4	5.6	HAZ
	A	2 wks.	37.5	52.6	4.8	HAZ
			36.6	52.4	4.8	HAZ
			37.2	52.0	2.9	FL
			39.1	52.3	3.8	HAZ
			37.6	52.1	4.3	HAZ
	B	2 wks.	37.5	52.0	4.7	HAZ
			38.0	52.3	4.3	HAZ
			38.2	52.8	4.6	HAZ
			36.4	51.5	5.3	HAZ
			36.4	52.0	5.0	HAZ
	A	4 wks.	37.2	51.6	2.2	FL
			38.5	52.9	5.6	HAZ
			38.0	53.1	4.3	HAZ
			38.6	53.1	5.1	HAZ
			39.1	53.0	4.6	HAZ

* HAZ = Heat affected zone
FL = Fusion line

TABLE A-VI (Continued)

RESULTS OF UNIAXIAL TENSILE TESTS ON 0.090 INCH THICK X7106-T63 WELDMENTS

Process and Filler Metal	Panel	Aging Time	Yield Str. 0.2% Offset ksi	Ultimate Strength ksi	Elong. in 2 in. %	Failure Location*
TIG X5180	B	4 wks.	36.8	53.0	5.6	HAZ
			37.1	52.2	5.2	HAZ
			39.0	53.5	5.2	HAZ
			39.1	53.6	4.7	HAZ
			38.9	53.3	4.7	HAZ
	A	8 wks.	41.1	52.3	3.9	HAZ
			41.6	51.3	2.7	FL
			39.4	52.4	4.1	HAZ
			39.5	53.3	4.8	HAZ
			39.4	53.2	4.3	HAZ
	B	8 wks.	40.4	52.7	4.4	HAZ
			38.7	52.0	5.2	HAZ
			39.0	53.2	4.7	HAZ
			39.1	52.3	4.8	HAZ
			37.9	52.0	4.5	HAZ
	A	12 wks.	40.8	54.6	4.9	HAZ
			41.7	55.0	4.8	HAZ
			39.8	53.6	3.0	FL
			41.5	55.1	5.1	HAZ
			40.6	55.3	5.5	HAZ
	A	19 wks.	41.2	55.2	4.3	HAZ
			42.8	56.3	4.6	HAZ
			40.7	56.3	5.0	HAZ
			41.7	55.3	4.2	HAZ
			41.6	56.0	4.4	HAZ
	A	24 wks.	41.0	55.0	5.3	HAZ
			41.6	55.4	5.5	HAZ
			40.7	56.3	4.3	HAZ
			41.5	55.4	5.1	HAZ
			40.7	55.7	4.4	FL
	B	24 wks.	41.2	55.5	5.9	HAZ
			41.5	54.3	5.3	HAZ
			39.6	50.8	3.9	HAZ
			41.8	55.0	4.5	HAZ
			41.0	54.9	5.9	HAZ

* HAZ = Heat affected zone
FL = Fusion line

TABLE A-VI (Continued)

RESULTS OF UNIAXIAL TENSILE TESTS ON
0.090 INCH THICK X7106-T63 WELDMENTS

Process and Filler Metal	Panel	Aging Time	Yield Str. 0.2% Offset ksi	Ultimate Strength ksi	Elong. in 2 in. %	Failure Location*
TIG 5356	C	1 day	27.3	43.6	5.1	FL
			30.1	44.3	3.5	FL
			30.0	45.1	4.4	FL
			28.9	45.5	6.0	HAZ
			29.5	44.8	4.3	FL
	C	1 wk.	34.2	51.3	5.1	HAZ
			34.0	50.8	4.4	FL
			34.1	50.6	4.0	FL
			35.7	51.1	4.8	HAZ
			36.8	51.3	4.5	HAZ
	C	2 wks.	36.4	52.0	3.5	FL
			37.5	52.3	4.3	HAZ
			36.5	50.6	4.8	HAZ
			35.3	52.5	7.1	HAZ
			35.9	49.9	2.9	FL
	C	4 wks.	38.0	53.1	4.7	HAZ
			37.9	53.6	4.5	HAZ
			38.0	52.0	3.2	FL
			39.7	52.6	3.2	FL
			36.4	50.3	2.9	FL
	C	8 wks.	39.5	52.8	3.2	FL
			39.4	53.2	5.0	HAZ
			37.3	52.0	4.6	FL
			38.5	53.1	5.4	HAZ
			38.8	52.5	4.0	HAZ
	C	12 wks.	39.4	53.5	4.3	HAZ
			39.1	54.1	4.6	HAZ
			39.7	50.3	3.5	FL
			40.0	54.6	5.1	HAZ
			39.5	53.6	5.0	HAZ
	C	24 wks.	40.0	55.1	6.2	HAZ
			40.0	54.7	4.6	FL
			39.8	54.8	6.2	HAZ
			41.2	54.8	6.3	HAZ
			42.0	55.6	6.3	HAZ

* HAZ = Heat affected zone
FL = Fusion line

TABLE A VI (Continued)

RESULTS OF UNIAXIAL TENSILE TESTS ON
0.090 INCH THICK X7106-T63 WELDMENTS

Process and Filler Metal	Panel	Aging Time	Yield Str. 0.2% Offset ksi	Ultimate Strength ksi	Elong. in 2 in. %	Failure Location*
TIG 5556	D	1 day	32.3	45.8	3.8	HAZ
			32.9	43.2	3.4	HAZ
			33.3	45.7	4.4	HAZ
			33.8	46.3	4.5	HAZ
			33.9	46.3	4.4	HAZ
	D	1 wk.	37.6	51.1	4.7	HAZ
			36.6	49.5	4.9	HAZ
			37.6	51.0	4.7	HAZ
			38.5	50.9	4.0	HAZ
			36.5	50.2	3.9	HAZ
	D	2 wks.	38.7	51.9	4.7	HAZ
			37.9	51.3	3.6	FL
			38.1	53.3	3.8	HAZ
			37.6	51.0	3.0	FL
			36.9	52.3	5.0	HAZ
	D	4 wks.	39.1	52.5	5.6	HAZ
			39.1	51.1	2.9	FL
			38.6	53.1	5.3	HAZ
			38.5	51.2	2.5	Weld
			38.7	53.1	4.7	HAZ
	D	8 wks.	37.9	52.1	5.4	HAZ
			39.2	51.6	3.8	FL
			39.0	51.6	4.5	HAZ
			38.6	51.5	3.3	FL
			38.6	53.0	4.8	HAZ
	D	12 wks.	39.7	54.4	4.5	FL
			40.0	54.2	5.8	HAZ
			41.0	54.1	5.4	HAZ
			39.7	53.9	4.9	HAZ
			38.5	53.3	5.2	HAZ
	D	24 wks.	39.1	54.6	6.0	HAZ
			39.2	54.0	4.5	HAZ
			39.4	52.5	3.5	FL
			38.9	54.3	5.2	HAZ
			39.1	53.6	4.6	HAZ

*HAZ = Heat affected zone
FL = Fusion line

TABLE A-VI (Continued)

RESULTS OF UNIAXIAL TENSILE TESTS ON
0.090 INCH THICK X7106-T63 WELDMENTS

Process and Filler Metal	Panel	Aging Time	Yield Str. 0.2% Offset ksi	Ultimate Strength ksi	Elong. in 2 in. %	Failure Location*
MIG X5180	E	1 day	32.8	46.8	4.2	HAZ
			31.8	46.3	4.8	HAZ
			31.5	46.7	3.9	HAZ
			31.4	46.4	5.0	HAZ
			31.8	46.5	4.9	HAZ
	E	1 wk.	35.3	49.2	5.2	HAZ
			34.5	49.0	4.6	HAZ
			39.7	53.2	5.6	HAZ
			34.3	48.9	5.3	HAZ
			34.3	50.1	5.7	HAZ
	E	2 wks.	36.8	51.3	5.0	HAZ
			37.2	50.0	3.4	FL
			38.7	51.0	3.4	HAZ
			36.6	50.0	5.3	HAZ
			35.5	50.0	5.3	HAZ
	E	4 wks.	36.2	50.6	5.8	HAZ
			38.1	51.9	4.5	HAZ
			37.2	50.5	3.5	FL
			35.2	50.4	5.8	HAZ
			36.8	50.4	4.6	HAZ
	E	8 wks.	38.5	52.4	4.8	HAZ
			37.4	51.8	4.7	HAZ
			39.5	53.9	5.2	HAZ
			37.0	51.0	5.0	HAZ
			37.7	51.5	4.9	HAZ
	E	24 wks.	40.8	52.6	3.4	HAZ
			38.2	52.3	4.6	HAZ
MIG 5356	F	4 wks.	35.2	48.9	4.2	HAZ
			35.3	50.4	5.1	HAZ
			37.4	51.3	3.9	FL
			36.3	50.7	4.6	HAZ
			36.2	49.5	4.5	HAZ

* HAZ = Heat affected zone
FL = Fusion line

TABLE A-VI (Continued)

RESULTS OF UNIAXIAL TENSILE TESTS ON
0.090 INCH THICK X7106-T63 WELDMENTS

Process and Filler Metal	Panel	Aging Time	Yield Str. 0.2% Offset ksi	Ultimate Strength ksi	Elong. in 2 in. %	Failure Location*
MIG 5356	F	24 wks.	39.8	53.6	4.2	FL
			39.1	53.3	4.7	HAZ
			37.7	51.4	3.3	HAZ
			39.9	51.8	2.6	FL
			37.1	52.9	5.5	HAZ
MIG 5556	G	4 wks.	35.7	49.4	4.4	HAZ
			36.4	48.5	2.5	FL
			38.0	50.2	4.9	HAZ
			36.2	50.3	5.0	HAZ
			35.2	49.3	5.8	HAZ
	G	24 wks.	38.6	51.5	4.4	HAZ
			----	53.1	5.2	HAZ
			38.9	52.0	3.4	HAZ
			43.4	53.4	4.0	HAZ
			38.6	51.7	3.9	HAZ

*HAZ = Heat affected zone
FL = Fusion line

APPENDIX B

APPENDIX B

STUDY OF APPLICABILITY OF MEMBRANE STRESS EQUATION

To complete the investigation, the applicability of the membrane stress equation to the bulge test was studied. One source of error in the use of the membrane stress equation might be a nonuniform bulge contour, since the radius of curvature enters into the derivation of the equation. The bulge contour of an annealed base metal panel (No. BMA-2) was determined by caliper measurements, while under pressure, at the center and on three chords of 4, 10 and 16-inches (concentric about the center of the panel). The average radius of curvature was computed over each chord. The results were:

Annealed Base Metal 2219 Panel No. BMA-2

Position	Chord (Inches)	Segment Height (Inches)	Average Radius of Curvature (Inches)
2" from center	4	0.14	14.4
5" from center	10	0.49	25.8
8" from center	16	1.13	28.9

The average radius of curvature calculated from the bulge height and die geometry (which is used in the membrane stress equation) was 28.2 inches. This indicates that the panel deviates somewhat from a spherical shape while being pressurized, and that most of the deviation occurs near the center of the panel. A similar set of measurements was carried out on the as-welded panel while under pressure. The results were as follows:

As-Welded 2219 Panel No. BP-60

Position	Chord (Inches)	Segment Height (Inches)	Average Radius of Curvature (Inches)
2" from center	4	.20	10.1
5" from center	8	.32	39.2
8" from center	16	.59	54.5

The average radius of curvature calculated from the bulge height and die geometry was 57.6 inches, agreeing quite well with the average radius of curvature over the 16-inch chord. Comparison of BP-60 and BMA-2 indicates that the more serious discrepancy might occur in welded panels than in base metal panels, since the welded panels fail at much lower values of pressure and deflection.

It is difficult to evaluate the true effect of this nonuniformity on the state of stress in the bulge panel. It apparently has no effect on the membrane stress per se, because the smaller radius of curvature at the panel center would minimize the calculated membrane stress there. Examination of failed panels revealed that in many cases failure initiated at the center of the panel. In the remainder of panels examined, the origin of fracture was not clear. The nonuniformity of bulge contour might be explained by the presence of bending stresses superimposed on the membrane stresses.

Another possible approach is to assume that the membrane stress equation is not applicable to the pressurization of a flat plate. The membrane stress equation was derived for a thin walled vessel with the form of a surface of revolution. Timoshenko [2] derived a set of equations pertaining to a thin, flat circular plate clamped at the edge and loaded with a uniform pressure. The equation for the stress at the center of the plate is given by:

$$\sigma = 0.423 \left(\frac{Eq^2a^2}{h^2}\right)^{1/3}$$

Where:
σ = stress, psi (circular plate)
E = modulus of elasticity, psi
q = applied uniform pressure, psi
a = radius of circular plate, inches
h = thickness of plate, inches

This equation does not make use of the radius of curvature of the bulged panel and the stress is not uniform over the entire area of the plate. It is maximum at the center and falls to approximately 3/4 of this value at the edge. This stress distribution could result in a nonspherical bulge. The equation is limited to use under conditions of elastic deformation.

The welded panels have all failed at low pressure levels because of the presence of a weld and/or heat-affected zone. In most cases, failure occurred with very little, if any, plastic deformation of the base metal. Therefore, it is possible to investigate the state of stress in a welded bulge panel by monitoring strain gages attached to the base metal.

A two element, 90° resistance strain gage rosette was mounted on the 2014-T6 base metal of Bulge Panel 54. It was located approximately one inch from the center of the panel and on the surface which would become convex during the test (outside surface). A number of data points (hydraulic pressure, bulge height, strain readings) were taken before the panel fractured. Membrane stresses were calculated from the pressure and bulge height data; circular plate stresses were calculated from the pressure data; and fiber stresses were calculated from the strain gage data. The stresses calculated by the three methods are summarized in the following table:

Welded (TIG 2014-T6/4043) Panel No. BP-54

Applied Pressure (psi)	Measured Deflection (Inch)	Membrane Stress (psi)	Circular Plate Stress (psi)	Outer Fiber Stress (psi)
10	0.5	5,700	9,150	12,500
64	1.0	17,800	31,500	36,400
82	1.1	20,700	37,300	42,000
102	1.2	23,500	43,300	47,400
123	1.3	26,100	48,900	53,300
147	1.4	28,900	54,900	58,200
171	1.5	31,300	60,900	63,600

The circular plate stress equation appears to produce a better estimate of the stress than does the membrane stress equation. The choice between the two methods should not be made, however, until additional work is initiated to determine the magnitude of bending stresses existing at the point of strain gage attachment.

APPENDIX C

APPENDIX C

EXAMINATION OF HYDRAULIC BULGE PANELS AND UNIAXIAL TENSILE SPECIMENS

A. Hydraulic Bulge Panels

The hydraulic bulge tests of Panels 17, 18 and 19 exhibited a range of 4.6 ksi for the calculated biaxial ultimate strength. In an effort to explain why this difference occurred an examination was made of the panels. The results of the tests of these panels were as follows:

Bulge Panel No.	Biaxial Ultimate Strength (ksi)
17	47.0
18	42.9
19	42.4

These panels were prepared by the TIG welding process, using 1/8-inch 2014-T6 base material and 2319 filler metal. The panels were of the tee weld configuration.

The panels were first visually examined and then measurements made of the height and width of the weld crowns and "drop throughs" (penetration crowns). Such measurements can provide an indication of any variations in current, voltage, travel speed, etc. occurring during the welding operation.

At most locations along the welds, the crowns and "drop throughs" of the bulged panels were distorted as a result of either clamping the panels in the bulge fixture of straining during bulge testing. The only locations on the welds that could be found in which the crowns and "drop throughs" had not been distorted are depicted in Figure C-1 as "A", "C" and "D". These locations were in the hold down area of the bulge fixture close to the location where the panels begin to deform into a bulge. Ridges machined in the top die of the fixture to prevent slippage of the panels during testing prevented the crowns and "drop throughs" from being distorted at these locations. The measurements of the crowns and "drop throughs" are listed in Table C-1.

Differences in the highest strength panel (No. 17) as compared to the other two were detected and may be summarized as follows:

1) In Panel No. 17 the crown of weld No. 1 at location "B" (Figure C-1) was partially ground off to lay a strain gage.

2) Weld No. 2 of Panel No. 17 had smaller width and height dimensions than the No. 2 welds in Panels 18 and 19 (Note Table C-1). The contour

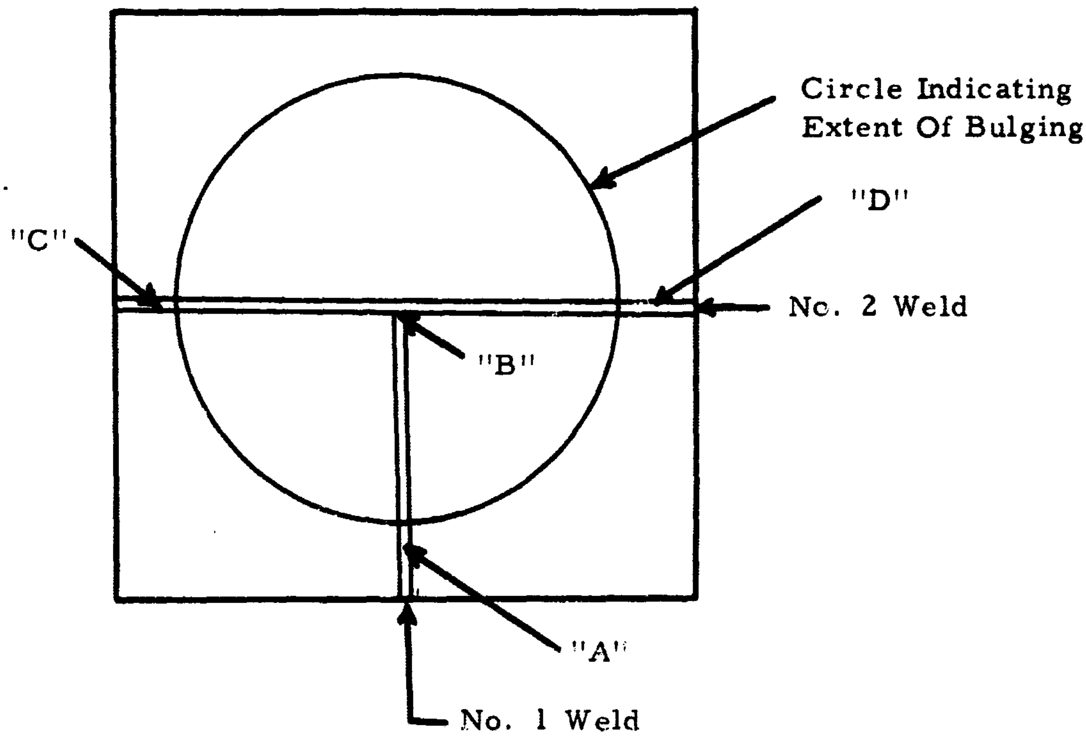

FIGURE C-1. LOCATIONS USED FOR WELD MEASUREMENTS
OF BIAXIAL PANELS 17, 18 AND 19

TABLE C-I

HEIGHT AND WIDTH MEASUREMENTS[1] OF WELD CROWNS AND "DROP THROUGHS" OF BULGE PANELS 17, 18 AND 19

Panel No.	Location		Weld Crown Height (In.)	Weld Crown Width (In.)	"Drop Through" Depth (In.)	"Drop Through" Width (In.)
17	A	Weld #1	.024	.208	.032	.116
	B	Weld #1	.006[2]	----	.026	----
	C	Weld #2	.022	.220	.027	.110
	D	Weld #2	.019	.210	.016	.070
18	A	Weld #1	.019	.220	.026	.112
	B	Weld #1	.020	.215	.032	.120
	C	Weld #2	.025	.240	.025	.125
	D	Weld #2	.022	.247	----	.105
19	A	Weld #1	.020	.230	.007	.120
	B	Weld #1	.019	.235	.030	.121
	C	Weld #2	.029	.235	.027	.120
	D	Weld #2	.025	.240	.027	.105

1 The location of these measurements schematically shown in Figure B-1.

2 Crown partially ground off.

of the "drop through" in weld No. 2 (Panel No. 17) was irregular for a 3-inch length at one end.

Visual examinations of the fracture also revealed differences in Panel No. 17. This panel had a relatively straight fracture along the fusion line. Panels 18 and 19 had part of their fractures in the heat-affected base metal. At the intersection of the welds the fractures in Panels 18 and 19 shifted from weld No. 2 into weld No. 1. This was not the case in Panel No. 17 where the entire length of the fracture was in fusion line of weld No. 2.

The differences noted in the three panels examined are not considered to be unusual and no indications of abnormal defects were noted in any of the panels. Thus, the observed differences in biaxial ultimate strength must be considered as inherent in bulge tests of these weldments or inherent in the methods presently used in the interpretation of bulge test results.

B. Uniaxial Tensile Specimens

In addition to biaxial ultimate strength variations in the bulge panels, scatter also occurred in some of the uniaxial ultimate strength results. To obtain the uniaxial strength of a panel, five or six uniaxial tensile specimens were machined from the panel and tested and the results averaged. Large variations in strength resulted within these groups of specimens in eight of the panels. In the worst case a 12.6 ksi spread between high and low ultimate tensile values existed. To determine the cause of this variation, the tensile specimens from eight bulge panels were examined. These bulge panels are listed below:

Bulge Panel No.	Weld Configuration	Welding Process/Base Metal/ Filler Metal
7	Single	TIG/2219-T87/2319
8	Single	TIG/2219-T87/2319
29	Single	MIG/2014-T6/4043
30	Single	MIG/2014-T6/4043
31	Cross	MIG/2014-T6/4943
33	Cross	MIG/2014-T6/4043
35	Tee	MIG/2014-T6/4043
36	Tee	MIG/2014-T6/4043

The fracture faces of each set of tensile specimens were examined for defects that might account for low tensile values. No relationship between the isolated defects observed and low strength specimens was found.

After this examination, the specimens were etched in mixed acid solution to identify the weld deposit in cross section. The resultant weld profile was studied. Measurements of the width and height of the weld crowns and "drop throughs" were made. The location of these measurements is depicted in

Figure C-2. Variations of weld profile within each set of specimens were observed. These variations were most pronounced in the MIG specimens. In addition to the weld profile varying from specimen to specimen, differences were noted across the width of some tensile specimens. The weld contours were also found to vary to some extent.

As a result of these variations, it was possible to separate most of the specimens into two general groups; wide weld profile and narrow weld profile. After separation, it was found that the specimens containing the large weld deposits were those having the lowest tensile strength. This was true in both MIG and TIG specimens. Measurements and observation of weld profiles in uniaxial tensile specimens are listed in Table C-II.

Although differences in the width of the weld crowns were noted, the magnitudes of these differences are considered to be comparable to the variations which may be expected in production. In addition, no other defects or abnormal variations were noted. Thus the scatter noted in the uniaxial tensile test results should be regarded as inherent in the particular types of weldments tested.

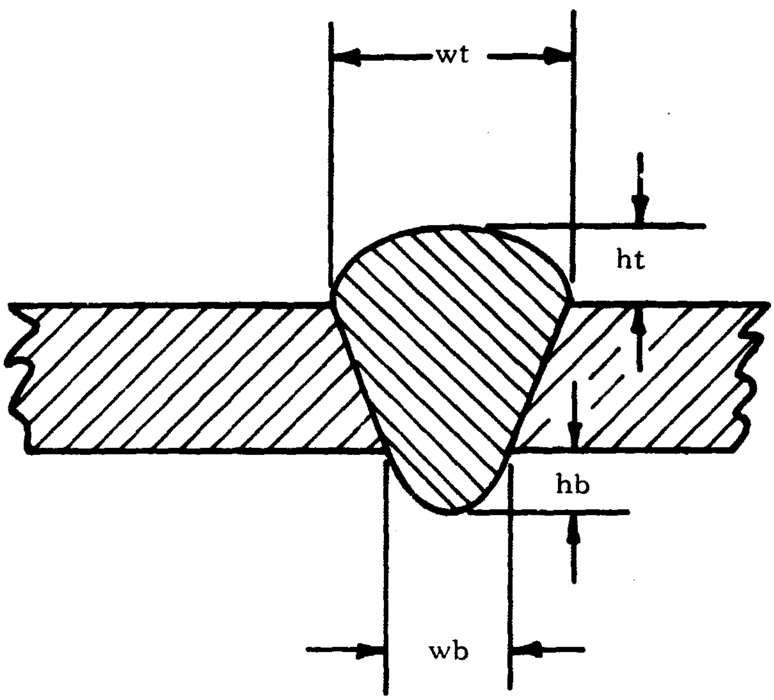

wt = width of crown
ht = height of crown
wb = width of drop through
hb = height of drop through

FIGURE C-2. MEASUREMENTS MADE ON WELD BEAD

TABLE C-II

RELATIONSHIP BETWEEN WELD PROFILE SIZE AND UNIAXIAL ULTIMATE STRENGTH

Bulge Panel Number	Panel Identification	Uniaxial Ultimate Strength, (ksi)	Relative Weld Profile Size[1]
7	TIG	41.8	Wide
	2219-T87/	41.9	Wide
	2319	47.8	Narrow
	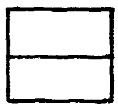	48.0	Narrow
		47.5	Narrow
		41.2	Wide
8	TIG	42.8	Wide
	2219-T87/	41.3	Wide
	2319	41.6	Wide
	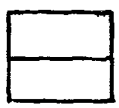	42.1	Wide
		47.8	Narrow
		40.9	Wide
29	MIG	48.9	Narrow
	2014-T6/	36.3	- - -
	4043	45.0	Narrow
	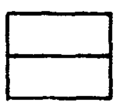	45.5	- - -
		38.1	Wide
30	MIG	46.1	Narrow
	2014-T6/	36.0	Wide
	4043	43.4	Narrow
	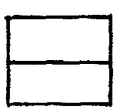	43.9	- - -
		39.2	- - -
31	MIG	44.4	- - -
	2014-T6/	40.7	- - -
	4043	34.0	Widest
	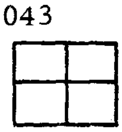	46.0	- - -
		45.1	- - -

TABLE C-11 (continued).

RELATIONSHIP BETWEEN WELD PROFILE SIZE AND UNIAXIAL ULTIMATE STRENGTH

Bulge Panel Number	Panel Identification	Uniaxial Ultimate Strength, (ksi)	Relative Weld Profile Size[1]
33	MIG	40.6	- - -
	2014-T6/	40.4	- - -
	4043	45.0	- - -
	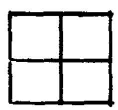	38.6	- - -
		47.8	- - -
35	MIG	42.4	Narrow
	2014-T6	31.4	Widest
	4043	35.4	Wide
		40.3	Narrow
	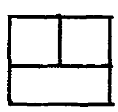		
36	MIG	44.4	Narrow
	2014-T6/	45.1	Narrow
	4043	43.6	Narrow
	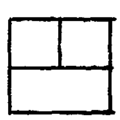	34.9	Wide
		45.5	Narrow

1 Weld profile size of MIG specimens determined by visual observation. Weld profile size of TIG specimens determined by measurements.

APPENDIX D

APPENDIX D

CALCULATION OF STANDARD DEVIATION AND LOWER TOLERANCE LIMIT

Symbols:

x_i = ultimate tensile strength (individual test)

$\bar{x} = \frac{\sum x_i}{N}$ = mean ultimate tensile strength

y_i = yield strength (individual test)

$\bar{y} = \frac{\sum y_i}{N}$ = mean yield strength

$S_x = \sqrt{\frac{\sum (x_i - \bar{x})^2}{N-1}}$ = standard deviation

LTL (U. S.) = $\bar{x} - KS_x$ = Lower Tolerance Limit of Ultimate Strength.

LTL (Y. S.) = $\bar{y} - KS_y$ = Lower Tolerance Limit of Yield Strength.

(K factor computed from non-central T distribution for 99% lower tolerance limit with 95% confidence.)

N = number of tests

Sample Calculations (TIG/2219-T87/2319 weldments)

Uniaxial Ultimate Strength

N = 48, K = 2.88

$\bar{x}$ = 43.5 ksi

$\sum (x_i - x)^2 = 228$

$S_x = \sqrt{\frac{228}{47}}$ = 2.20 ksi

LTL = 43.5-(2.88)(2.20)= 37.2 ksi

Biaxial Ultimate Strength

N = 9, K = 4.14

$\bar{x}$ = 35.3 ksi

$\sum (x_1 - x)^2 = 78.4$

$S_x = \sqrt{\frac{78.4}{8}}$ = 3.13 ksi

LTL = 35.3-4.14(3.13)= 22.3 ksi

Sample Calculations: (TIG/X7106-T63/X5180 Weldments aged 24 weeks)

Ultimate Strength

$N = 10,\ K = 3.98$

$\overline{x} = 54.8$ ksi

$\sum (x_i - \overline{x})^2 = 20.5$

$S_x = \sqrt{\dfrac{20.5}{9}} = 1.51$ ksi

LTL (U.S.) = 54.8-(3.98)(1.51)=48.8 ksi

Yield Strength

$N = 10,\ K = 3.98$

$\overline{y} = 41.1$ ksi

$\sum (y_i - \overline{y})^2 = 3.68$

$S_y = \sqrt{\dfrac{3.68}{9}} = 0.64$

LTL (Y.S.) = 41.1-(3.98)(0.64)=38.5 ksi

APPENDIX E

APPENDIX E

DISCUSSION OF MEASUREMENT OF RESIDUAL STRESS

The analysis of residual stress in structures has been done for many years and has, in many cases, been found to be a significant factor in the load carrying ability of a structure. Considerable dispute exists over what effect residual stress has on the fracture of ductile materials.

A few comments are in order on the effect of residual stresses in welded panels.

The measurement of residual stresses, especially in welded structures, requires careful attention to detail. Some technique development is also necessary. In the terms of Campus[38] "... measurement of residual stresses requires still more caution than the measurement of ordinary stresses. The measurement of residual stresses often has more the qualitative significance of a proof of the existence of residual stresses rather than the quantitative significance of a precise determination. In other words, it is difficult to evaluate and to verify the degree of approximation, the measurement indicates rather an order of magnitude".

Certainly, the magnitude of the stresses measured in the TIG and MIG welds and areas of heat-affected base metal should be interpreted as an order of magnitude measurements rather than as an "absolute" measurement. Due to welding variables no more accuracy than this should be expected. It is therefore, considered that the data reported (Table VIII) are typical results and are within normally expected deviation. Drucker[39] states "Residual stress has been blamed for much of the difficulty in welded structures. Generally, it is not residual stresses on a very small scale which are worried about, but rather stresses which exist over appreciable regions compared with any holes, notches, or other flaws existing in the welds in their neighborhood. A small amount of plastic deformation clearly wipes out residual stresses because they are associated with strains of elastic rather than plastic magnitude. Therefore, residual stresses do not matter in a slightly, or very ductile fracture". Drucker goes on to explain that the "exhaustion of ductility" in tension may be the net result of residual stress, which is to say that in achieving the residual stress, the weld may have had to plastically deform some during cooling, and "used up some ductility", thus there is "less ductility left before fracture". This seems to be the most plausible way of looking at residual stresses in these welded plates, although it is by no means quantitative. It is difficult to measure the amount of strain which occurs during welding; however, this might be an important factor for investigation.

It is, therefore, difficult to assess the importance of residual stress on fracture. This does not, however, appear to be the explanation for the lower biaxial to uniaxial strength ratio as observed in the hydraulic bulge tests.

APPENDIX F

N 6

262

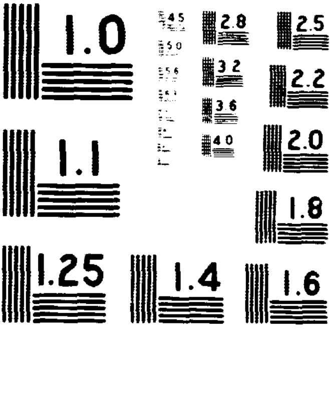

MICROCOPY RESOLUTION TEST CHART
NATIONAL BUREAU OF STANDARDS-1963

APPENDIX F

LITERATURE SURVEY

1. 7XXX Series Aluminum Alloys

The 7XXX series aluminum alloys constitute a group of Al-Zn-Mg alloys which exhibit natural age-hardening characteristics. The inherent high strength of this series of alloys provides a potential for wide application in the aircraft and aerospace industry. The early application of these alloys, however, was limited by a general lack of weldability. One particular alloy of this series, X7106, has been recently developed by the Aluminum Company of America, and it has been reported that this particular alloy combines high strength with good weldability(5). The alloy exhibits a low quench sensitivity and its natural aging characteristics provide high weld joint efficiencies without post weld heat treatments. An obvious potential application for this alloy is in the fabrication of large aerospace vehicles and components where post-weld heat treatment is impractical.

Numerous weldable alloys of the Al-Zn-Mg series have recently been developed throughout the world(6). Table F-I lists the alloy designation, country, manufacturers and composition of these alloys. The range of zinc for these alloys is 2.7-5.0 percent and the magnesium contents vary from 0.75-3.00 percent. An important consideration for these alloys is total Zn + Mg content. This range for these alloys is 4.75-7.00 percent and is below the nine percent value which has been considered responsible for a brittle structure in wrought alloys(7).

The zinc and magnesium content of X7106 is compared against Kaiser 7039 and Reynolds X7002 in Figure F-1. The relationship of these weldable alloys is also compared against the difficult to weld high-strength 7075. For the three weldable alloys the Mg + Zn range is 6.00-7.00 percent while 7075 has a Zn + Mg content of 9.1 percent. The chemical composition of X7106 is listed in Table F-II. Zinc and magnesium are the major alloying elements with additions of Zr, Cr, Mn and Ti. The zirconium is added because if its strong grain refining effect. Alcoa previously marketed an alloy X7006 with the same composition as X7106 except for the zirconium addition. The beneficial effect of grain refining by zirconium and the reduction of cracking tendencies on welding was such that X7006 was withdrawn and replaced by X7106.

The chromium content in the Al-Zn-Mg system has been found to enhance the precipitation hardening mechanism(8). It has also been reported that the addition of Cr to these alloys reduces the susceptibility to stress corrosion(9).

The 7XXX series alloys can be precipitation hardened by solution heat

TABLE F-1

COMMERCIAL AND EXPERIMENTAL WELDABLE Al-Zn-Mg ALLOYS*

Alloy Designation	Country and Manufacturer	Nominal Composition Percent						Nominal (Zn+Mg)%
		Zn	Mg	Zr	Mn	Cr	Cu	
X7106	U.S.A. - Alcoa	4.25	2.25	0.12	0.25	0.10	0.05	6.50
7039	U.S.A. - Kaiser	4.00	3.00	-	0.3	0.20	0.05	7.00
X7002	U.S.A. - Reynolds	3.5	2.5	-	0.3	-	0.75	6.00
Hiduminium 48	U.K. - High Duty Alloys	4.5	2.5	-	0.20	0.15	-	7.00
Impalco 710	U.K. - (Imperial) (Aluminum)	3.0 5.0	2.25 1.25	- -	0.50 0.50	0.20 0.15	- 0.40	[illegible].25 6.25
GBD74S	U.K. - Alcan	4.5	1.20	-	0.30	0.20	-	5.70
74S	Canada - Alcan	4.3	1.7	-	0.30	-	0.10	6.00
C7[illegible]S	Canada - Alcan	4.0	0.75	-	0.10	-	0.10	4.75
V92T	Russia	2.7	3.9	-	0.80	-	-	6.60
Superalumag-T.35	France(Trefimataux)	3.25	2.25	-	0.30	0.2	-	5.50
Konstruktal 21/55	(Germany -V.L.W. (Sweden - Svenska (Metallverken (Switzerland (Aluminum Suisse S.A.	4.6	1.2	-	0.3	0.2	-	5.8

* Based on information in Reference 6.

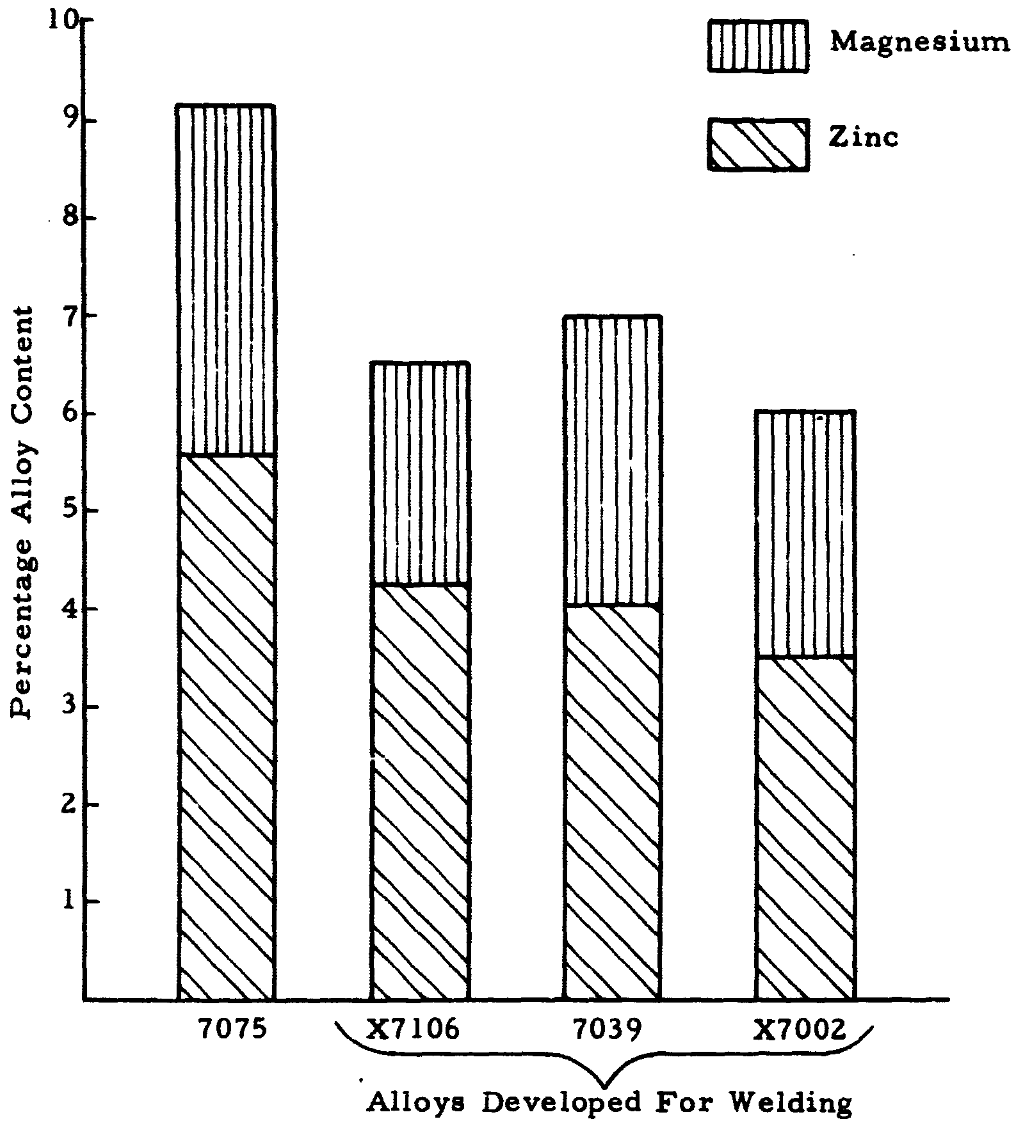

FIGURE F-1. BAR GRAPH COMPARING Zn AND Mg CONTENT OF X7106 WITH OTHER Al-Zn-Mg ALLOYS

TABLE H-II

CHEMICAL COMPOSITION OF ALUMINUM ALLOY X7106 (Reference 5)

	Composition Limits*Percent
Fe + Si	0. 35
Cu	0. 10
Mn	0. 10 - 0. 40
Mg	1. 7 - 2. 8
Zn	3. 7 - 4. 8
Ti	0. 01 - 0. 06
Cr	0. 06 - 0. 20
Zr	0. 08 - 0. 25
Others each	0. 05
Others total	0. 15

* Composition is maximum unless a range is indicated

treatment and aging cycles. The majority of opinions[4, 10, 11] hold that age hardening results from the precipitation of $MgZn_2$ but it also has been stated that the $Al_2Mg_3Zn_3$ phase is involved[12]. Figure F-2 shows the phase relationship at 824 and 392°F for the aluminum-rich corner of the Al-Zn-Mg ternary system. There is a rapid reduction in the solubility of the $MgZn_2$ and $Al_2Mg_3Zn_3$ phases with decreasing temperature. The apex of the $MgZn_2$ phase field lies at 12.3 percent Mg and 1.6 percent Zn at 824°F while at 392°F it lies at 2.8 percent Mg and 0.2 percent Zn. It is this decrease in solubility with temperature that makes precipitation hardening possible for alloys in this system.

The high solution heat treatment temperatures and close temperature control associated with age hardening of Al-Cu alloys are not necessary for alloys of the Al-Zn-Mg system. Solution heat treatment can be carried out in the range 860-920°F. Another aspect of X7106 is the low quench rate sensitivity. After solution treatment the alloy will respond to artificial aging or to natural aging.

A number of studies of the aging process in Al-Zn-Mg alloys have been made. The precipitation process in these alloys has been shown[8] to consist of three stages as indicated by the reaction:

(supersaturated solid solution) $\rightarrow$ G. P. zones $\rightarrow$ M' $\rightarrow$ ($MgZn_2$).

The G. P. zones are coherent with the aluminum matrix while M' is partly coherent. Maximum hardness results when a mixture of G. P. zones and M' is present as the result of aging the solution heat treated material. $MgZn_2$ is the equilibrium phase.

The strength of X7106, following a solution quench, is an approximately logarithmic function of aging time at room temperature. The maximum strength attained on natural aging is reported to be realized after a period of from one to three months[5]. Artificial aging greatly reduces the time required to obtain maximum strength. The aging characteristics of a four percent Zn, two percent Mg high-purity alloy have been studied by Polmear[10]. Figure F-3 presents plots of hardness versus time for several aging temperatures for this alloy. These curves indicate that the time requirement for maximum hardness is reduced by increasing the aging temperature, however, the peak hardness attained is lower than that reached at lower temperatures. At a temperature of 248°F, a peak hardness of 95 V. P. N. is reached at approximately 20 days, followed by loss of hardness with continued aging. The 302° and 392° aging temperature resulted in a further reduction of the peak hardness and overaging at shorter times. The overaging process has been found to be associated with the instability of G. P. zones at high temperatures[13].

The mechanical properties of X7106 and X7006 aluminum alloys have been reported in several publications[5, 14, 15]. The ultimate strength, yield strength and elongation of these alloys in four conditions of heat treatment are listed in Table F-III. These results represent a limited number of tests at various temperatures. The indicated range of ultimate strength at room temperature is 58.2 to 61.0 ksi.

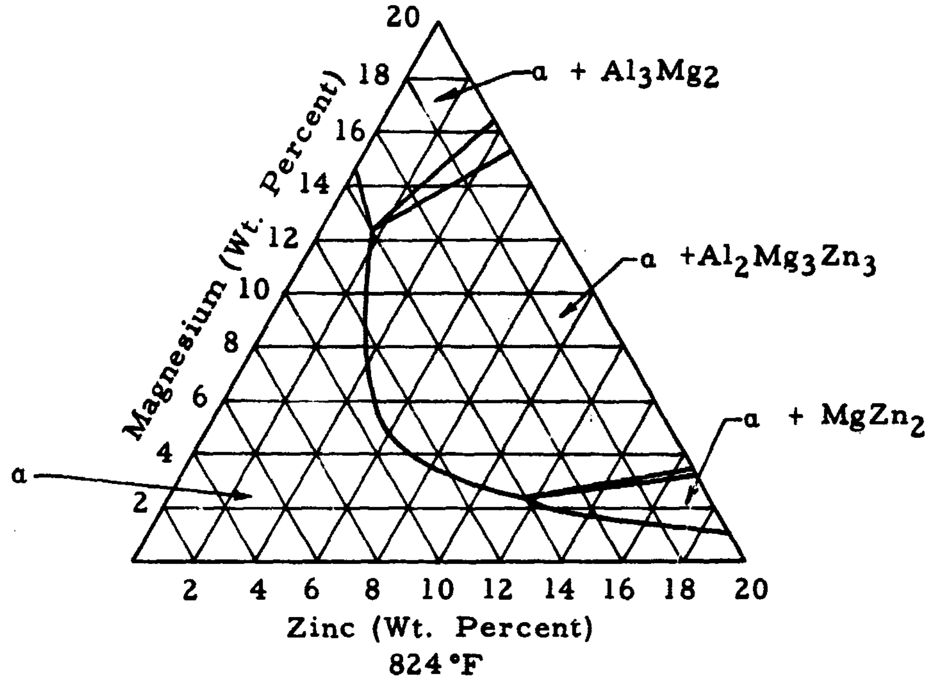

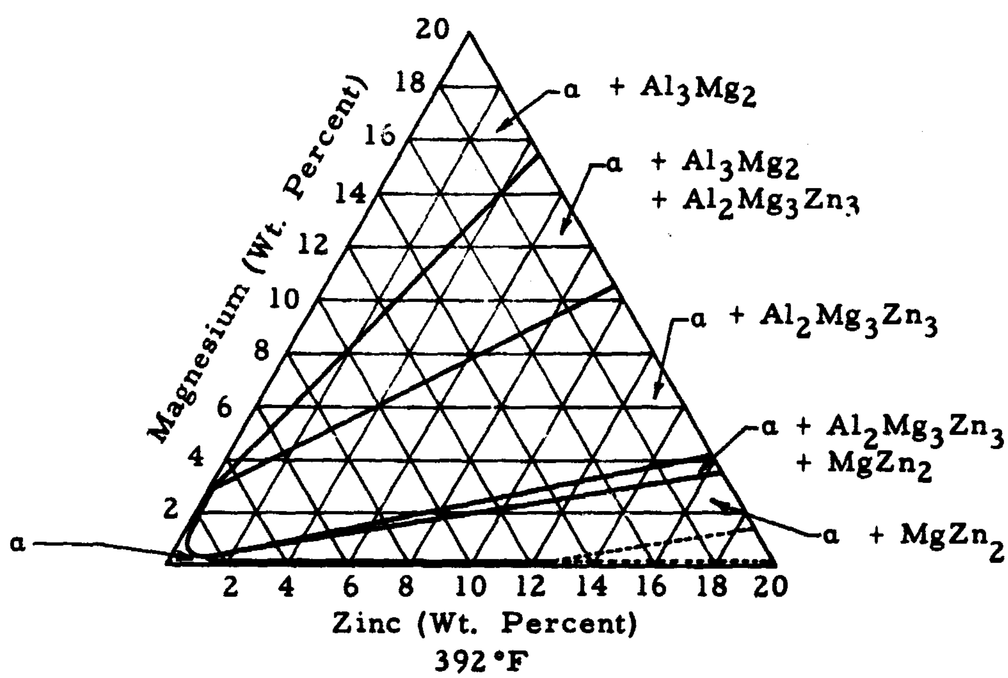

FIGURE F-2. PHASE RELATIONSHIPS AT 752 °F AND 392 °F IN THE ALUMINUM RICH CORNER OF THE Al-Zn-Mg SYSTEM

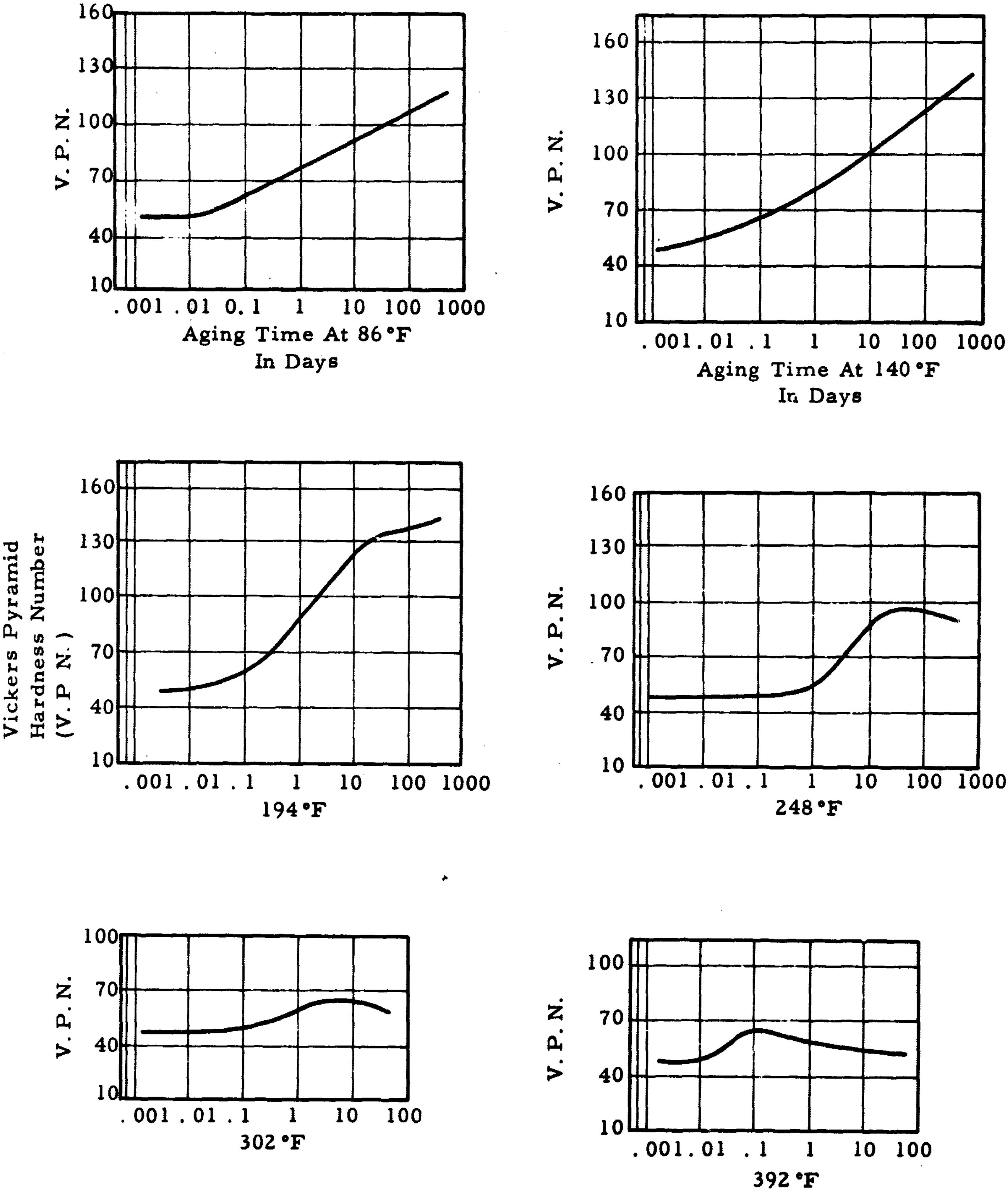

FIGURE F-3. HARDNESS/TIME CURVES FOR A 4 PERCENT ZINC 2 PERCENT MAGNESIUM ALLOY. AGED AT VARIOUS TEMPERATURES. POLMEAR[10]

TABLE F-III

BASE MATERIAL MECHANICAL PROPERTIES FOR X7106 AND X7006 (T6, T62, T6351 CONDITIONS)

Grain Direction	Temperature of Test	Yield Strength ksi	Ultimate Strength, ksi	Elongation Percent	Bibliography References	Thickness	Number of Samples
Long.	75°	54.2	58.8	20.0	14	3/8 Inch	3 samples
Trans.	75°	52.7	58.2	19.0	14	3/8 Inch	3 samples
Long.	75°	52.0	60.0	11.7	15	.063 Inch	3 samples
Long.	75°	50.5	58.4	15.0	15	1/4 Inch	5 samples
- - -	75°	55.0	61.0	15.0	5	"Typical Properties"	
Long.	-320°	64.2	76.2	18.2	14	3/8 Inch	3 samples
Trans.	-320°	61.3	75.2	17.3	14	3/8 Inch	3 samples
Long.	-320°	51.9	78.1	15.8	15	.063 Inch	3 samples
Long.	-320°	60.9	77.0	18.5	15	1/4 Inch	5 samples
- - -	-320°	67.0	80.0	- - -	5	"Typical Properties"	
Long.	-423°	69.0	90.3	18.5	14	3/8 Inch	3 samples
Trans.	-423°	69.2	91.5	17.8	14	3/8 Inch	3 samples
- - -	-423°	76.0	96.0	- - -	5	"Typical Properties"	

The fracture toughness and notch tensile strength of X7106 have been investigated by Anderson, et al[16]. The results of these studies indicate that X7106 is relatively insensitive to notch effects at temperatures ranging from 70°F to 432°F. Other studies utilizing precracked Charpy specimens also indicate that this alloy exhibits a relatively high fracture toughness[36]. The characteristics of 7039 aluminum alloy at cryogenic temperatures has been reported by DeMoney[37].

Stress corrosion problems in the original Al-Zn-Mg structural alloys have been reported[9, 17, 18]. Part of the problem is attributed to the high alloy content of these alloys. The alloying element level of X7106 is lower than these structural alloys and hence superior stress corrosion resistance may be expected. This relationship between alloy content and stress corrosion is demonstrated in Figure F-4. Curves for the stress corrosion lives of several extruded Al-Zn-Mg alloys of various compositions are compared. The six percent and five percent zinc levels have poor lives while the four percent zinc is superior. It has been established that for stress corrosion considerations, the safe limit for zinc should be fixed at slightly higher than four percent. Alloy X7106 meets this requirement. Alcoa reports that X7106-T6 sheet (based on limited data) has high resistance to stress corrosion[5].

II. Weldability of X7106

A. Metallurgical Considerations

The low quench sensitivity, natural aging and overaging mechanisms are of importance when considering X7106 weldments. The degree of insensitivity to quench rate of X7106 is such that at locations in the vicinity of a weld, where the solution temperature is attained, solution heat treatment results. Thus, solution heat treatment will occur in the weld deposit and also in part of the heat-affected base metal adjacent to the weld. Two other conditions prevail in the heat affected base metal: 1) a region will exist where the heat from welding will not produce a solution heat treatment but will result in overaging, and 2) in some regions a temperature sufficient to cause overaging will be attained but the time at temperature is insufficient for this overaging. A detailed study of these effects has been made on a 4.7 percent Zn, 2.3 percent Mg alloy after welding[4]. It was found that the zones of the weldment could be related to temperature and heat treatment effects as summarized in Table F-IV. Weldments of X7106 can be expected to show related behavior as the aging mechanisms and solution treatment temperatures are similar. Thus the location in the heat-affected base metal where reversion occurs can be the weakest region of the weldment. This is accounted for by the low level of response to subsequent aging.

Multipass welds (6 passes on 1-inch plate) for 4.5 percent, Zn,

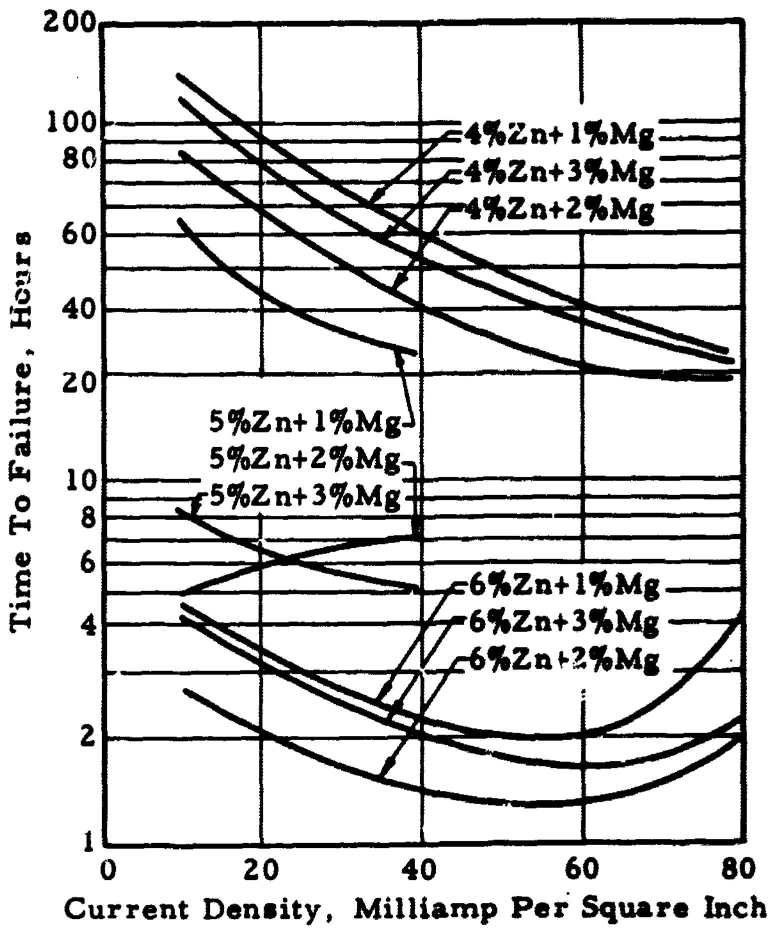

FIGURE F-4. COMPARISON OF STRESS CORROSION SUSCEPTIBILITY OF EXTRUDED TERNARY Al-Zn-Mg ALLOYS. All were stressed at 50% of the 0.2% yield strength. Taylor(17)

TABLE F-IV

SUMMARY OF TIME-TEMPERATURE EFFECTS ON WELDING AN Al-Zn-Mg ALLOY. Rogerson[4]

Temperature °F	Effect
>662	Solution heat treatment occurs. Responds to aging.
392-482	Reversion. Some dissolution of precipitated particles occurs. Partial response to subsequent aging.
302-356	No degradation with welding time cycle because of insufficient time exposure.

2.5 percent Mg have also been studied[8]. The superposition of several thermal cycles on the weldment was found to produce precipitates in part of the heat-affected base metal (on the electron microscope scale). This condition resulted in a softer structure and the loss of strength was not recovered on aging. Because of this deleterious effect of repeated heating, the full, inherent strength of X7106 weldments may not be obtained when repair welding or multipass procedures are employed.

B. Filler Metal Selection

The selection of a filler metal for welding X7106 involves the following considerations:

(a) Mechanical properties of the weld joint.
(b) Natural aging potential of the weld deposit.
(c) Crack susceptibility of the filler metal-base plate combination.
(d) Stress corrosion possibilities.

The efficiency of weld joints of X7106 is dependent on the artificial aging or natural aging characteristics of the weld deposit. This requires that the weld deposit contain zinc and magnesium since small additions of magnesium to the Al-Zn system have a pronounced effect on the age hardening of such alloys. For optimum hardening the zinc to magnesium ratio should be in the range of 4:1 to 2:1. The amounts of these two elements in the weld deposit are obviously governed by the composition of the parent metal and filler metal.

The ideal composition of the weld deposit would be that of base material (4 percent Zn and 2 percent Mg). However, this condition cannot be met because of a weldability problem associated with low magnesium and high zinc contents[19]. The cracking tendency of various Al-Mg filler metals, as a function of magnesium content, is illustrated in Figure F-5. Maximum cracking is encountered in the 1-1/2 percent Mg range. On the basis of this curve, freedom from cracking results at magnesium levels of five percent and greater.

Studies of the effect of zinc content in filler metals have also been made[20]. Cracking propensity was found to increase with higher zinc contents. This is indicated by the curves in Figure F-6. The family of curves in Figure F-6 (a), shows the relationship between zinc composition and cracking at three levels of superheat in ring casting tests. The lower curve, Figure F-6 (b), indicates the cracking tendencies measured in weld restraint tests. Both evaluations suggest that increased cracking will result as the zinc level is increased in the range of 0-6 percent.

The filler metals currently used for X7106 are X5180, 5356 and 5556. The chemical compositions of these alloys are as follows:

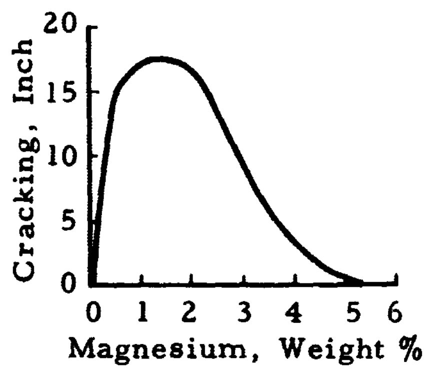

FIGURE F-5. EFFECT OF MAGNESIUM CONTENT ON WELD DEPOSIT ON CRACKING IN Al-Zn ALLOYS. Dowd[19]

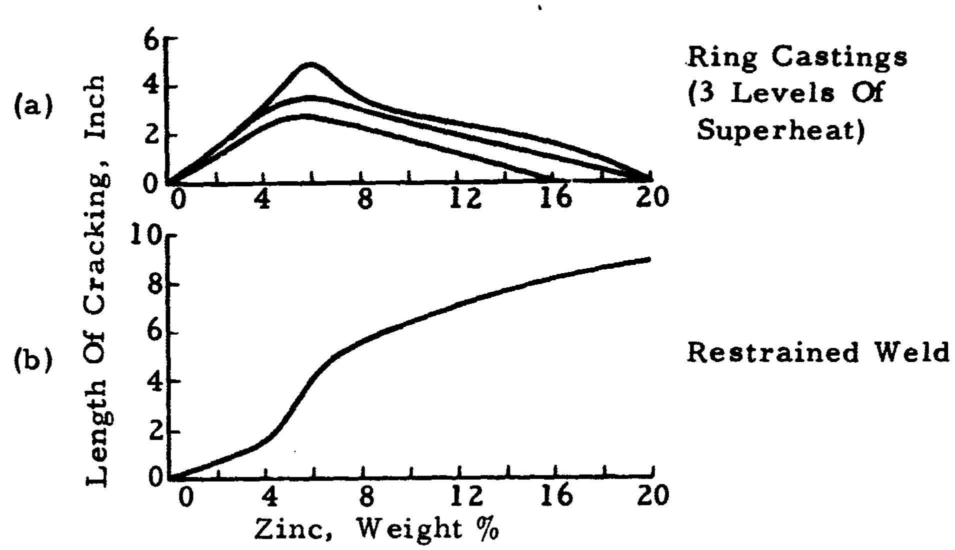

FIGURE F-6. INFLUENCE OF ZINC CONTENT ON CRACKING AS INDICATED BY RING CASTING AND RESTRAINED WELD TESTS. Pumphrey & Lyons[20]

	Nominal Percentage						
Alloy	Mg	Zn	Zr	Mn	Cr	Cu	Ti
X5180	4.0	2.0	0.1	0.5	0.1	-	0.1
5356	5.0	-	-	0.1	0.1	-	0.1
5556	5.25	-	-	0.8	0.1	-	0.1

Filler metals 5356 and 5556 are known to have good weldability when used with 5XXX series alloys. These two filler metals contain five percent magnesium, suggesting that they would be suitable for use with X7106 (See Figure F-5).

The filler metal designated as X5180 was developed expressly for use with X7106. Joint strength and resistance to stress corrosion of weldments prepared with X5180 is reported to be superior to 5356 and 5556 weldments[5]. The higher strength of X7106/X5180 weldments, as compared to weldments made with 5356 or 5556 filler metal, can be attributed to the presence of both magnesium and zinc in the filler alloy.

A useful indication of the probable composition of the weld deposit with parent metal and filler metal combinations is provided by the dilution nomogram in Figure F-7[21]. The analysis of weld metal for the close butt preparation with the three filler metals is considered in Table F-V (zinc and magnesium losses in the arc are not considered). The use of X5180 filler metal results in less zinc in the weld deposit than is in the X7106 parent metal, however, zinc still remains in the major alloying element and **a** Zn:Mg ratio of 1.4 is obtained. The use of 5356 and 5556 filler metals results in a lower Zn:Mg ratio and a correspondingly lower strength.

Studies of filler metal for aluminum alloys have indicated that a grain refiner could be beneficial in reducing cracking tendencies[22]. Zirconium is used in X5180 for this purpose. The results of previous studies appear to eliminate certain potential alloying additions such as Cu and Si[23]. Copper in the filler metal would provide hardening by the formation of Al_2CuMg, however, an undesirable delay in response to natural aging is attributed to this phase[12]. In addition, the presence of copper in the filler metal, induces poor weldability and increases the stress-corrosion susceptibility.

Large additions of silicon have been made to filler metals used to weld Al-Mg alloys for the purpose of improving weldability. Although silicon may be used to improve weldability of X7106 it is not usually employed because the resultant formation of Mg_2Si would interfere with the age hardening mechanism and thus lower the strength of the weld deposit. For this reason the silicon level in filler metals for X7106 is likely to be in the order of 0.15 percent which is used in filler metals for welding other 7XXX series alloys[20, 21].

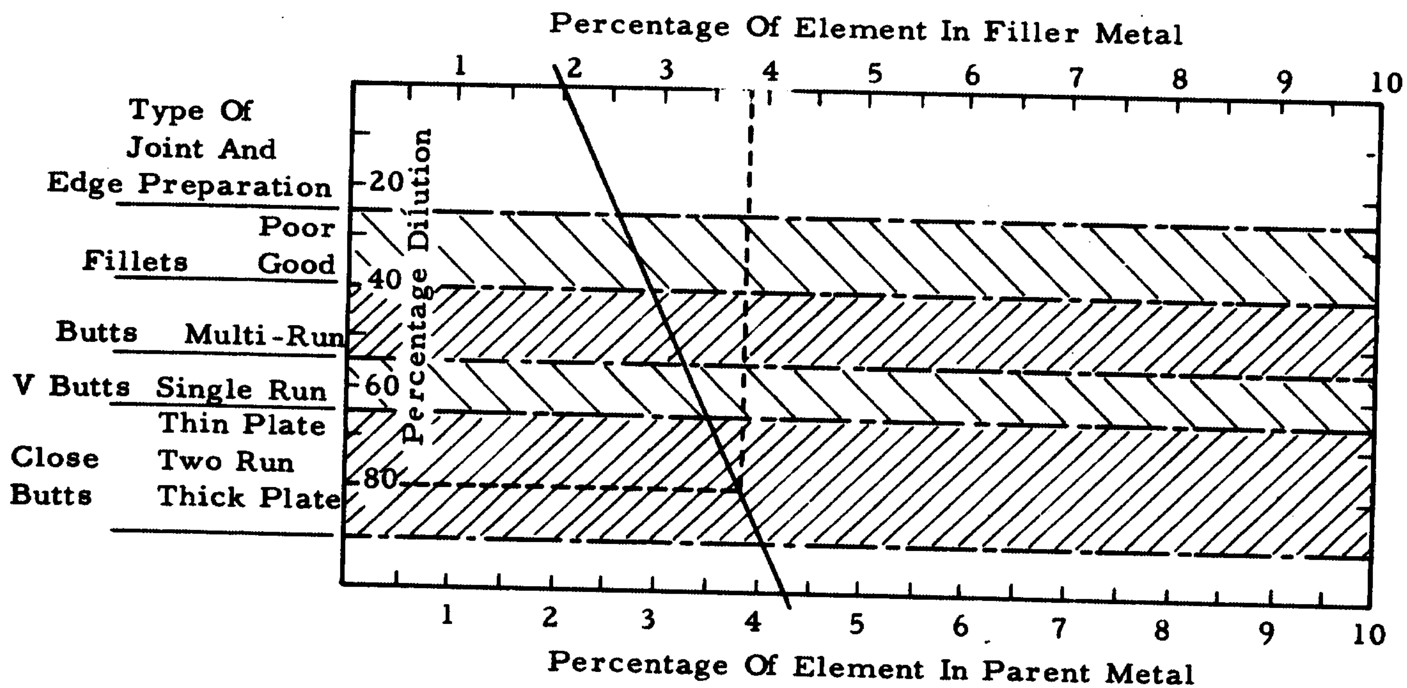

FIGURE F-7. DILUTION NOMOGRAM. EXAMPLE SHOWS PREDICTED ZINC CONTENT OF WELD METAL FOR X7106, X5180 FILLER AND 80 PERCENT DILUTION. Houldcroft[21]

TABLE F-V

PREDICTED WELD METAL COMPOSITION OBTAINED FROM DILUTION NOMOGRAM (Figure F-7)

Filler Base Metal	Filler Composition Mg	 Zn	Weld Composition Mg	 Zn
X5180 - X7106	4	2	2.6	3.6
X5356 - X7106	5	-	2.8	3.1
X5556 - X7106	5.25	-	2.9	3.1

C. Crack Susceptibility of X7106 Weldments

From this survey the weldability of X7106 appears to be quite good[24, 25, 26, 27]. In one investigation of the hot-cracking characteristics of this alloy conducted by Alcoa (employing the tee test, see below) the test results indicated that alloy X7106 is comparable to alloy 2219 in this respect[24]. Hot shortness due to low melting eutectics is responsible for the small amount of cracking that does occur. The weld surface appearance was generally reported as being good. One undesirable feature was the release of considerable fumes during the welding operation. These fumes are attributed to the high percentages of zinc and magnesium in both metal and filler metal. Dross (high Zn constituent) has been observed with TIG process by some investigators[28]. This dross was noted in the weld fusion zones and toes of welds.

One of the aspects of this survey was to investigate restraint tests and determine from available information which test would be most applicable for the X7106 study. Most of the restraint tests were originally developed to study the weldability of steels, and the reliability of these tests for studying aluminum is not well known. However, information is being generated by different investigators which should increase the confidence level of these tests when applied to aluminum. Some of the more salient tests are cruciform, circular restraint, Houldcroft, window restraint test and Tee test. Each of these tests is discussed in detail below:

1. Cruciform Test: The cruciform test was primarily developed for an underbead or heat affected zone cracking test[29]. However, some have found it useful as an acceptance test for aluminum filler metals[25, 30]. This test has been used in filler metal development programs at Kaiser Aluminum Corp. with good results[25]. There appears to be a trend toward using the test for material one inch and greater in thickness. However, a survey by Randall, et al showed that thinner gages were used by some investigators[29].

The cruciform test consists of three 12-inch long plates joined together to form a 90° cross with four 6-inch legs as shown in Figure F-8. Other dimensions have been used by some investigators. To test for crack susceptibility, fillet welds are deposited in sequence between the legs of the specimen. As each bead is deposited a higher degree of restraint is developed. Resultant crack lengths are a measure of the weldability. In most cases, one test is made to evaluate crack susceptibility.

2. Houldcroft Test: The Houldcroft test, utilizing the specimen shown in Figure F-9, has been used to study the weldability of aluminum alloys[1, 31]. The test specimen consists of a single sheet 3-inches x 1-3/4 inches. Eight equally spaced slots 1/32-inch wide are machined in each side of the 3-inch dimension. The first two corresponding slots are 1/8-inch in length. Additional slots progressively increase in length to 5/8-inch. These dimensions are recommended for 1/16-inch thick sheet. For tests on 1/8-inch thick sheet all dimensions are increased by 50 percent and the slot spacing to

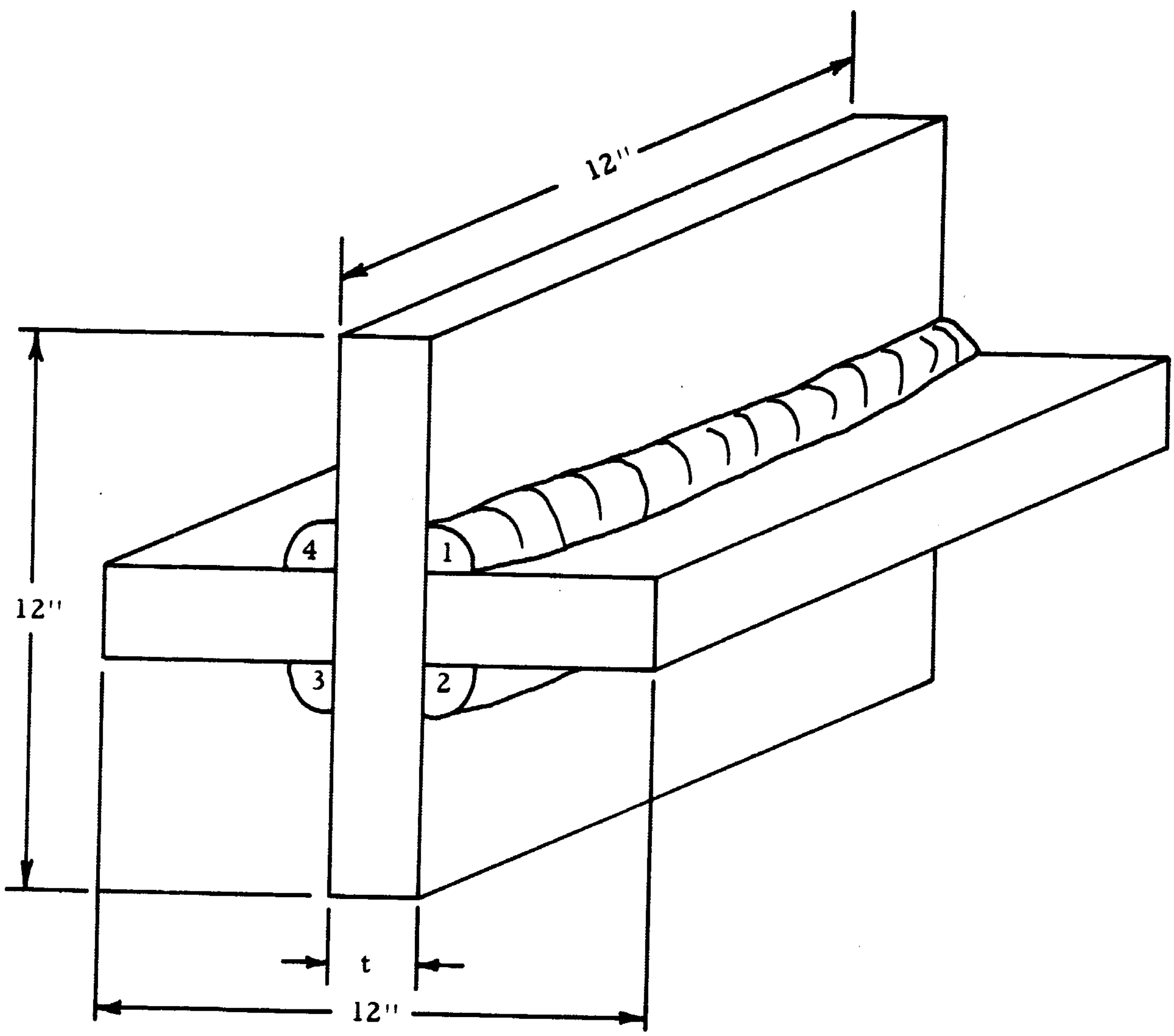

FIGURE F-8. CRUCIFORM TEST

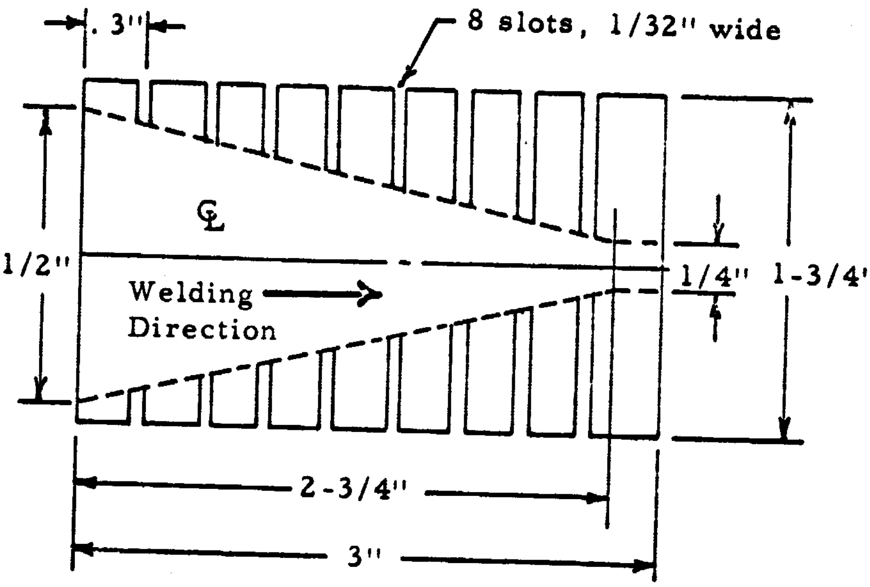

FIGURE F-9. HOULDCROFT TEST SPECIMEN

0.5-inch. In the test a single, bead-on-plate weld is made along the center line of the specimen. By the arrangement and dimensions of the slots, the stress level on the weld is constantly diminished as the weld progresses down the center line of the test. Cracking severity is determined by the resultant length of the crack.

The test can be used to evaluate both parent metal and parent metal-filler metal combinations. The test was previously developed to study magnesium-base and aluminum-base alloys in thin sheets. The inert gas tungsten arc welding process has been used in the preparation of this test. However, it is believed that the test could be extended to consumable electrode welding, provided filler wire diameter is sufficiently small. Complete penetration must be obtained and a constant bead width must be maintained. The test is sensitive to both welding current and speed. Conditions can be deliberately altered to increase the range of the test. Usually six tests are made to determine cracking severity for any one condition. This test has the advantages of being economical and simple in design.

Rogerson, et al(3), have conducted a program to obtain a better understanding of the fundamental reasons for hot cracking in welds and castings. In this program the Houldcroft Test modified to the 1/8-inch thickness was used extensively. An integral, unslotted, 2-1/2-inch, run-on-tab allowed the heat flow pattern to stabilize before the arc reached the first slot.

3. Circular-Patch Test: Another type of restraint test is the circular-patch weld test. The dimensions and joint geometry of the patch test specimens are by no means standardized. A typical test specimen is shown in Figure F-10. It consists essentially of a root pass deposited in a double V joint formed with a circular patch inserted into a plate. The extent of cracking is measured and expressed as a percentage of the total circumferential length of weld metal. The test has been used to evaluate the cracking susceptibility of several materials(29). This test is used to evaluate both hot and cold cracks of welds and heat-affected zones. A quantitative evaluation of cracking susceptibility can be obtained by varying the patch diameter. As the diameter is decreased the restraint is increased.

Levy and Kennedy investigated the residual stresses in circular-patch specimens of various plate and patch sizes(32). They showed that the residual tensile stresses in the order of yield stress of the material were present in specimens where the patch diameter to plate width ratio was in the range of 0.200 to 0.300. They also indicated that very small patches were undesirable because the cooling rate of the weld deposit was lower than encountered in a normal weld. Patches four to five-inches in diameter seem to offer the best geometry for test specimens.

Borland and Rogerson studied the patch test to assess hot cracking tendencies of weld metal and reported good reproducibility(33). On the

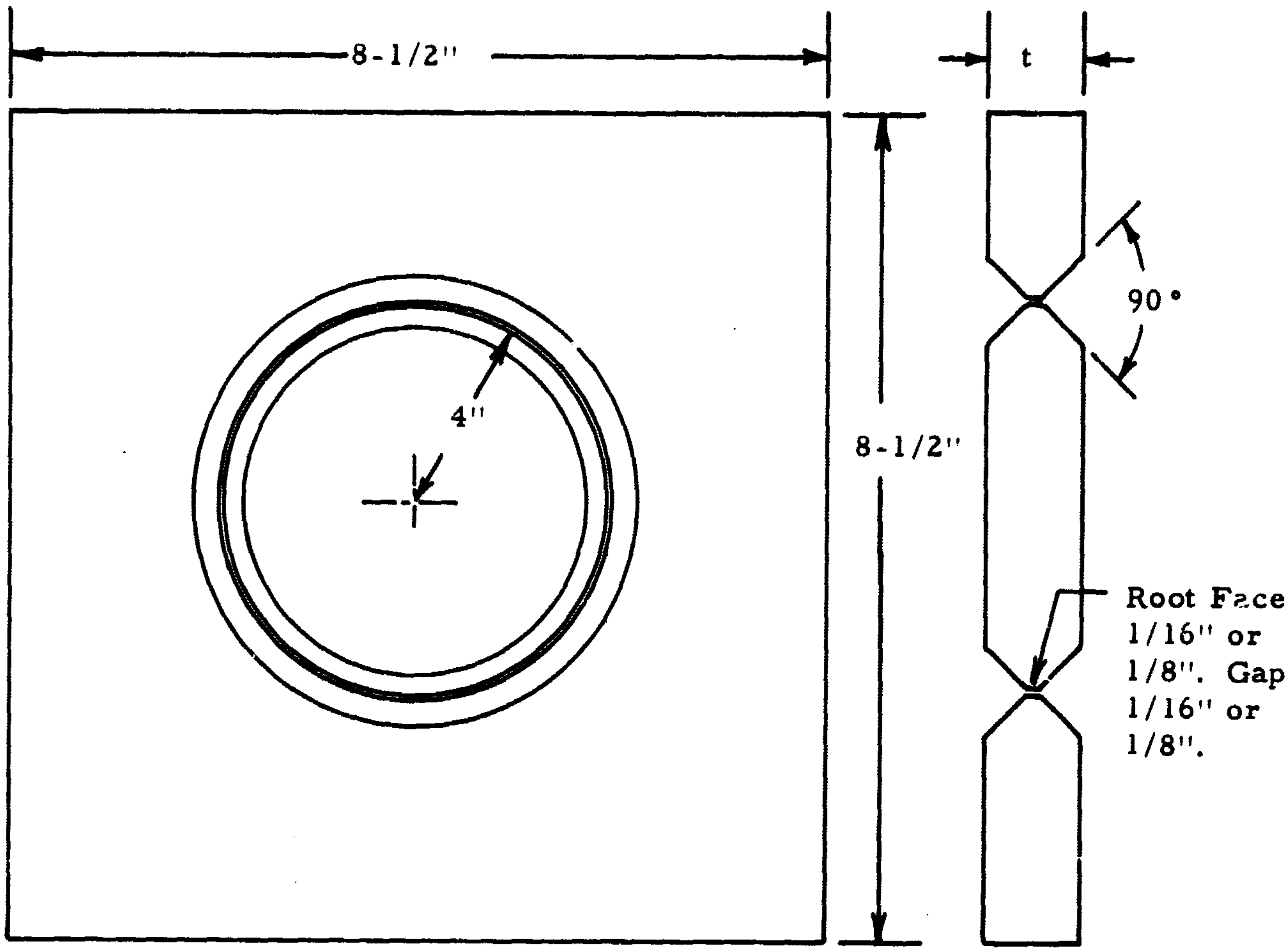

FIGURE F-10. CIRCULAR-PATCH TEST SPECIMEN other hand, Baysinger[31] and Manary[26] reported the test to be poor from the standpoint of reproducibility. In addition, Manary indicated the patch had a tendency to draw to one side due to the shrinkage forces of the weld. Baysinger indicated the results from thin sheet could not be extrapolated to thicker materials. Both Baysinger and Manary indicated the test to be very sensitive to the welding procedure and the least variation from any one parameter could result in erroneous results.

4. Tee Test: A fourth weld cracking test was developed by the Aluminum Company of America, and is described by Dowd[19]. The test is shown in Figure F-11 and consists of an inverted tee. The vertical member is 1/2-inch x 4-inches x 10-inches and the base member is 1-inch x 4-inches x 10-inches. Fillet welds are manually deposited and crack sensitivity evaluated by the extent of the longitudinal cracking in the fillets. This test is used primarily to evaluate filler metals. In essence, this is one-half of a cruciform test. Dudas indicated that this test gives more consistency and interpretable results than the Houldcroft, circular-patch or other tests evaluated[24].

5. Window Restraint Test: A window restraint test discussed by Arnold[34] is shown in Figure F-12. The test fixture consists of a 2-inch x 48-inch x 48-inch plate with a 12-1/2-inch x 18-1/2-inch opening or window cut in the center. Two plates of the material to be evaluated are welded to the edges of the window to form a butt joint. The edge weldments highly restrain the plates as the butt joint is welded. This is a very severe test and will always result in cracking if the base metal and/or filler metal is the least bit prone to hot or cold cracking. It has been pointed out, that all window restraint tests made from the 7XXX and 2XXX series aluminum had resulted in severe cracking[35].

D. Mechanical Properties of X7106 Weldments

Limited data is available for the mechanical properties of welded X7106. Some of this data has been reported by the Aluminum Company of America[5]. In addition, work conducted on X7006 by D'Annessa serves as a useful guideline to the expected behavior of X7106 weldments[15].

A comparison of the ultimate strength of as-welded and naturally aged X7106 and post-weld aged X7106 for three thicknesses (.125, .375 and 1.250-inches) is given in Figure F-13. Artificial aging produced higher strengths in the two thinner gages. Post-weld aging did not increase the strength of the thicker material. The range of ultimate strength for the three thicknesses is 52.0 - 58.0 ksi.

D'Annessa[15] reported the effect of natural aging on the mechanical properties of 0.063 and 1/4-inch thick X7006 weldments. These properties are shown in Figure F-14. One point on the graph in this figure represents the mechanical properties of specimens artificially aged after welding. This information indicates that the strength obtained by artificial aging is less

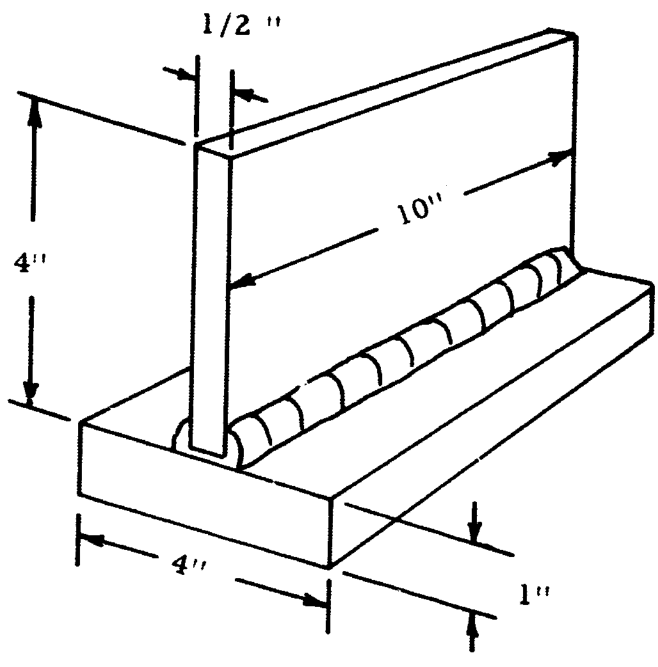

FIGURE F-11. TEE TEST

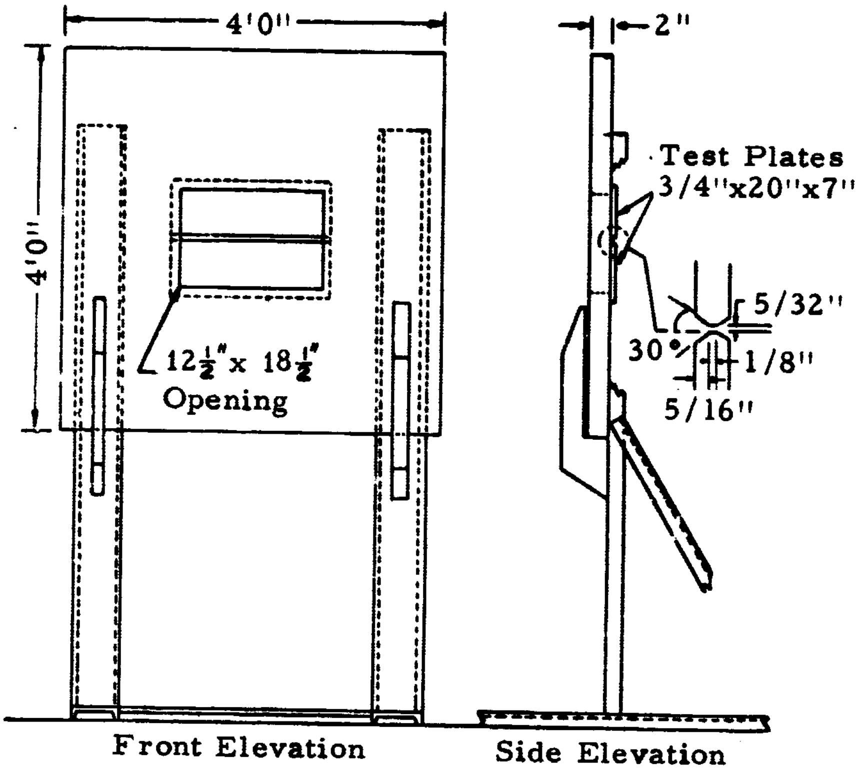

FIGURE F-12. WINDOW RESTRAINED TEST PLATE SET-UP

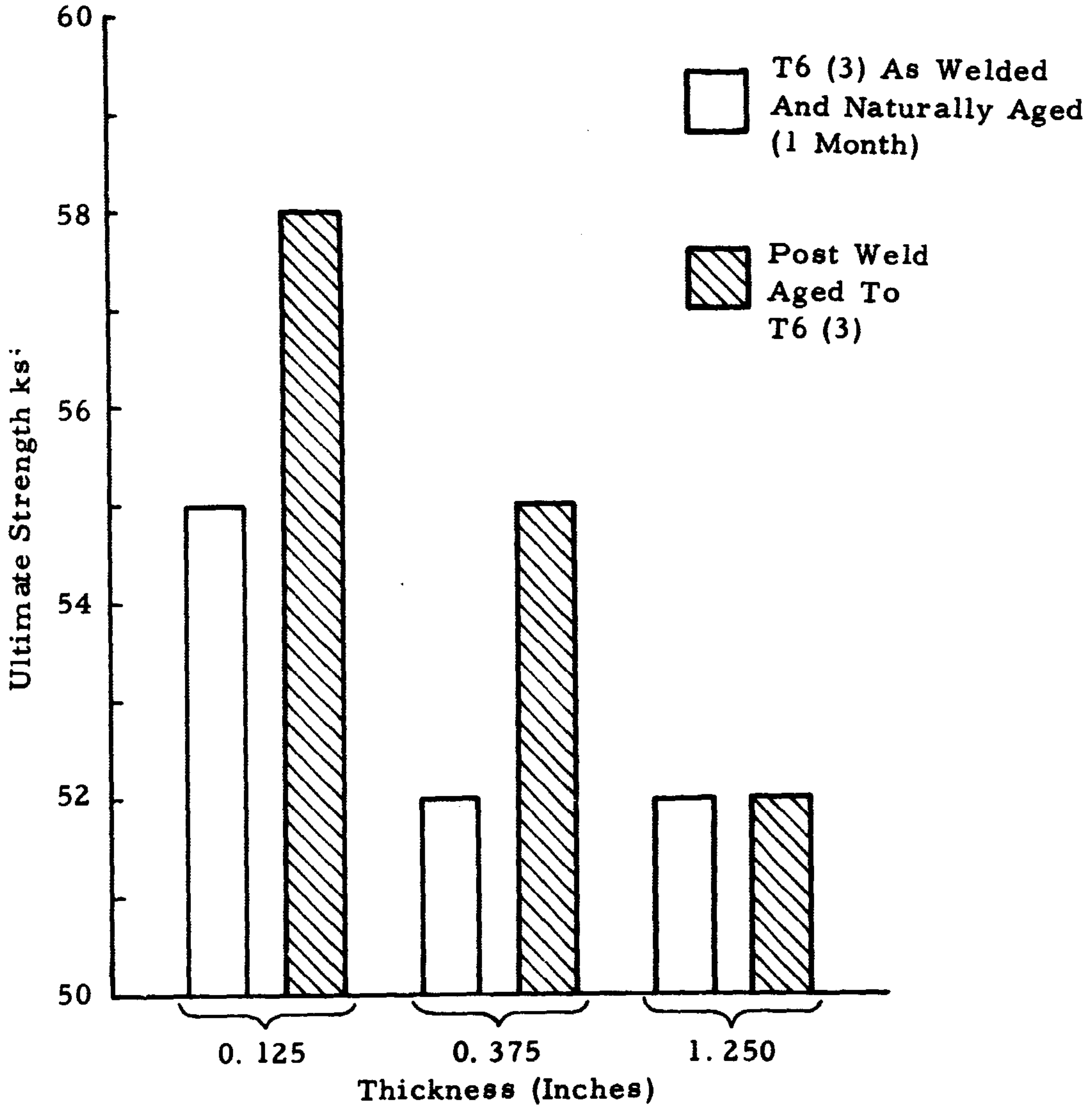

FIGURE F-13. BAR GRAPH OF ULTIMATE STRENGTH OF X7106-X5180 WELDMENTS FOR NATURALLY AND ARTIFICIALLY AGED CONDITIONS (Reference 5)

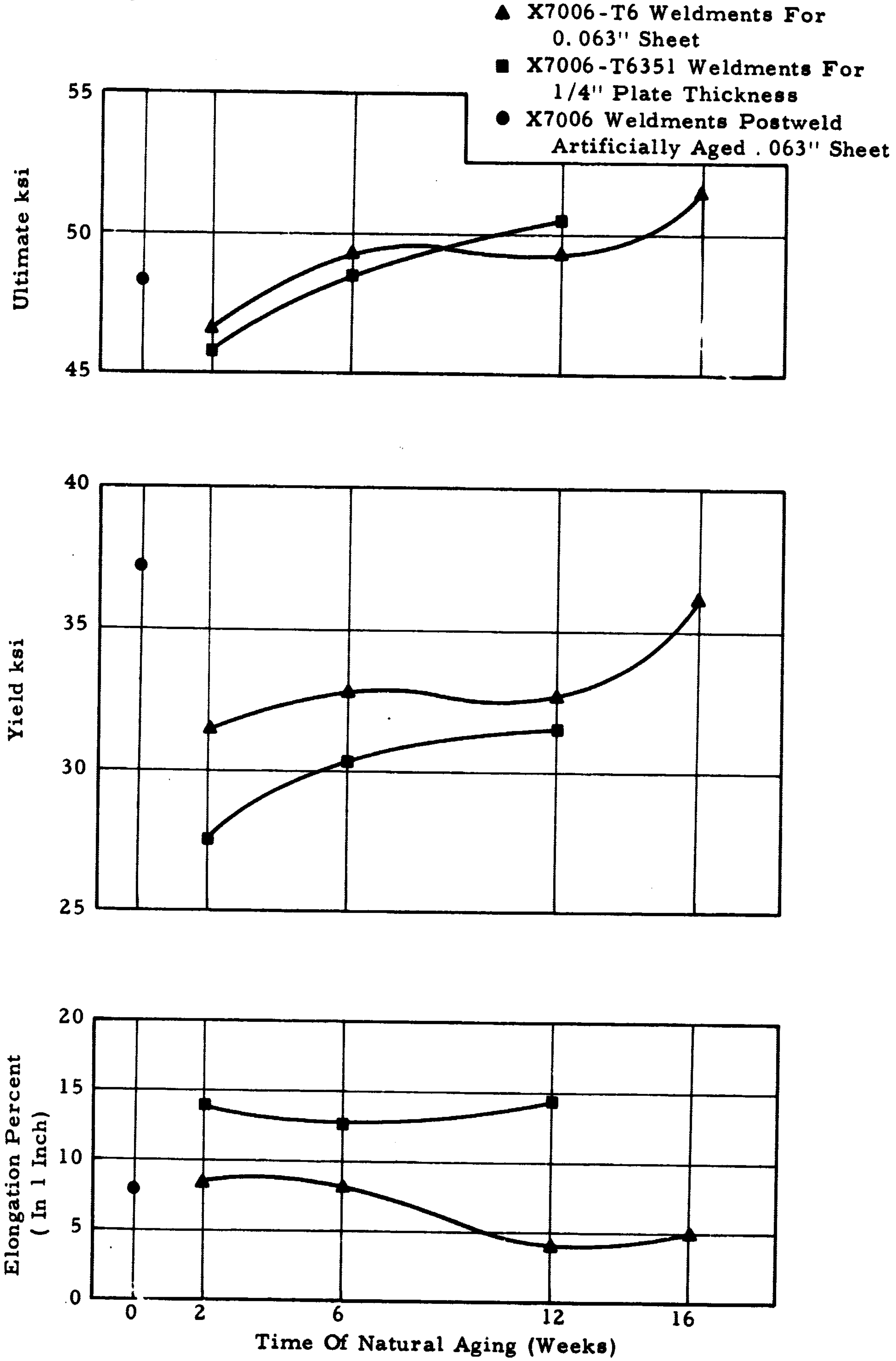

FIGURE F-14. MECHANICAL PROPERTIES OF X7006-X5080 WELDMENTS ON NATURAL AGING. D'Annessa[15] than that obtained from natural aging for six weeks or longer. Weldments of the 0.063-inch gage were also solution heat treated and artificially aged. It was pointed out that the weld fusion lines did not respond fully to the heat treatment. The mechanical properties of this material in the post weld solution heat treated and artificially aged, naturally aged and post-weld, artificially aged conditions are shown below:

MECHANICAL PROPERTIES OF 0.063 INCH, X7006-X5080 WELDMENTS[1] AFTER VARIOUS TREATMENTS

Condition	Ultimate, ksi	Yield, ksi	Elongation Percent (2 inches)
Post weld solution heat treated and artificially aged	44.4	40.0	3.1
Naturally aged (12 weeks)	49.1	32.9	5.7
Post weld artificially aged	48.2	37.3	4.2

The post-weld solution heat treated and artificially aged specimens did not respond to the heat treatment. This was reported to be due to the high magnesium content of the X5080 filler metal. This causes the chemistry of the weld fusion zones to approach the three-phase (α+Al_3Mg_2+$AlMG_3Zn_3$) field and possibly alters the precipitation hardening mechanism[12].

E. Summary

The results of this survey indicate that X7106 is reasonably weldable. From the published data, it appears that X5180 filler metal is the most suitable for use with this alloy. However, further evaluation of the three applicable filler alloys is necessary.

Partly because of its recent development only limited data on the mechanical properties of X7106 weldments are available. Information on X7006 weldments indicates that natural aging of the weldment results in substantial strengthening. This information can be extrapolated to X7106 because the chemical analysis is the same except for a small amount of zirconium addition to X7106. However, before extensive application of this alloy, further investigations should be carried out. In particular, the mechanical properties of the plate material and weldments for various thicknesses need to be firmly established. Another area that needs to be explored is the effect of different welding procedures on natural aging.

One of the objectives of this survey was to study the various restraint tests and recommend which would be the most applicable for the X7106 study. To investigate the weldability under restraint, it appears that possibly two restraint tests should be used. One type of test would be used to evaluate thin sheet and the other to test thicker materials. Probably the Houldcroft test would be the most applicable for thin sheet. A considerable amount of data obtained from this test is available and the results appear to be reliable. For thicker material, the cruciform test would probably be most applicable. This test has been used for several years and the results appear to be reliable. The test is relatively inexpensive and does not require an excessive amount of preparation time. It is to be emphasized that the results obtained from one test and one thickness of material cannot be extrapolated to the other test or to another thickness of material.

Assuming that the Houldcroft and cruciform tests are selected for evaluation of the crack susceptibility of X7106, it is recommended that another material known to be satisfactory or at least usable, from past experience, be tested along with the X7106. This other material could represent a standard to which the X7106 would be compared. Possibly, 2219 welded with 2319 filler metal would be a satisfactory material for use as a standard.